Coronal Mass Ejections & SEP Events

Nat Gopalswamy
NASA Goddard Space Flight Center
Greenbelt MD 20771 USA
nat.gopalswamy@nasa.gov
http://cdaw.gsfc.nasa.gov

Thanks to:
S. Yashiro, P. Mäkelä, S. Akiyama, H. Xie, N. Thakur, G. Michalek, A. Lara, E. Aguilar-Rodriguez, M. L. Mays, B. J. Thompson, J. M. Davila, O. C. St. Cyr, R. A. Howard, M. L. Kaiser, R. J. MacDowall

CCMC June 14, 2016

A Total Solar Eclipse Revealing the Coronal Structure

Prominences during eclipse
reported in
The Chronicle of Novgorod: AD 1185

The streamer structures are blown off occasionally as coronal mass ejections (CMEs). CMEs contain million-degree plasma with embedded magnetic field

CME in Old Eclipse Pictures: 1860 July 18

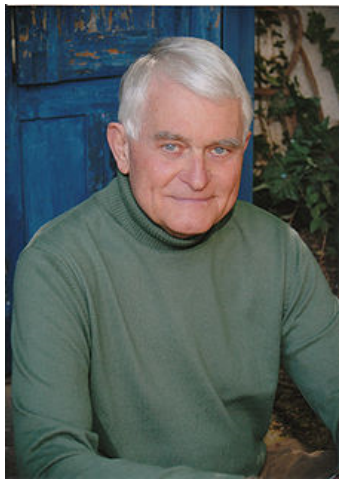

J. A. Eddy (1931 – 2009)

Chen et al 1997

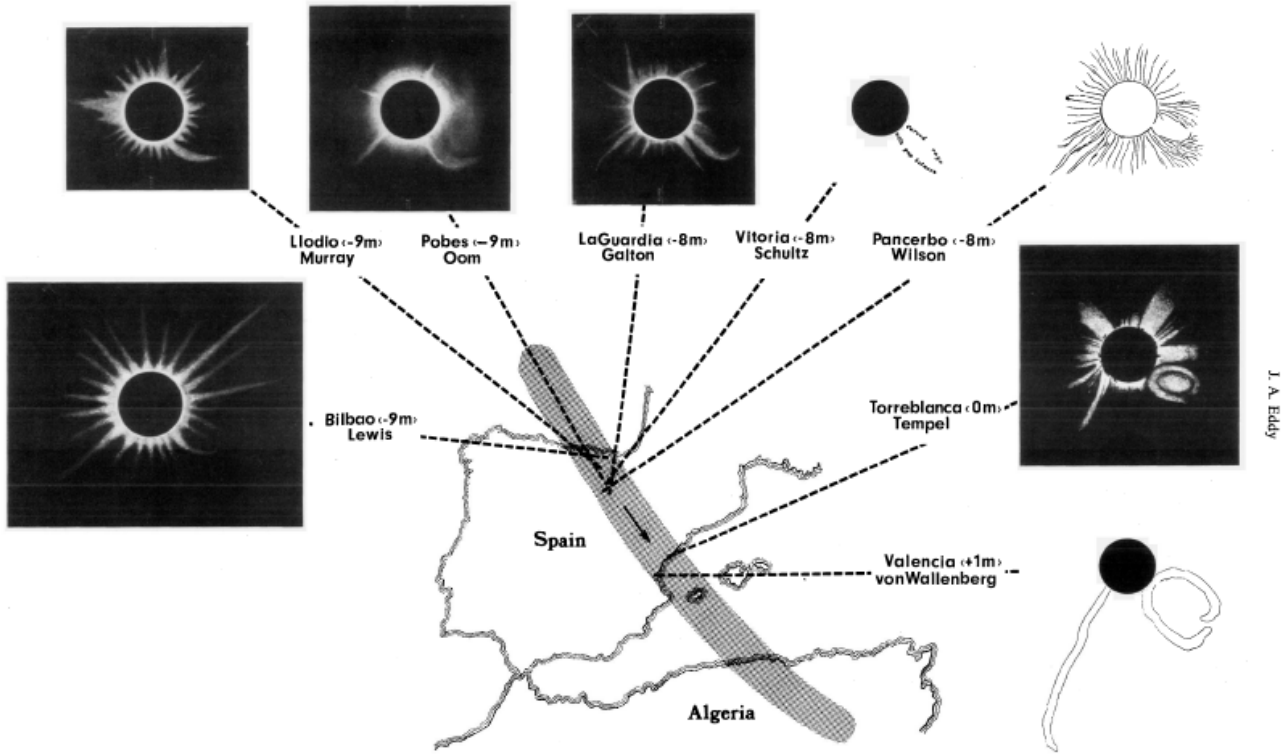

Fig. 4. Selected drawings of the corona (from Ranyard, 1879), made by different observers along the path of totality in Spain during the 1860 eclipse. Times are relative to mid-totality at Tempel's station at Torreblanca

Eddy, 1974 estimated the CME speed to be 200-500 km/s

A CME during a recent eclipse (2012 Nov 13)

Mareeba, Queensland, Australia (16S145E, the maximum eclipse 20:39:36 UT)

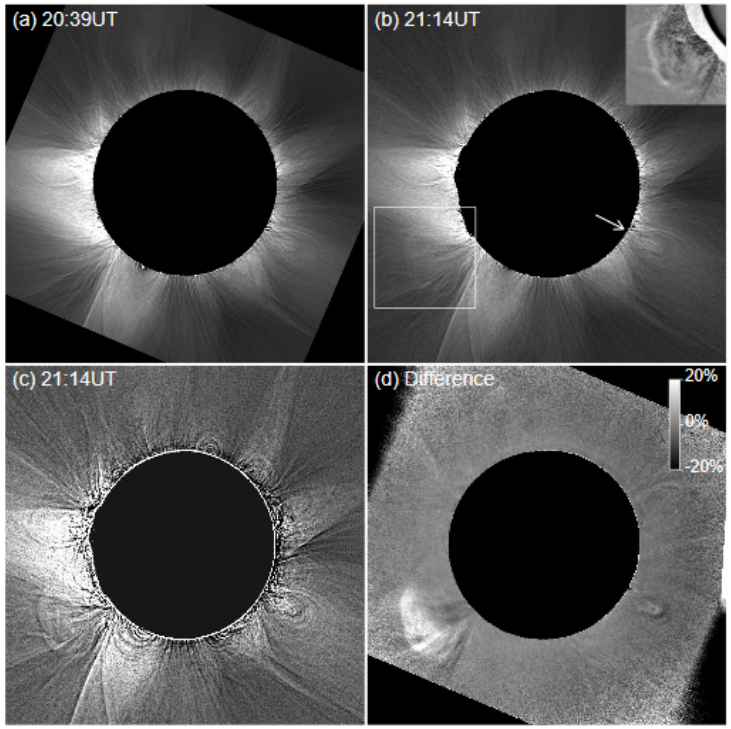

Commercial tour ship Pacific Venus (30S173E, the maximum eclipse 21:14:49 UT)

Hanaoka et al. 2014

CMEs, Flares, SEPs

Coronagraphs made it possible to observe the corona outside of eclipses (Lyot, 1932)

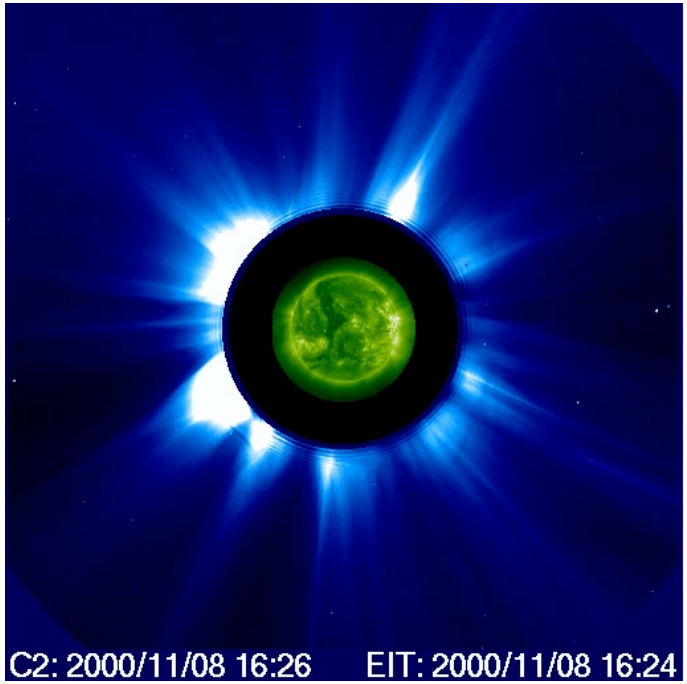

SOHO/LASCO and EIT

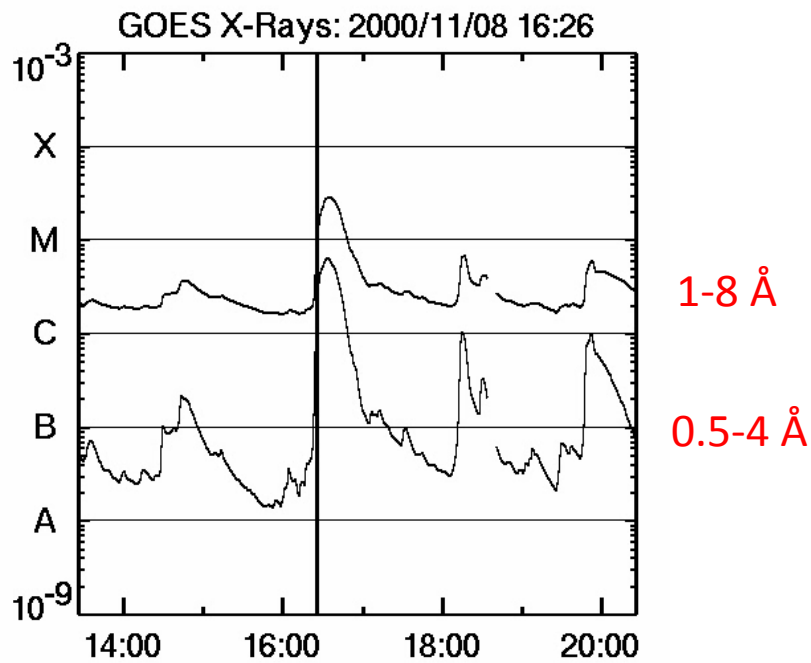

http://cdaw.gsfc.nasa.gov

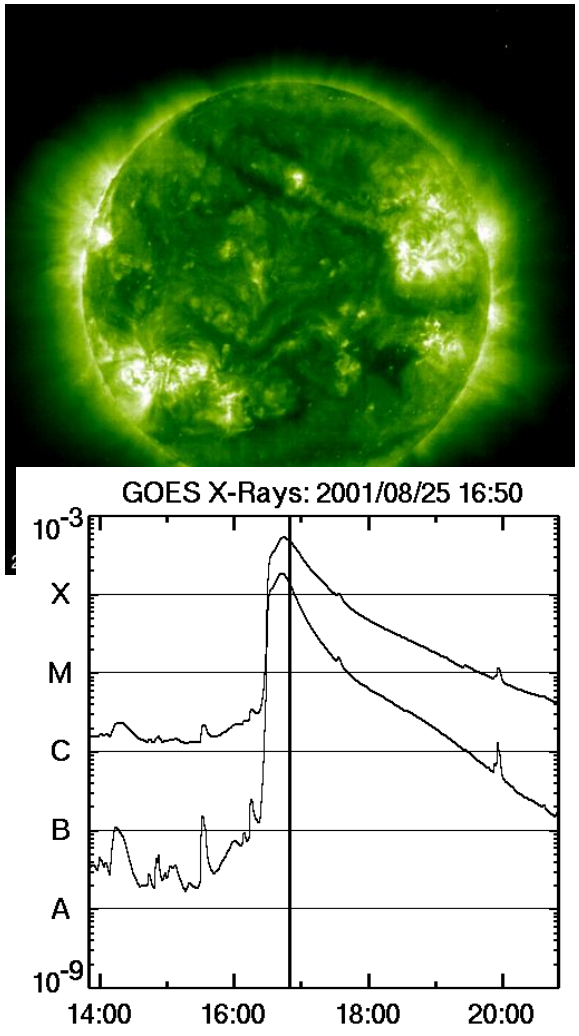

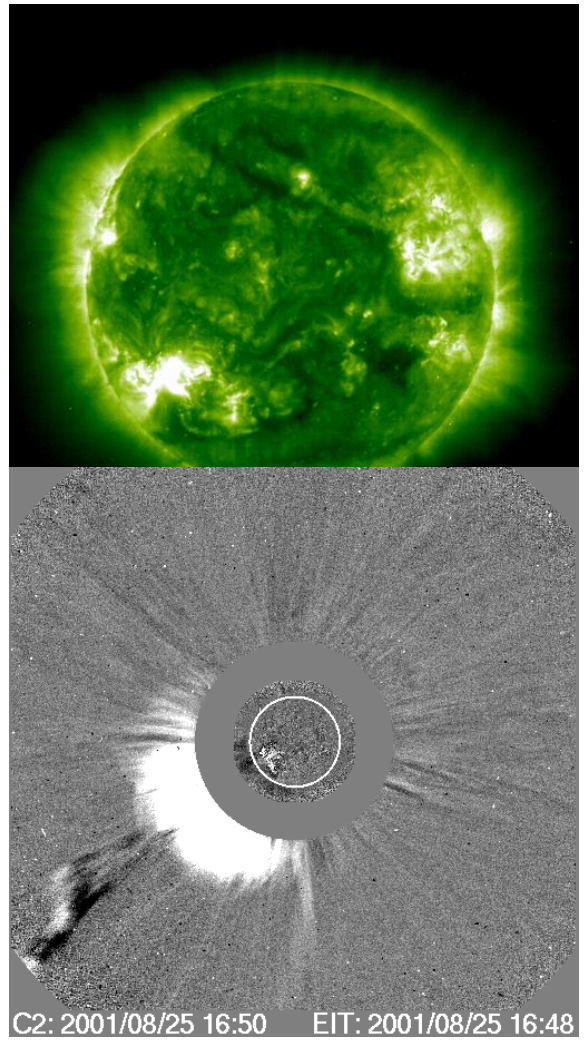

CME-Flare Relation

CME Mo

A CME is a multi-thermal , coherent magnetized plasma structure

Temperature ranges from tens of thousands to tens of million K

Densities from 10^8 to 10^{12} cm^{-3}

Speeds range from <100 km/s to >3000 km/s

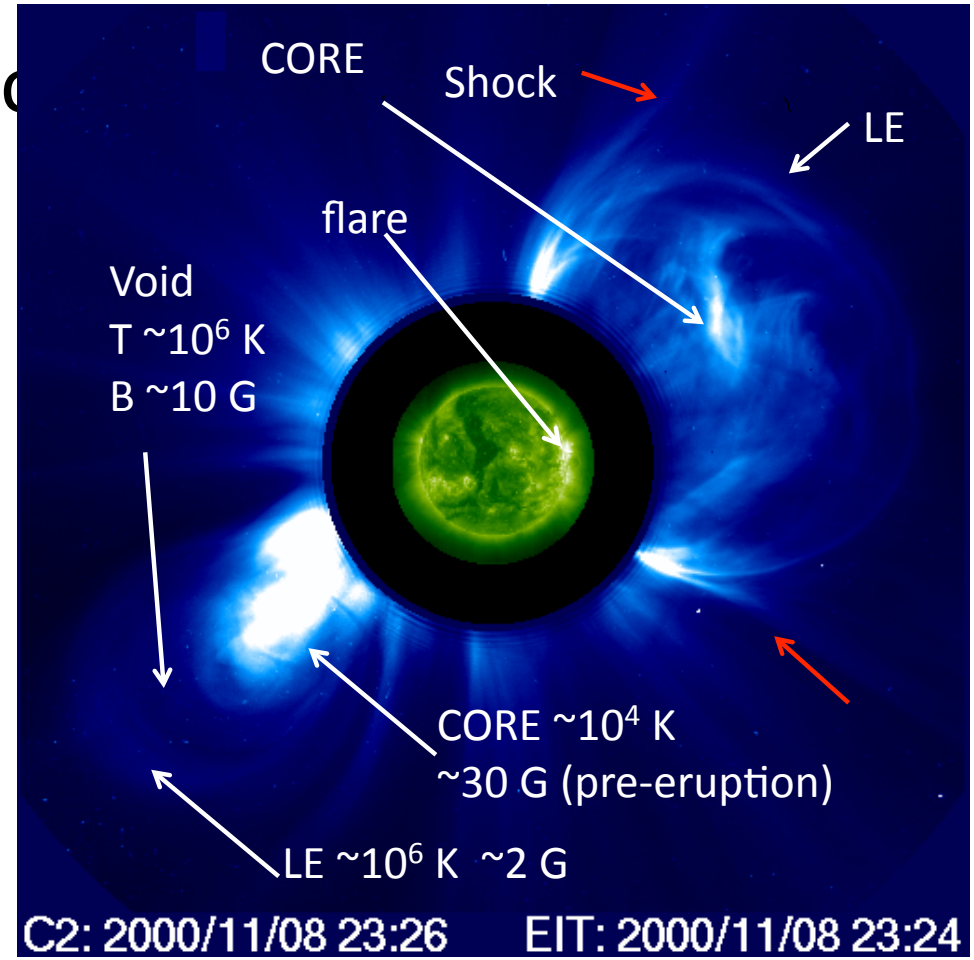

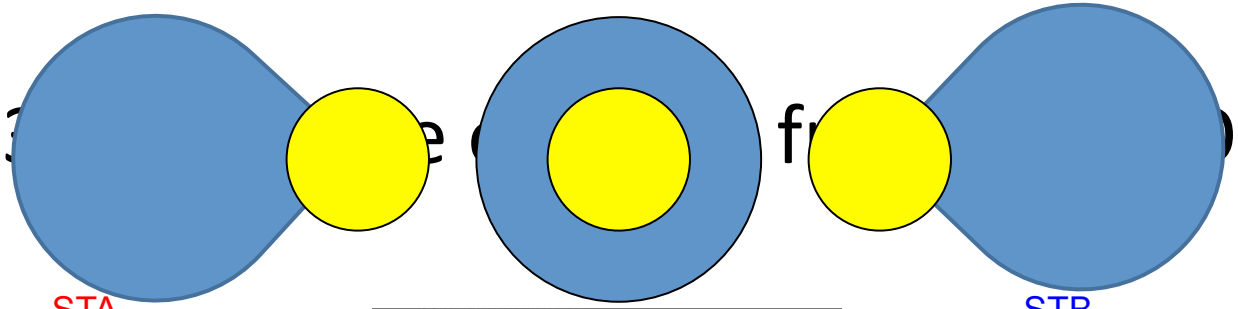

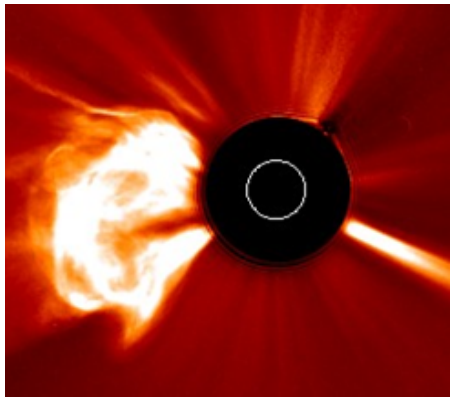

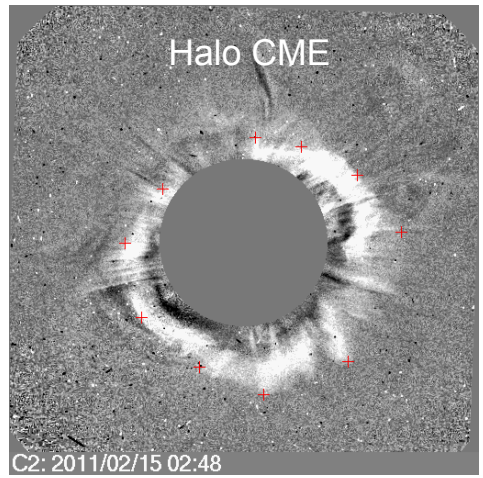

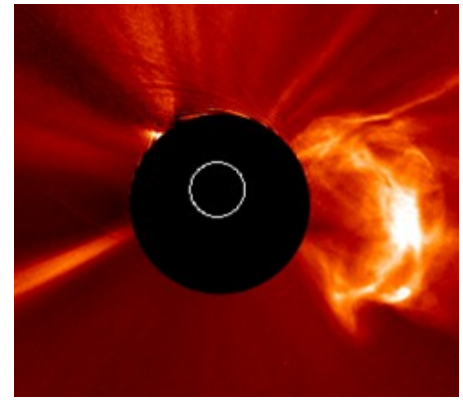

Limb CME

Limb CME

3-D Structure of CMEs: look like a balloon as is clear from three views

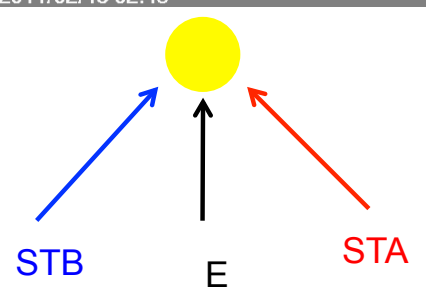

STEREO-A & B and SOHO coronagraphs

Natural Hazard: Geomagnetic Storms & SEPs

59% of reporting S/C and 18% of onboard instrument groups reported problems

Barbieri & Mahmot 2004
Gopalswamy et al. 2005

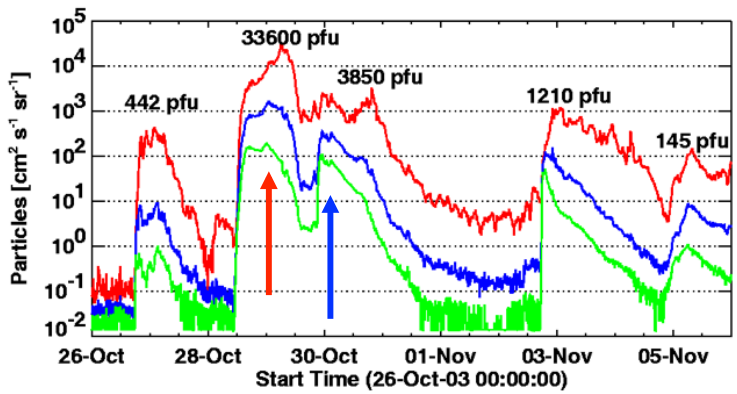

Two halo CMEs: 10/28 and 10/29 2003

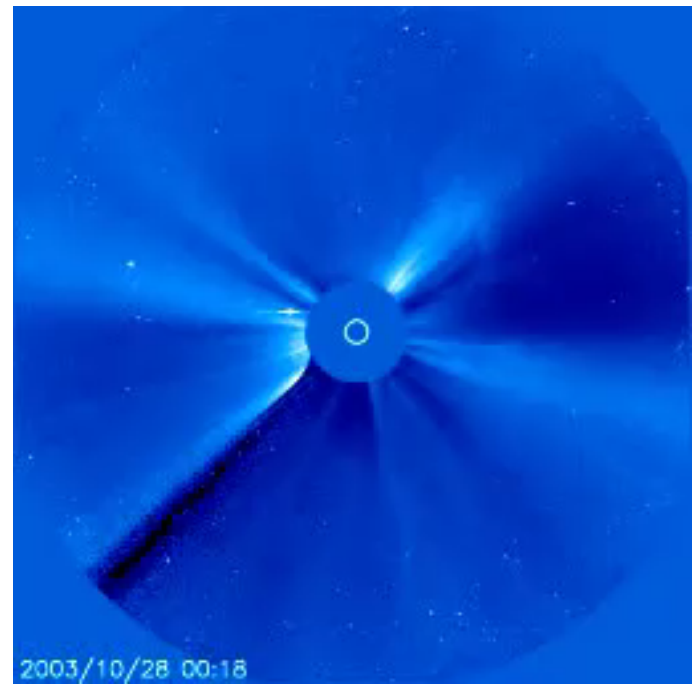

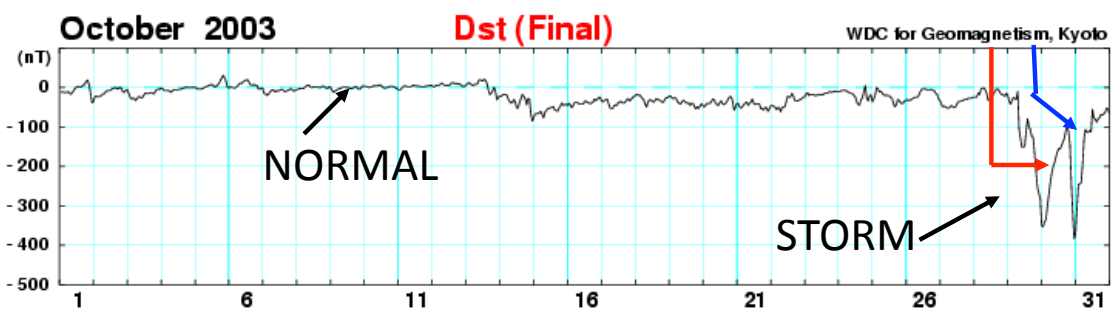

Transformer oil heated by 10° in Sweden; 50,000 people in Malmo had power blackout

SOHO/LASCO

MARIE: The Martian Radiation Environment Experiment

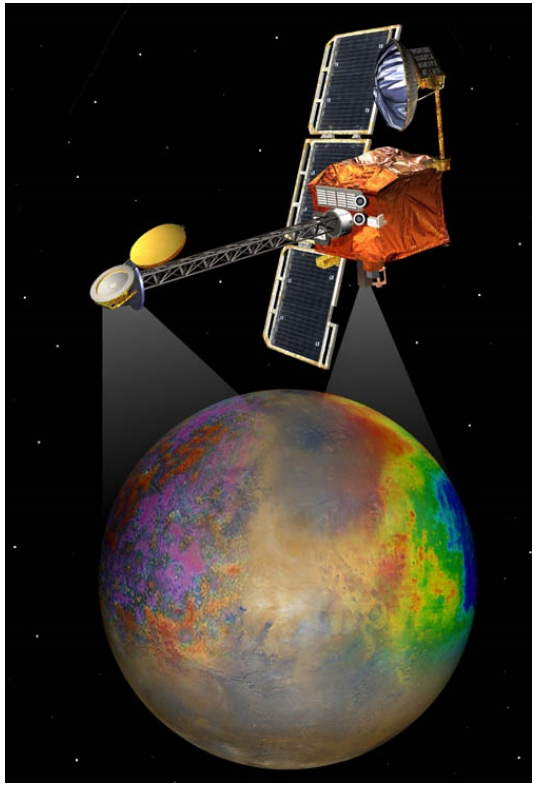

Mars Odyssey

The MARIE instrument on Mars Odyssey observed the radiation levels on the way to Mars and in orbit, so that future mission designers could plan the trips of human explorers to Mars.

One of the October 2003 SEP events rendered MARIE inoperative. It is ironic, as MARIE was designed to measure the radiation environment at Mars.

Nozomi

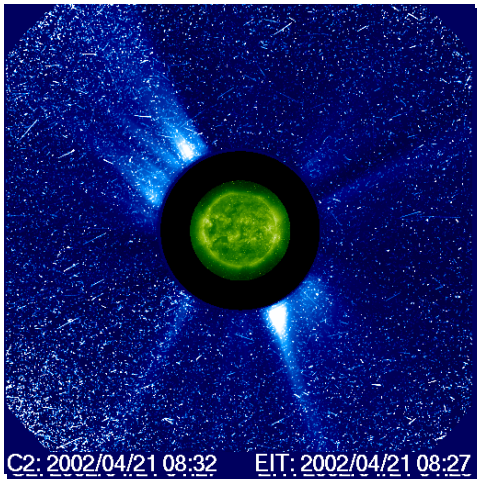

Protons penetrating Earth's Atmosphere

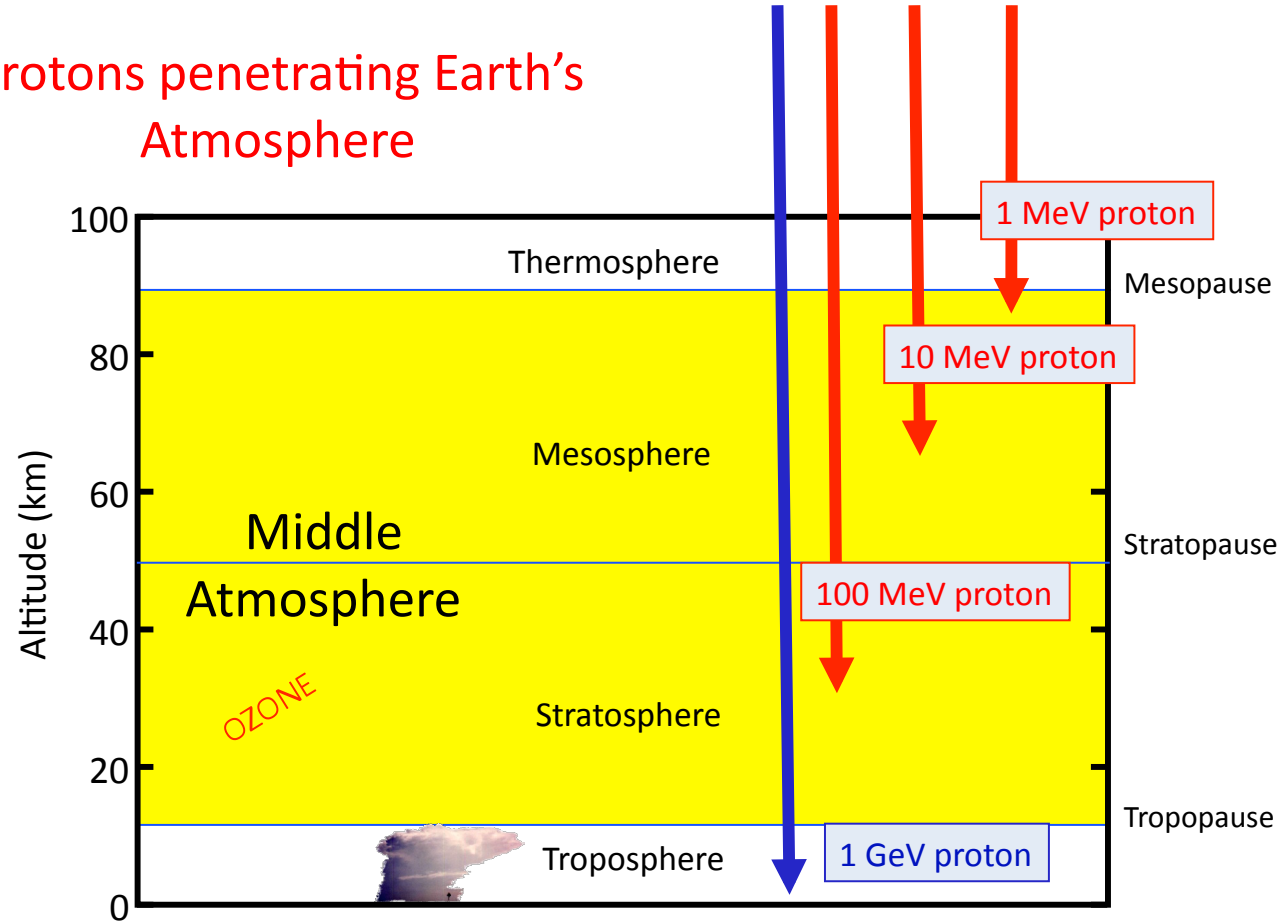

100 MeV protons penetrate to the stratosphere and can destroy ozone.

Courtesy: C. Jackman

GeV particles can affect airplane crew/passengers in polar routes

Range of Phenomena: 2005 May 13

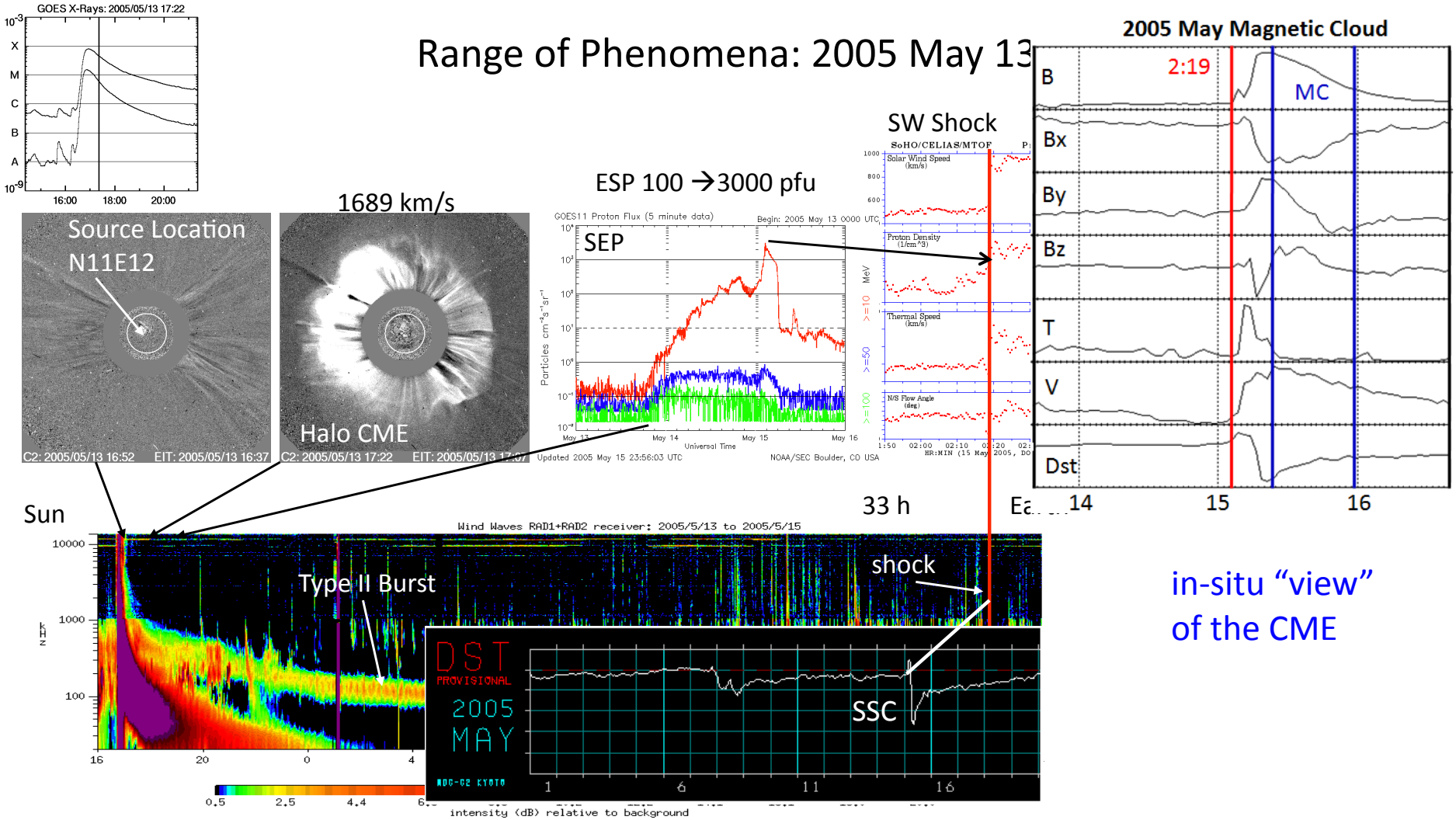

in-situ "view" of the CME

Animation of Halloween 2003 CMEs

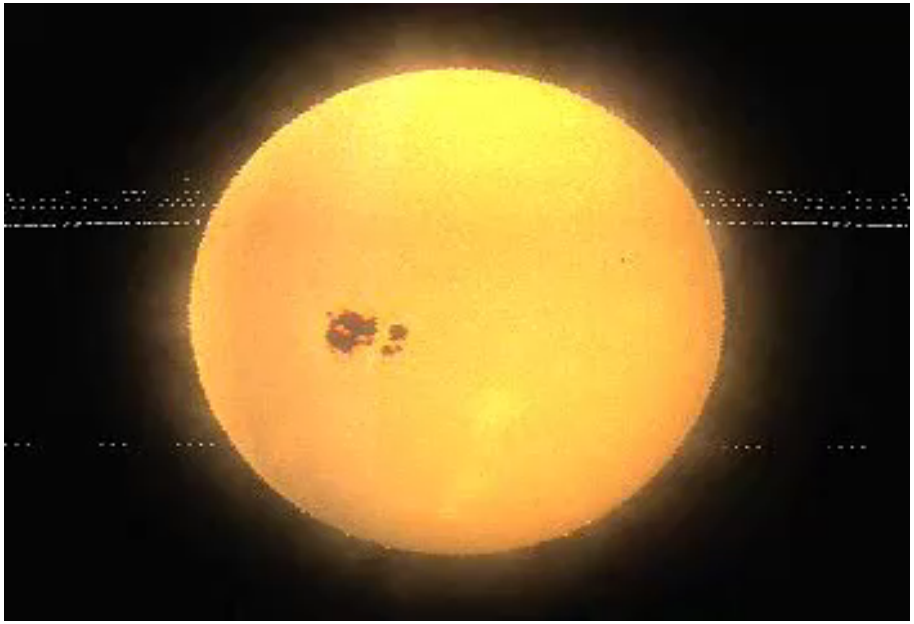

Consequences of the CMEs were observed at Earth, Jupiter, Saturn and even at the edge of the solar system where the Voyagers were located. The CMEs took 6 months to reach the termination shock.

CMEs represent the most energetic phenomenon in the heliosphere

Solar Disturbances can affect the entire solar system!

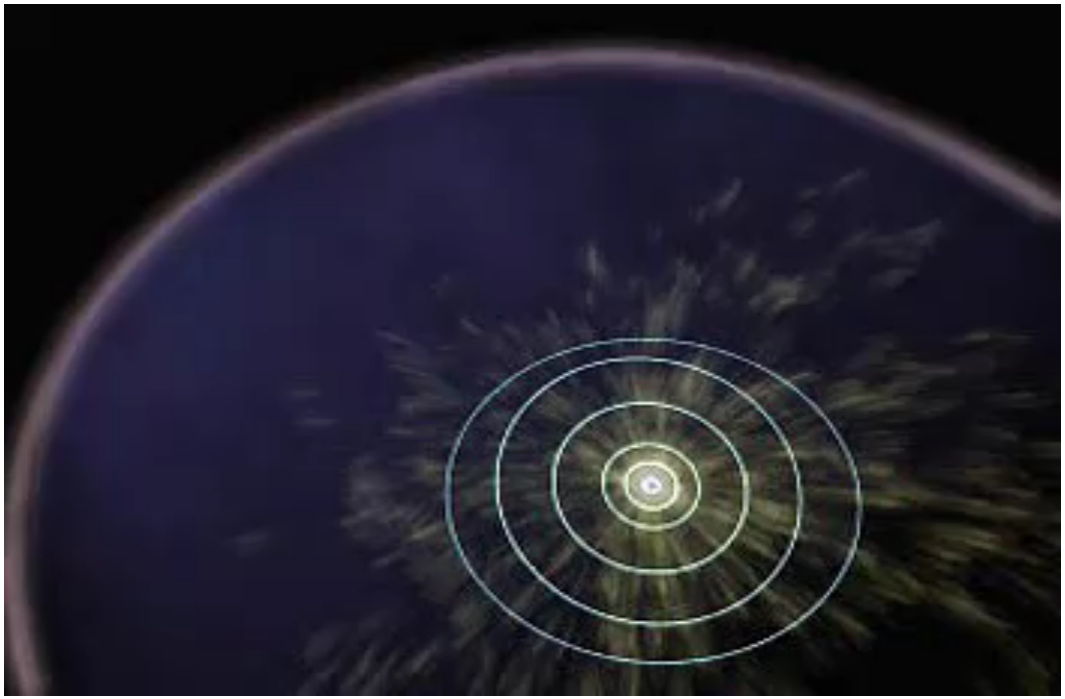

Animation showing the 2003 October November solar eruptions (based on Voyager 1 and 2 observations). Demonstrates the impact of solar events throughout the heliosphere

A Brief History: Solar and Interplanetary Milestones

- 1634: Variation in geomagnetic field (Gellibrand, in Fleming 1939)
- 1740s: geomagnetic disturbances correlated with aurora (Graham, Celsius, Hirorter)
- 1801: Low sunspot activity and high wheat prices (Wilhelm Herschel)
- 1806: Humboldt coins "magnetic storm", sets up worldwide magnetic observatories; aurora connection
- 1859: R. C. Carrington observes a flare from a sunspot region followed by the the great storm of 1859
- 1892: G. Fenyi finds prominence eruptions as fast as several 100 km/s; Fitzgerald: corpuscular connection
- 1908: G. E. Hale discovers magnetic field in sunspots; sets up worldwide H-alpha flare patrol (1931)
- 1937: S. E. Forbush world-wide decrease in cosmic rays
- 1943: H. W. Newton estimates the corpuscular stream extent of ~90°
- 1946: S.E. Forbush reports energetic particles associated with flares
- 1947: R. Payne-Scott discovers Type II radio bursts suggesting connection to filament eruption
- 1953: T. Gold proposes interplanetary shock to explain sudden commencement
- 1957: A. Boischot discovers moving type IV bursts (radio-emitting plasmoids); Parker's tangled field
- 1960: Pioneer 5 detects Forbush decrease outside Earth's magnetosphere - due to flare plasma
- 1962: Mariner II detects an interplanetary shock
- 1970: Hansen reports K-corona transient associated with moving type IV burst
- 1971: OSO-7 observes the first white-light CME

Solar Eruptions and Space Weather

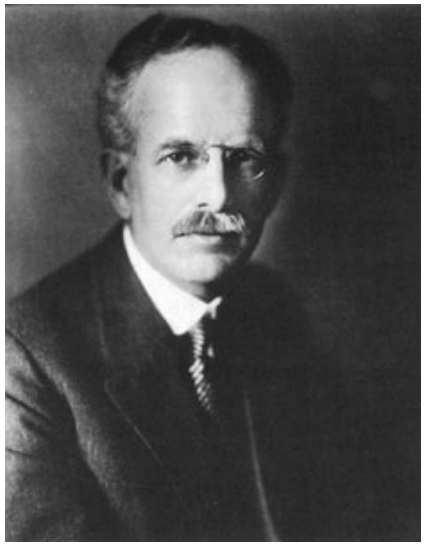

G E Hale 1868 - 1938

- Discovered magnetic field in sunspots (1908)
- Brought flares to central position via his paper in 1931: "The spectrohelioscope and its work, Part II: Solar eruptions and their apparent terrestrial effects"
- Average delay ~26 h (flare to storm)

12 May1909 Flare

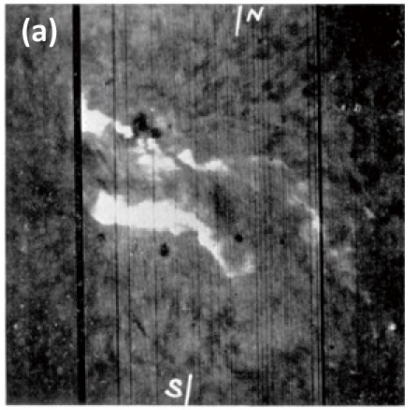

Hale 1931

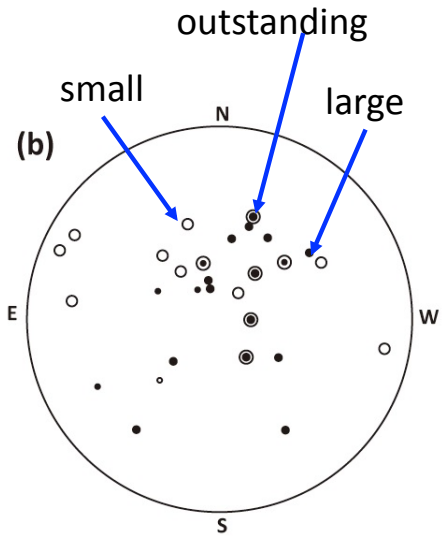

Newton 1943

1943 Newton: Flare – geomagnetic storm connection
- angular extent of the plasma stream ~90° (similar to modern ICME extent)
- Possible storms from filament eruptions outside of sunspots

Forbush Decrease, SEPs

Forbush (1946) Phys. Rev. Lett.

A full account of the experiment will be submitted for publication to the *Canadian Journal of Research*.

[1] C. Lapointe and F. Rasetti, Phys. Rev. **58**, 554 (1940).
[2] John Marshall, Phys. Rev. **70**, 107 (1946).
[3] J. Mattauch, *Kernphysikalische Tabellen* (Verlagsbuchhandlung Julius Springer, Berlin, 1942).

Three Unusual Cosmic-Ray Increases Possibly Due to Charged Particles from the Sun

SCOTT E. FORBUSH
Department of Terrestrial Magnetism,
Carnegie Institution of Washington, Washington, D. C.

October 10, 1946

SEVERAL world-wide decreases in cosmic-ray intensity have been observed[1,2] during magnetic storms. These decreases have been ascribed[3] to ring currents, or their equivalents, required to account for the observed world-wide magnetic changes.

In about 10 years of continuous records of ionization in Compton-Bennett meters (shielded by 11-cm Pb) three obviously unusual increases in ionization have been noted. For Cheltenham, Maryland, geomagnetic latitude, $\Phi = 50°$ N, these are shown in Fig. 1, in which the bi-hourly means were corrected for barometric pressure. Curves very similar to the upper one in Fig. 1 obtain[2] simultaneously for Godhavn, Greenland, $\Phi = 78°$ N; and for Christchurch, New Zealand, $\Phi = 48°$ S. Except for the absence of significant increases on February 28, 1942; March 7, 1942; and July 25, 1946, the curves for Huancayo, Peru, $\Phi = 1°$ S, are otherwise quite similar to those for Cheltenham.

Figure 1 indicates each of the three unusual increases in cosmic-ray intensity began nearly simultaneously with a solar flare (bright chromospheric eruption)

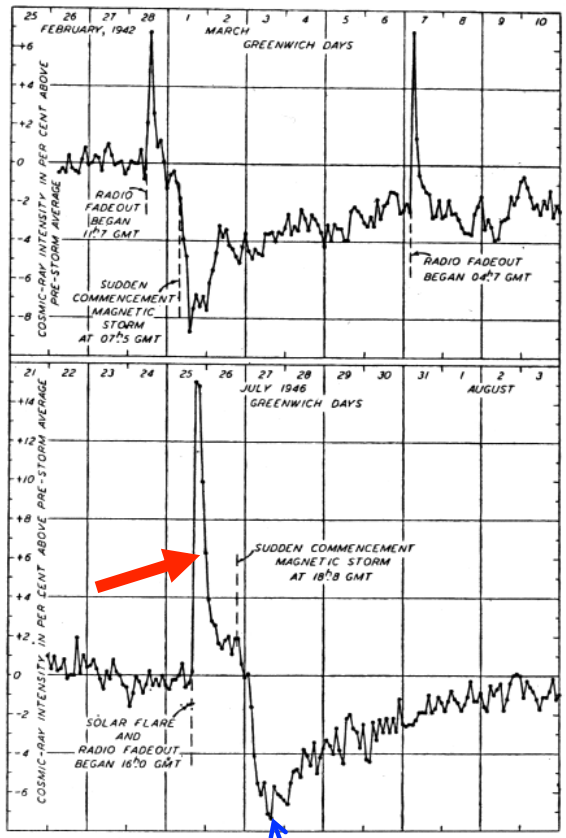

FIG. 1. Three unusual increases in cosmic-ray intensity at Cheltenham, Maryland, during solar flares and radio fadeouts.

Forbush decrease (1937)

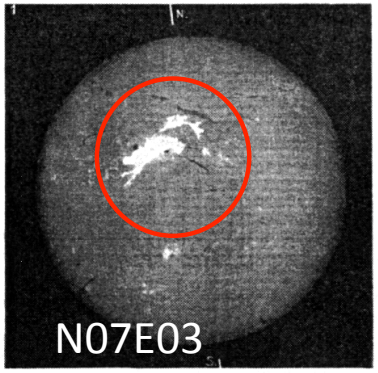

25 July 46 GLE Flare

Scott E. Forbush
(1904-1984)

Type II Radio Bursts are caused by electrons accelerated in the CME shock

Ruby Payne-Scott
1912 – 1981

The whole pattern drifts;
140 MHz in 6 min
df/dt = 0.4 MHz/s

Plasma density
5.0 x10^8 cm^{-3}

1.2 x10^8 cm^{-3}

0.4 x10^8 cm^{-3}

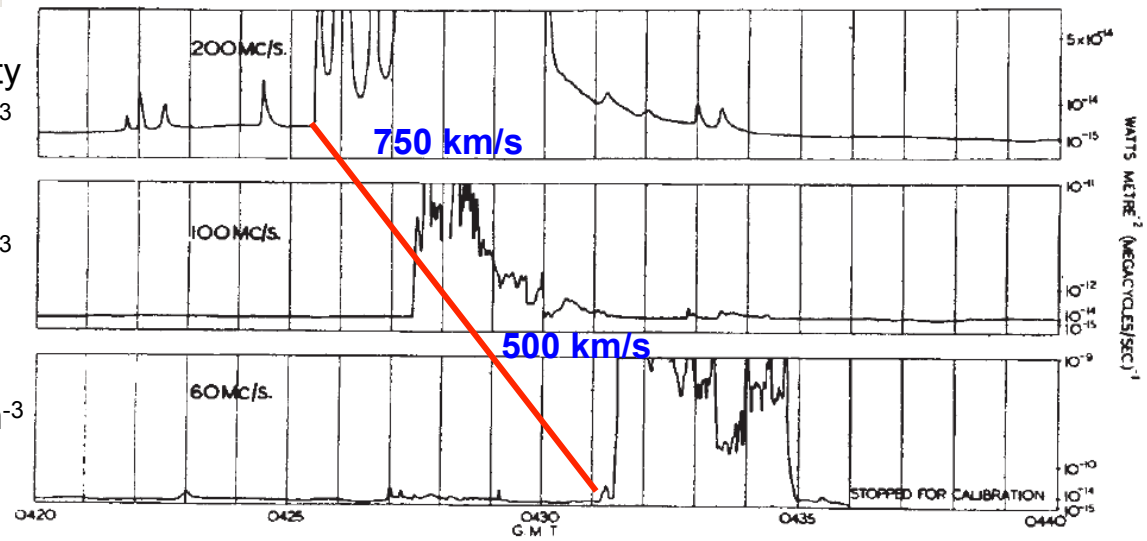

Nature 260, 256, 1947

LARGE OUTBURST OF MARCH 8, 1947

Moving type IV bursts

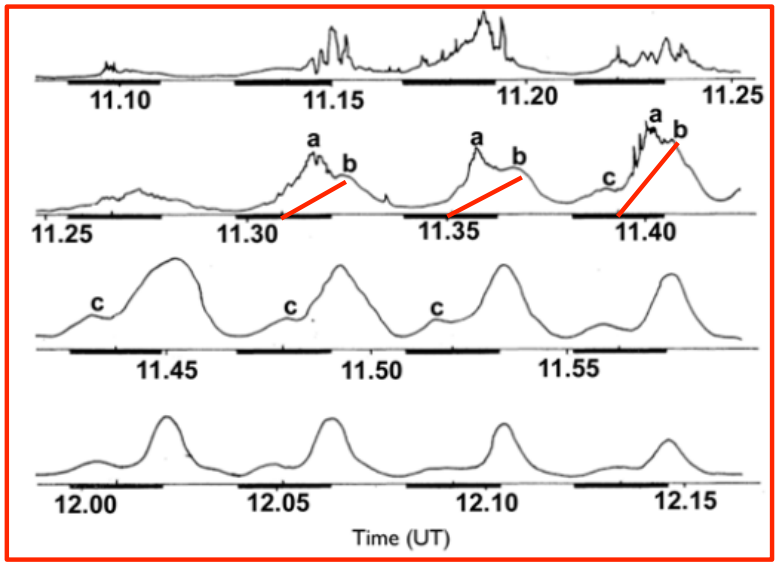

- 7 November 1956 moving Type IV burst at 169 MHz from E-W Nancay Interferometer Array
- One-dimensional scans (source “b”)
- Source “a” is a type II burst
- Discovered by A. Boischot in 1957 (From Pick et al. 2011)

Type IV image from at 80 MHz from the Culgoora Radioheliograph in Australia
Due to 100s of KeV electrons in moving magnetic structures

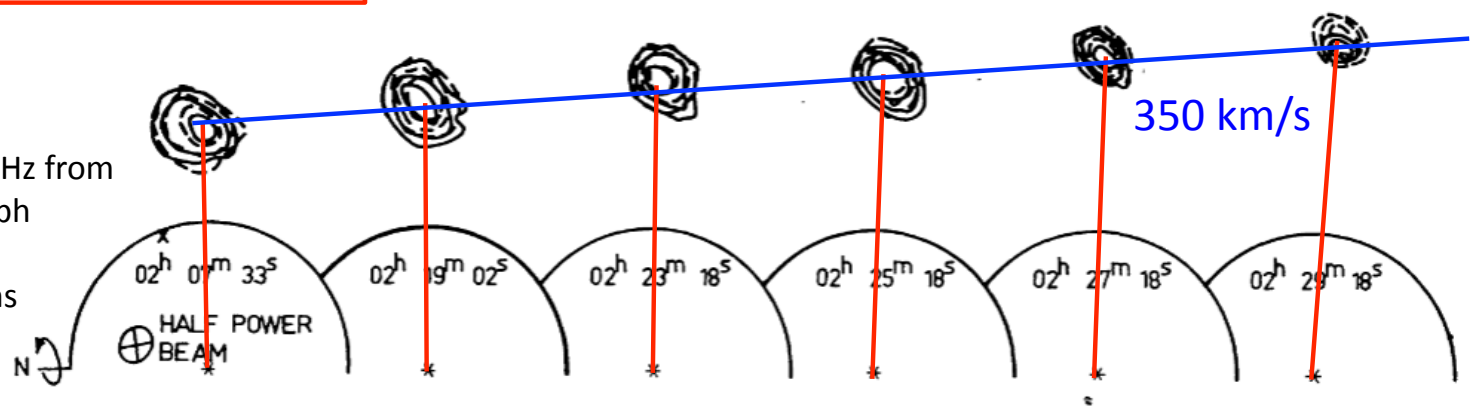

1970 Dec 26

Schmahl 1972

A Complete Picture of Solar Eruptions

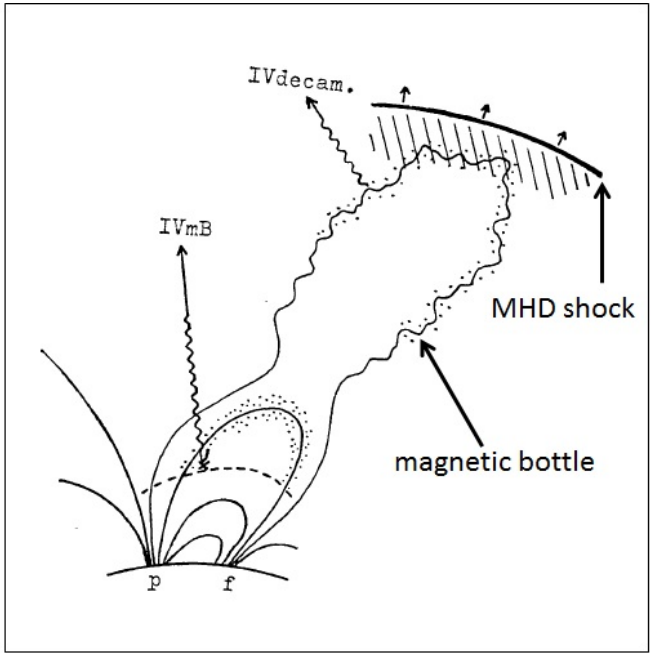

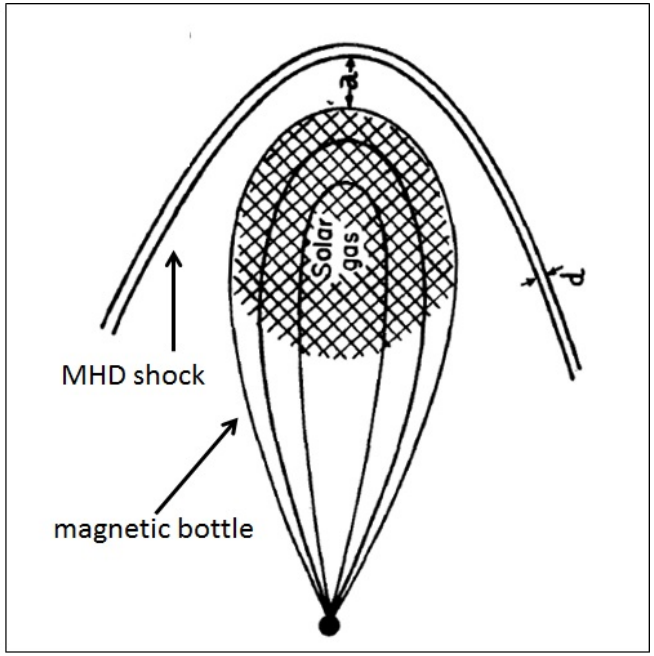

Fokker (1963)

solar

interplanetary

Gold 1962

CMEs Waiting to be Discovered…

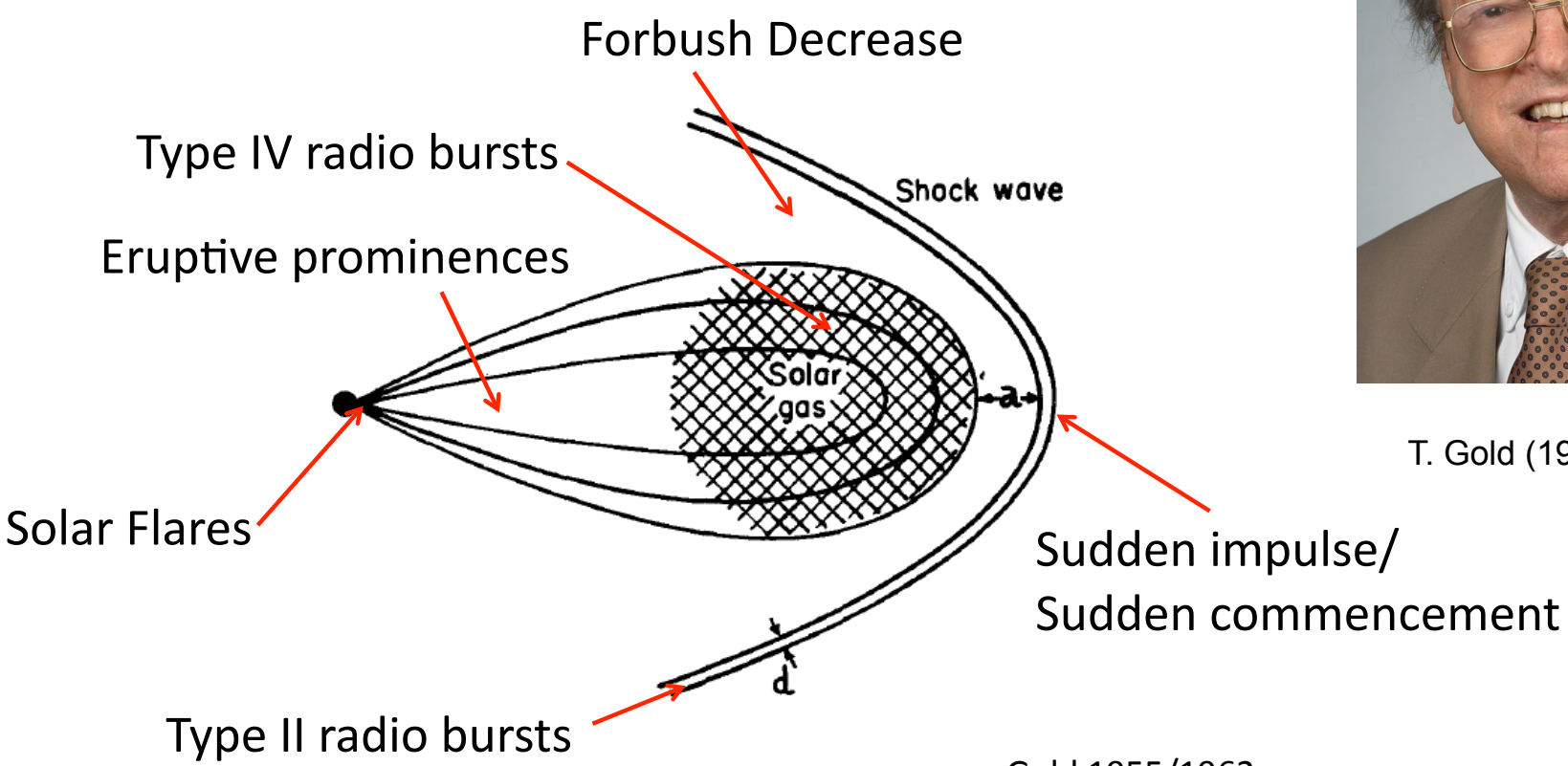

Gold 1955/1962

T. Gold (1920 – 2004)

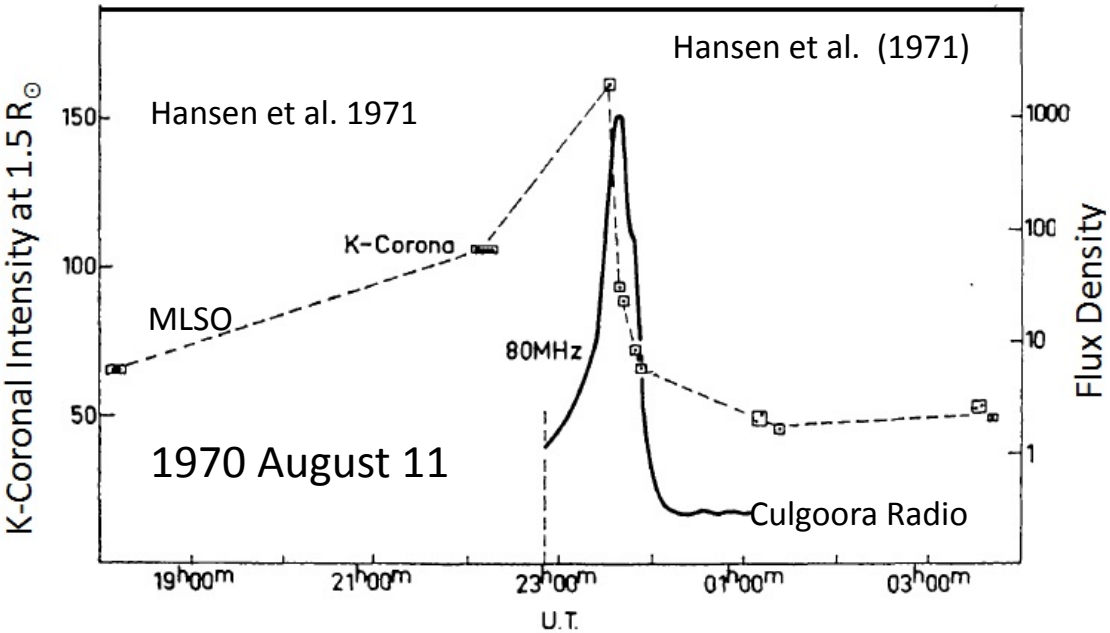
Hansen et al. (1971)
Hansen et al. 1971
K-Coronal Intensity at 1.5 R⊙
150
100
50
K-Corona
MLSO
80MHz
1970 August 11
Culgoora Radio
1000
100
10
1
Flux Density
19h00m
21h00m
23h00m
01h00m
03h00m
U.T.

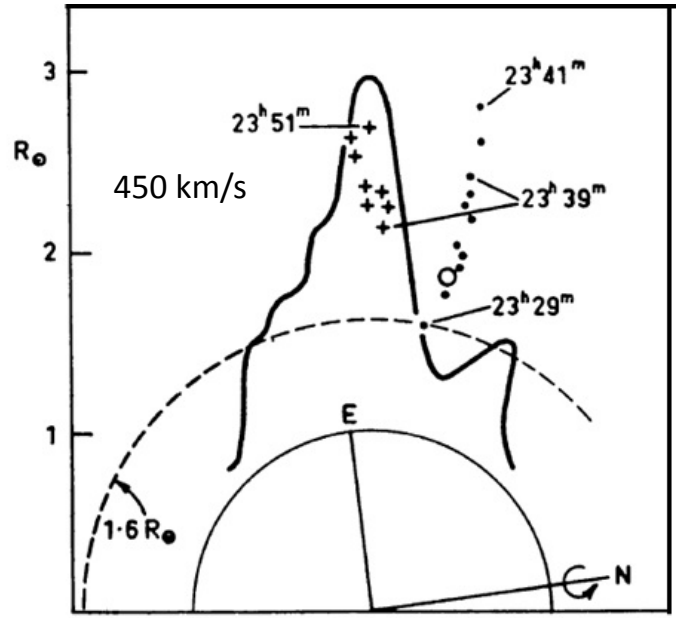
3
2
1
R⊙
450 km/s
23h41m
23h51m
23h39m
23h29m
E
1·6 R⊙
N

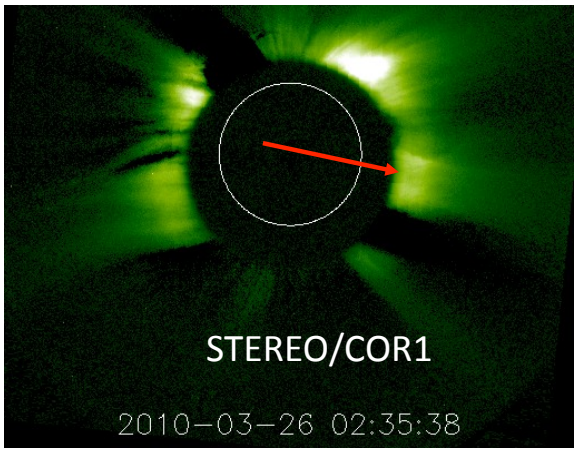
STEREO/COR1
2010-03-26 02:35:38

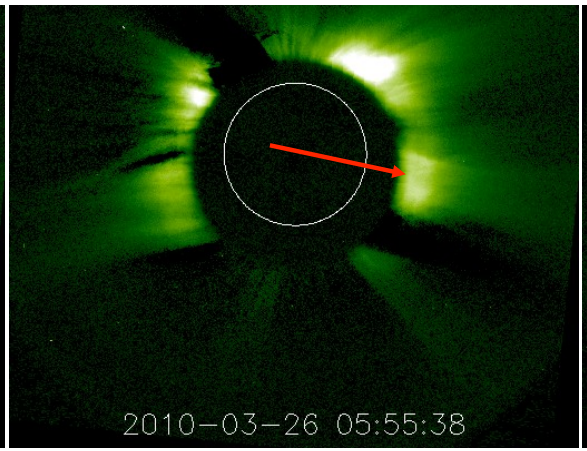
2010-03-26 05:55:38

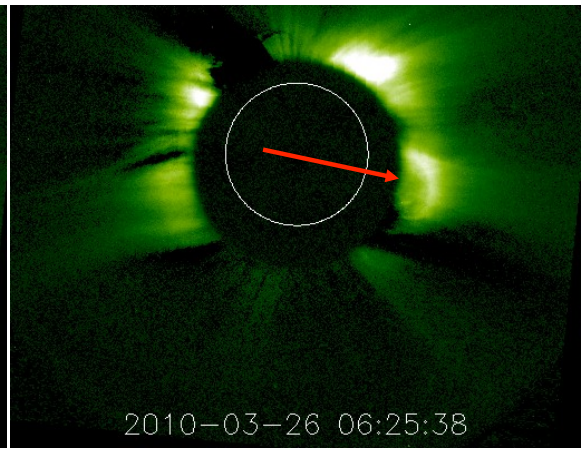
2010-03-26 06:25:38

The first white-light CME from OSO-7

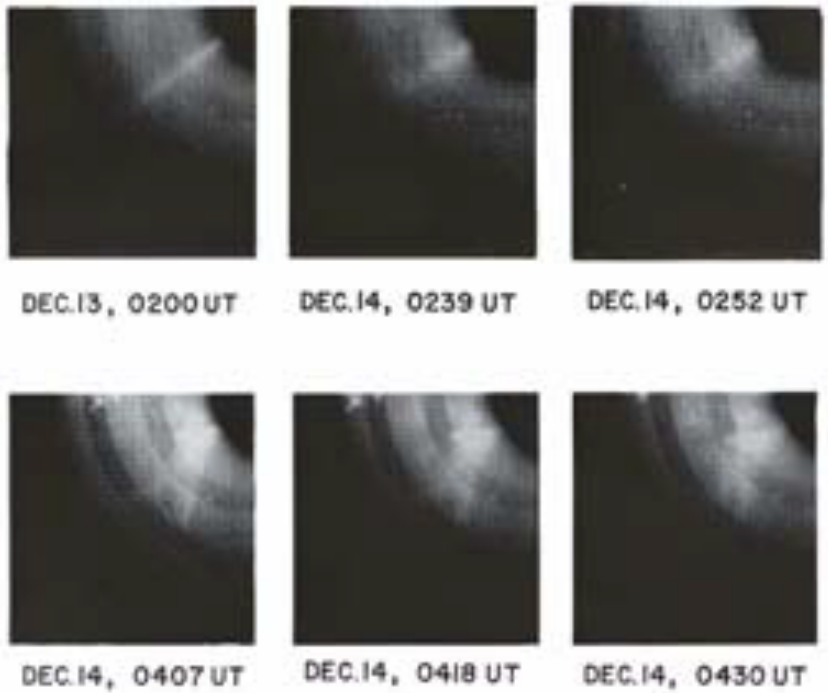

David Roberts, the electronics engineer noticed the change and thought his camera was failing…

Tousey, 1973
reported on the 13-14 Dec 1971 coronal transient (1000 km/s)

Skylab
Solwind on P78-1
Coronagraph/Polarimeter on SMM
SOHO/LASCO ←
STEREO/SECCHI
MLSO Mark IV K -Coronameter

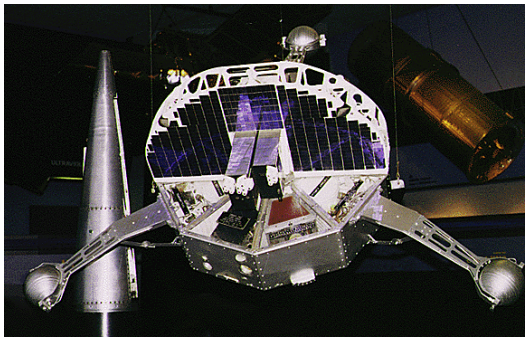

NASA's OSO-7

Kinematic Properties

- Based on height-time measurements of CMEs at the leading edge.
- The measurements refer to the sky plane, so they may be subject to projection effects
- Linear fit to the height-time data points gives average speed within the coronagraphic field of view
- Quadratic fits give acceleration

Basic Attributes of a CME:

Speed, Width & CPA

Base Difference: $F_n - F_o$
Running Difference: $F_n - F_{n-1}$
F_n, F_{n-1}, F_o are images at times t_n , t_{n-1} and t_o

CPA = Angle made by CME apex with Solar North

Width = PA2 – PA1

Speed = dh/dt
Acceleration = d^2h/dt^2

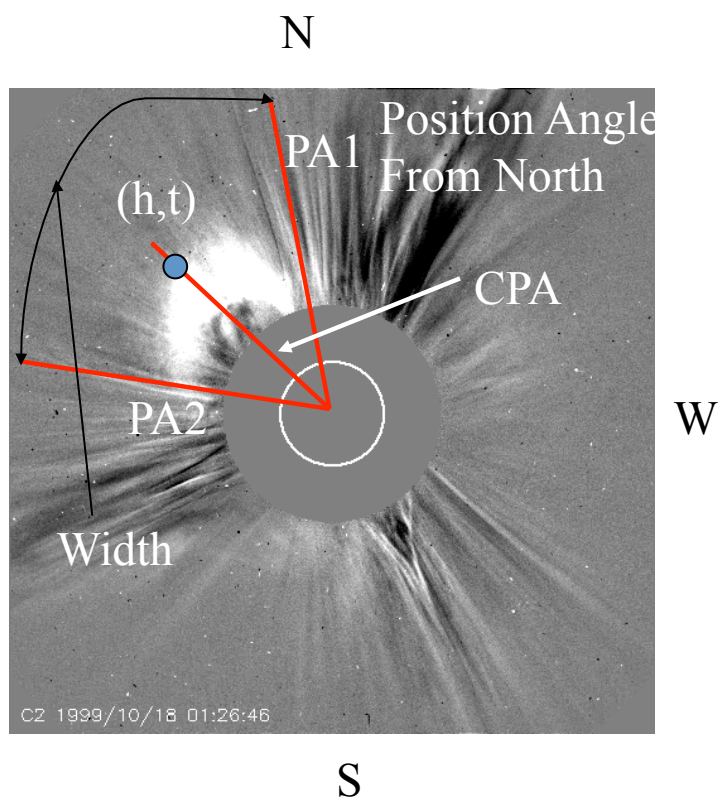

In the exercise session you will measure the speed and width of two CMEs

Kinematic Properties: Speed & Width

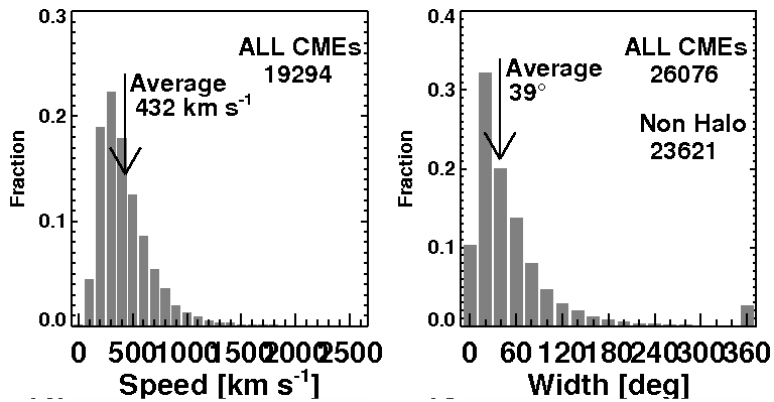

Acceleration in LASCO C2/C3 FOV

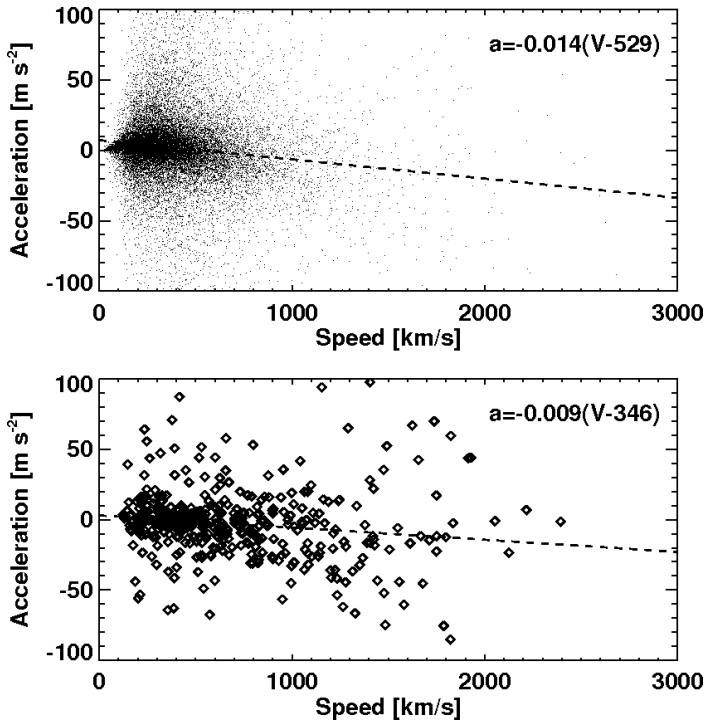

The measured acceleration is a combination of accelerations due to the propelling force, gravity, and aerodynamic drag.

$a = a_p - a_g - a_d$

In the SOHO coronagraph, the measurements are made beyond 2.5 solar radii

By this distance a_p and a_g are weakened significantly

Therefore, the measured acceleration is mostly due to aerodynamic drag:
$a = - a_d$
and is referred to as residual acceleration

a_p can be 2-3 orders of magnitude higher than the residual acceleration.

Acceleration from LASCO C1, EIT

Gopalswamy & Thompson 2000

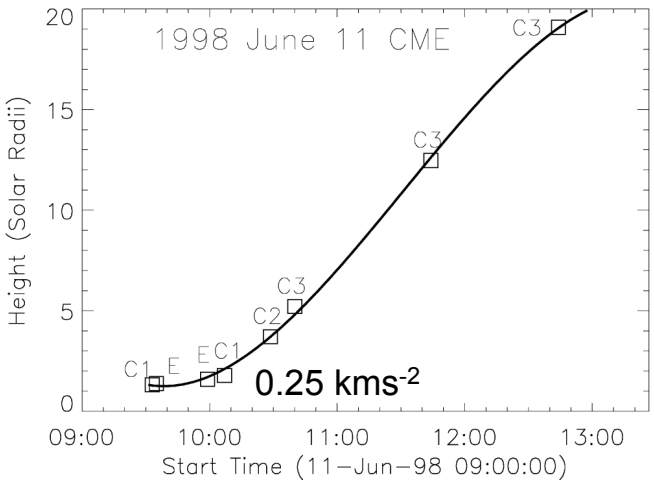

$h = 3.1 - 0.1t + 1.5\times10^{-3}t^2 - 3.4\times10^{-6}t^3$

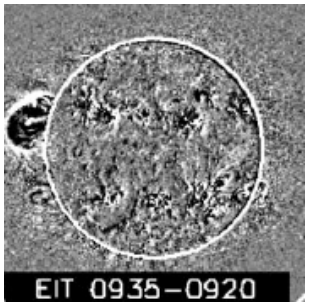

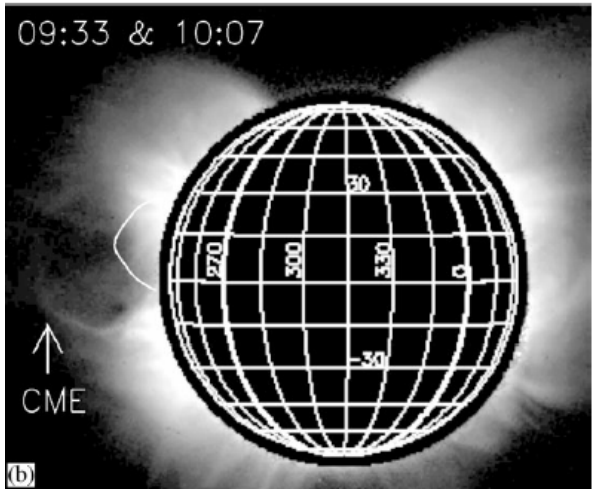

Before June 1998, SOHO had inner coronagraph that measured CMEs close to the surface. The height-time measurement can be fit to a 3rd order polynomial indicating early acceleration and later deceleration (a_p = 0.25 kms^{-2} and residual acceleration = -36 ms^{-2})

Initial Acceleration of CMEs

Bein et al., 2011

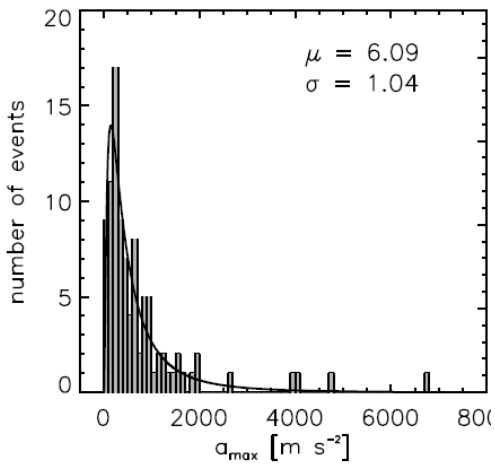

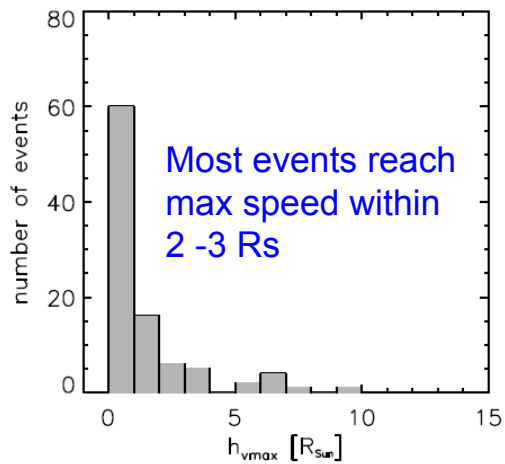

Gopalswamy et al. 2011

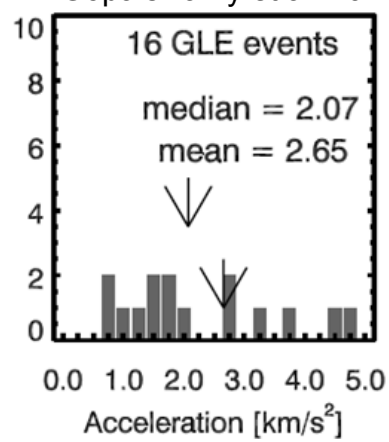

- STEREO/EUVI COR1
- 95 CMEs
- a_{max}: 0.02 to 6.8 kms^{-2}
- Height at Vmax: 1.17 to 11 Rs

- Ultrafast CMEs
- CME acceleration = Flare acceleration
- a: 0.5 to 7.5 kms^{-2}

Mass & Kinetic Energy

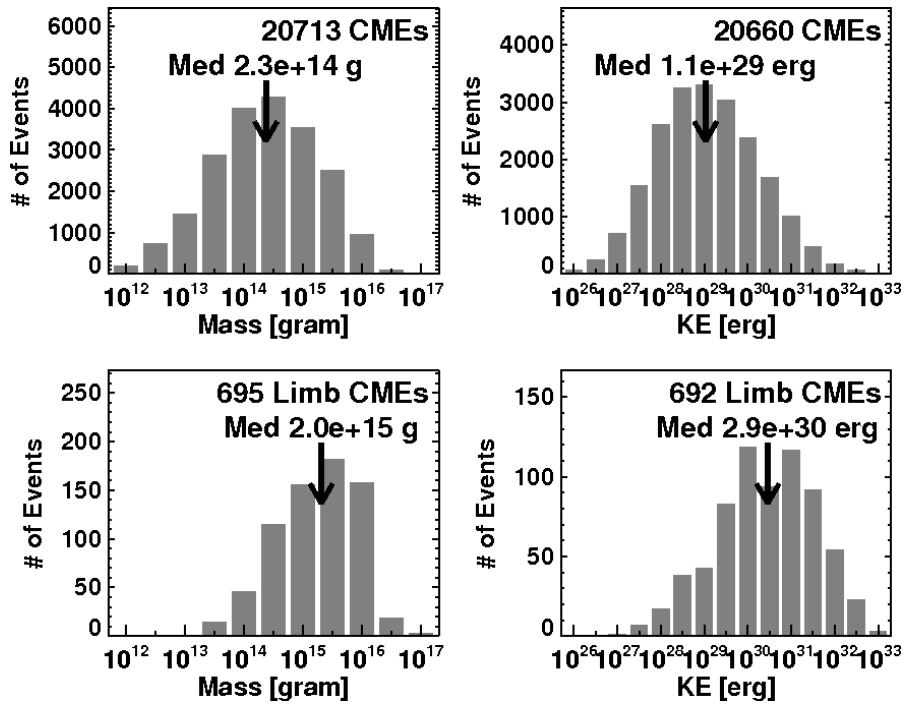

The CME mass can be determined from the excess brightness due to the CME and how many electrons are needed to produce this brightness. Once the mass and speed are known, the CME kinetic energy can be determined. Limb CMEs give the true distribution because they are not subject to projection effects

Solar Cycle Variation

- CMEs come from closed field regions on the Sun (e.g. Sunspot regions).
- CME speed and rate in phase with sunspot number (CME rate SSN are well correlated)
- There are exceptions especially during solar maximum phase
- Cycle 23 and 24 (when good CME observations are available) give details of this correlation

CME Rate & Speed (Rotation Averaged)

#CMEs per year ~10^3

Mass per CME ~4×10^{14} g

Mass loss due to CMEs
~4×10^{14} kg.yr^{-1}
= 2×10^{-16} Ms. yr^{-1}

Solar wind mass loss:
~2×10^{-14} Ms. yr^{-1}

During solar maximum, CME mass loss up to 10% of solar wind flux

Daily Rate

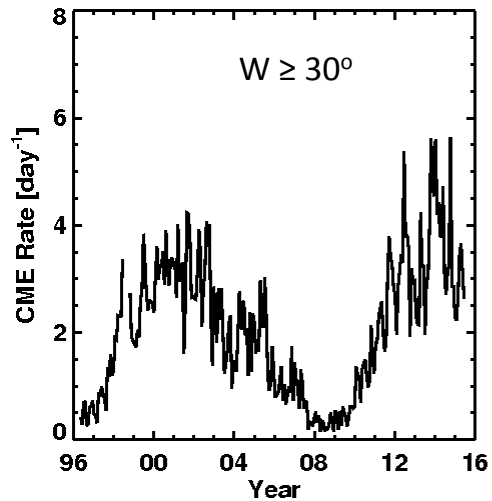

Average CME speed

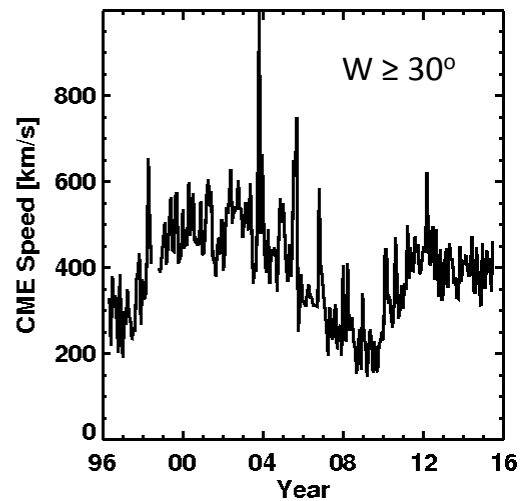

The rate is ~0.5 per day during the solar minimum and exceed ~4 per day during solar maximum

The CME speed also varies with solar cycle: CMEs are generally faster during solar maxima

CME Rate Compared with Sunspot Number (SSN)

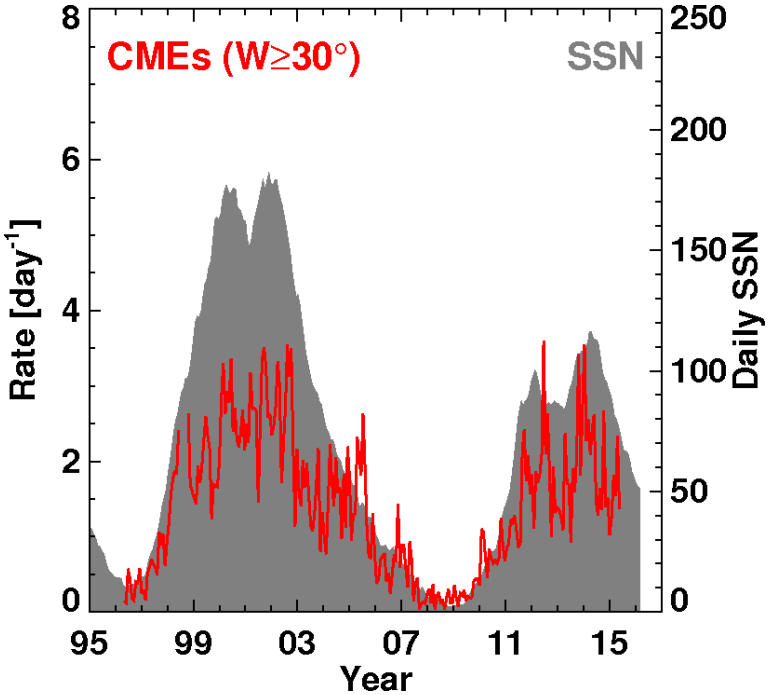

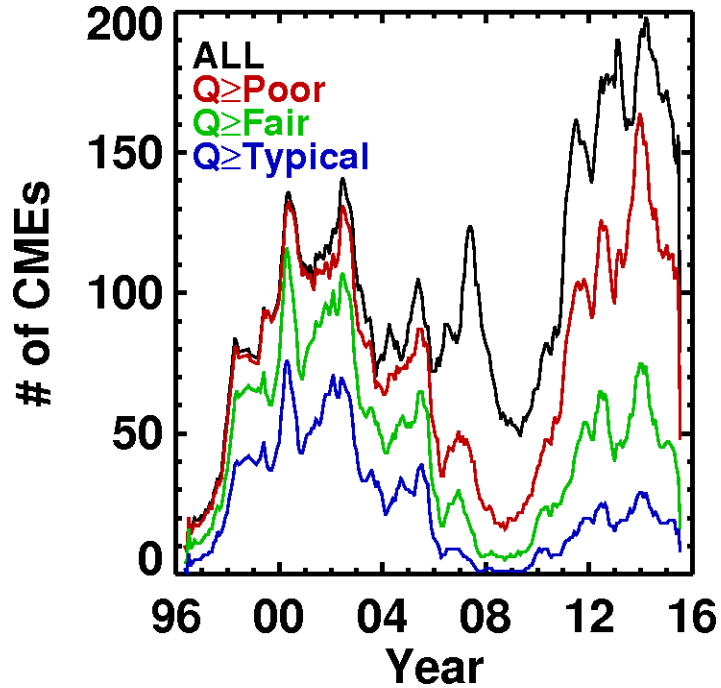

CME Rate well correlated with SSN

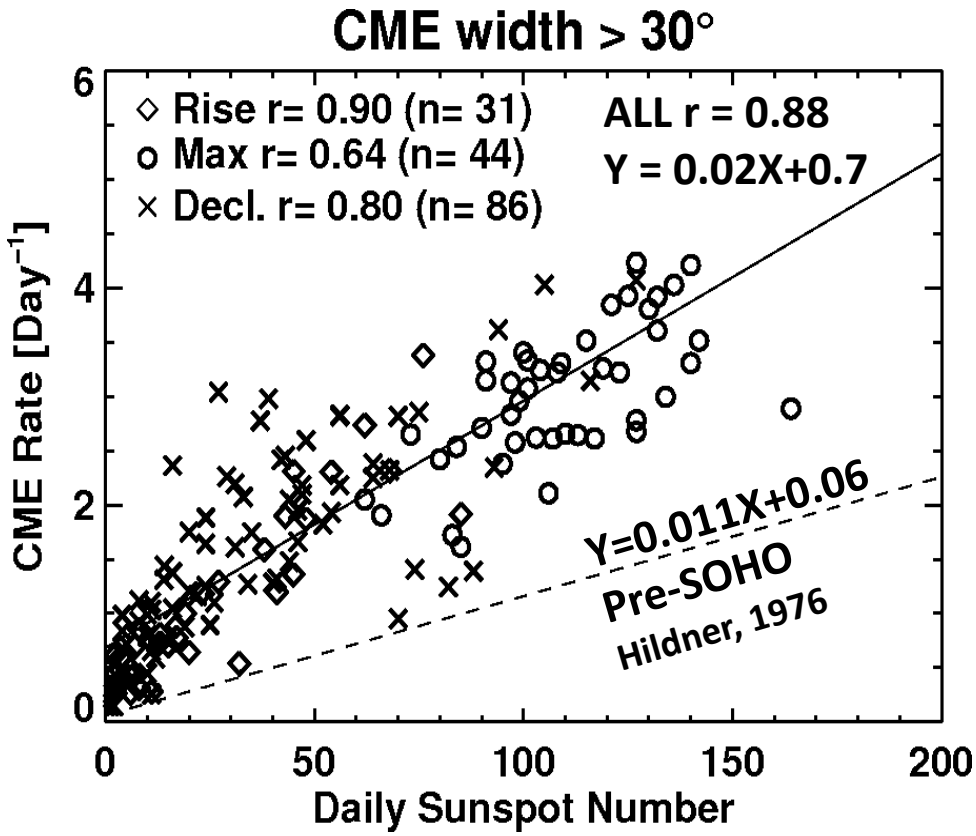

Weaker correlation during maximum phase: CMEs from outside sunspots – Polar crown filaments

The pre-SOHO (SMM, Solwind) data indicate a smaller slope because of the lower sensitivity and smaller field of view compared to the LASCO coronagraphs.

CME Rate vs. SSN

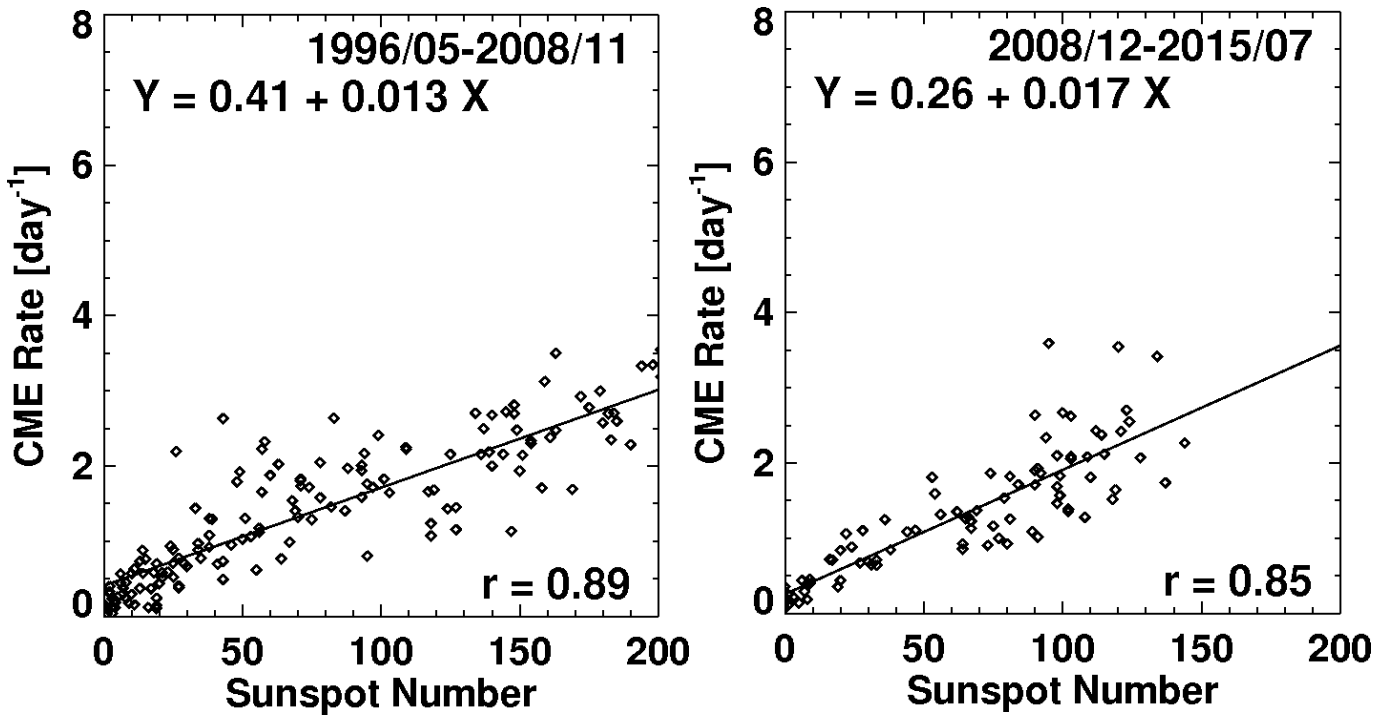

Halo CMEs

- CMEs that appear to surround the occulting disk in sky-plane projection
- No different from other CMEs, except that they must be faster and wider on the average to be visible outside the occulting disk
- Halos affect a large volume of the corona
- Most of the halos may be shock-driving
- Halos can be heading away or toward Earth. Those heading toward Earth are important for space weather

Halo CMEs

Halo CMEs, discovered in Solwind data (Howard et al. 1982), have been recognized in the SOHO era as an important subset relevant for space weather (Gopalswamy et al., 2010)

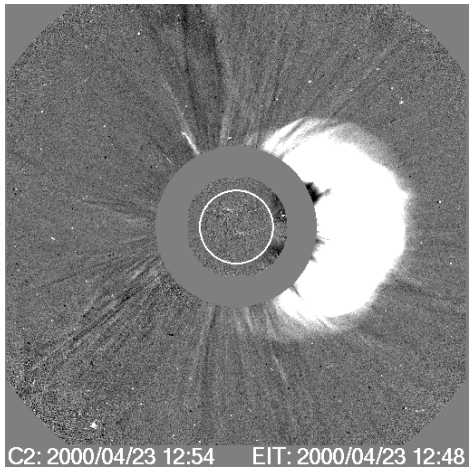

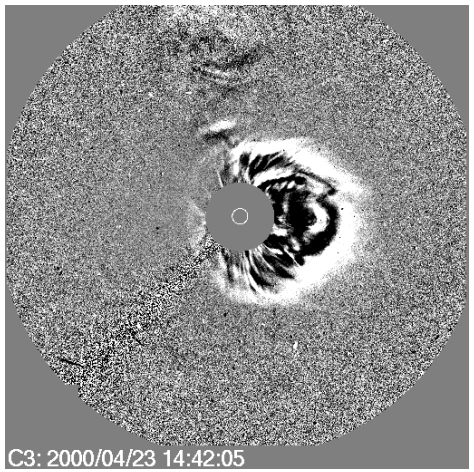

Partial halo becomes asymmetric halo

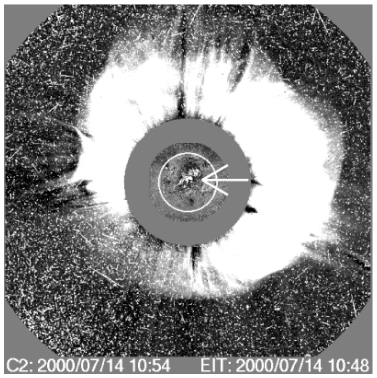

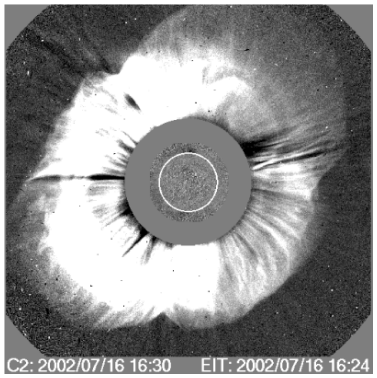

Front-side halo

back-side halo

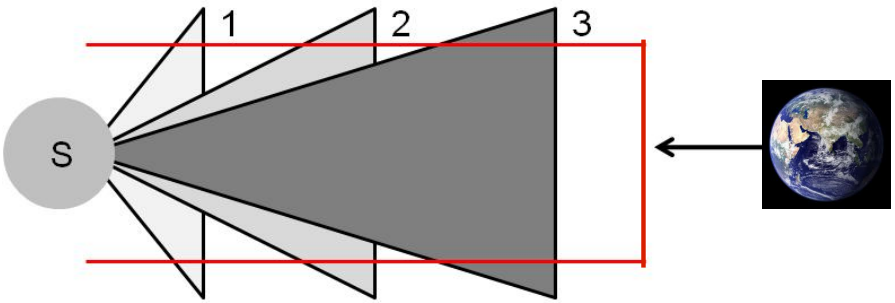

Halo CMEs are generally wide

The three cones 1, 2, 3 represent 3 CMEs

Frontside halos (earth-directed)

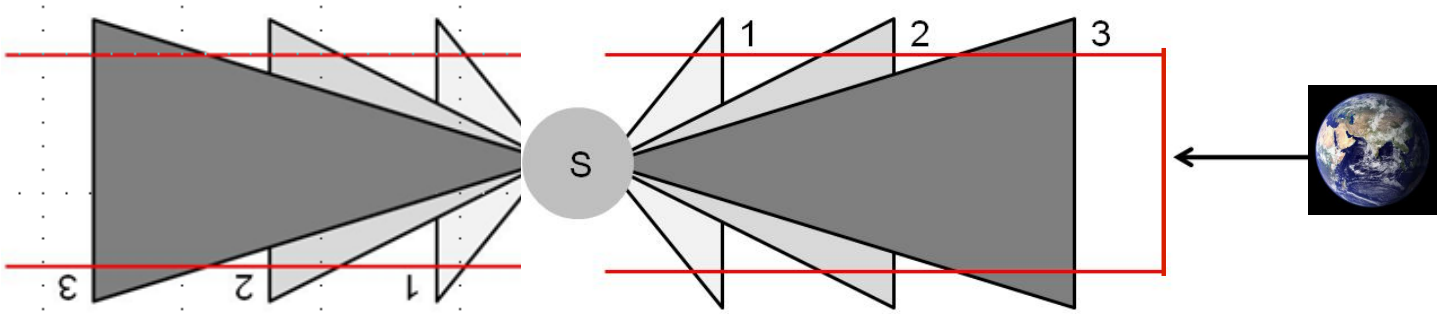

backside halos
(anti-earthward)

Portions outside the red lines appear as halos
1, 2, 3 represent three CMEs with decreasing widths. 1 will appear as halo immediately. 3 has to travel a long distance before appearing as halo. Some may never become a halo or fade out before becoming a halo.

Halo CME Properties

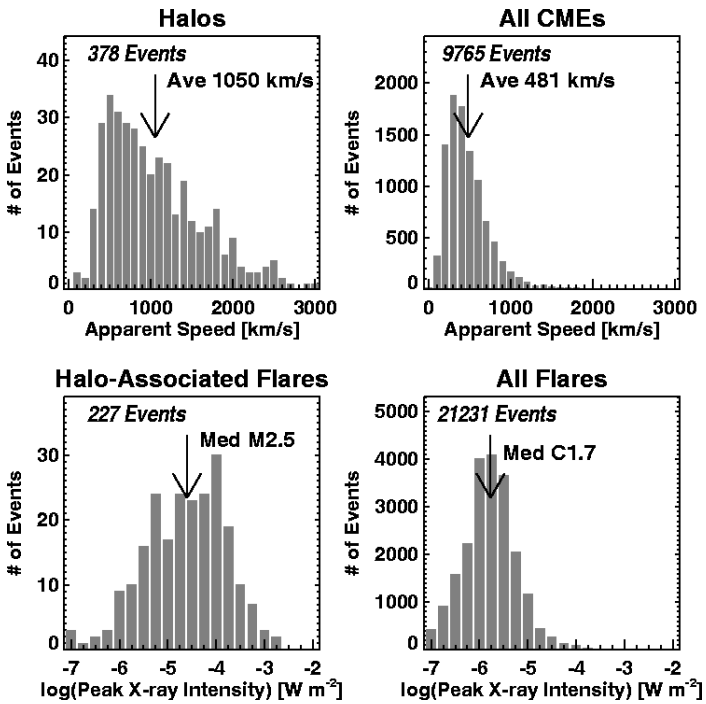

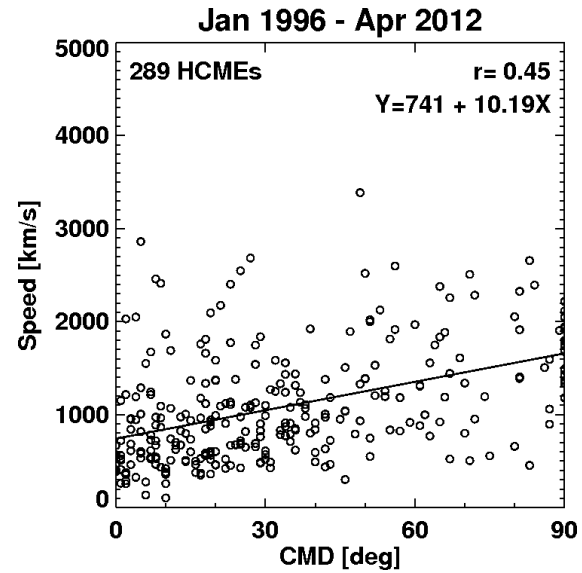

Only ~3.5% of all CMEs are halos

Halos are ~ 2 times faster than the average CME (halo CMEs are subject to large projection effects)

Flares associated with halo CMEs are larger

Higher kinetic energy: travel far into the interplanetary medium and impact Earth

Faster and Wider CMEs are More Energetic

Wider CMEs are faster

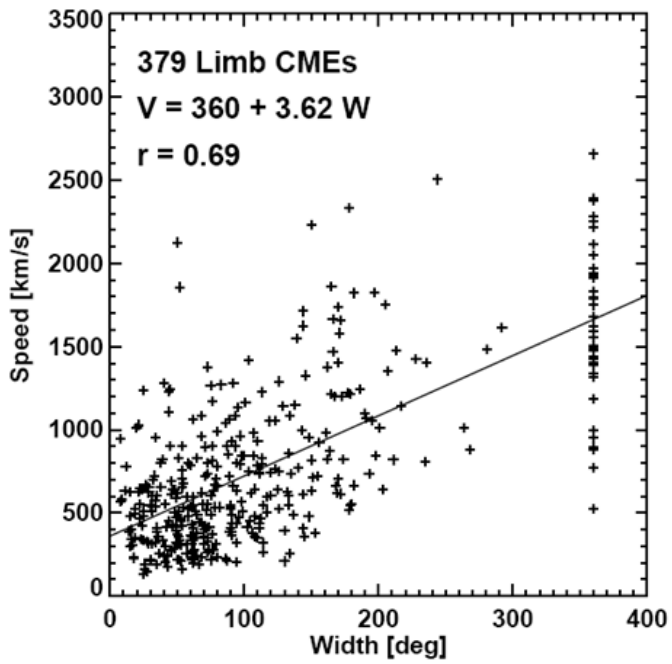

Wider CMEs are more massive

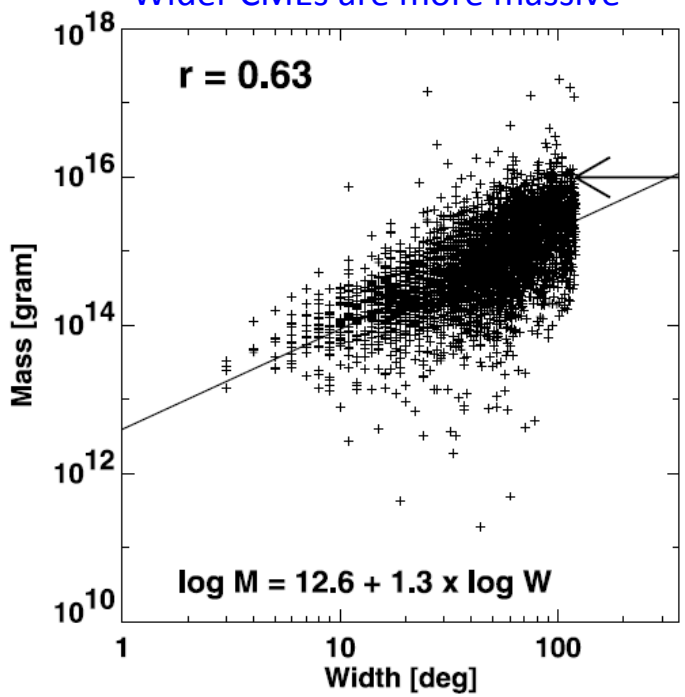

Halo CMEs are more energetic

Fraction of halos is a measure of the energy of a CME population

Halo Fraction of Some CME Populations

Table 1 Speed and width of the special populations of CMEs

	Halos	MCs	Non-MCs	Type IIs	Shocks	Storms	SEPs
Speed (km s^{-1})	1,089	782	955	1,194	966	1,007	1,557
% Halos	100	59	60	59	54	67	69
% Partial halos	–	88	90	81	90	91	88
Non-halo width (°)	–	55	84	83	90	89	48

Gopalswamy et al. 2010

Solar Source Regions

- CMEs originate from closed magnetic field regions (bipolar or multipolar configurations)
- Active regions
- Filament regions
- Loops connecting two active regions
- CME source regions are easily identified from the associated flare (close connection between CMEs and flares)

An Eruption Region

Photospheric Magnetogram

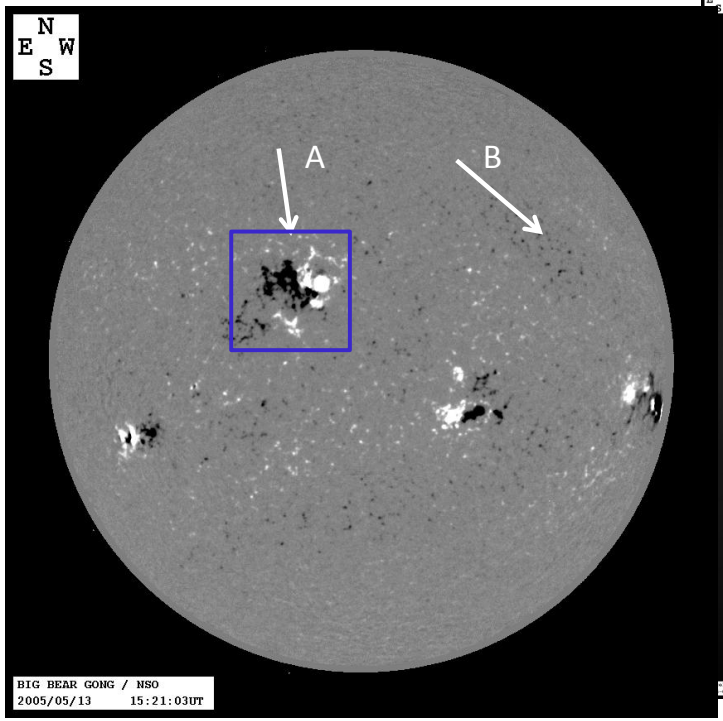

A: active region
B: Filament region (also bipolar, but no sunspots)

Chromosphere (H-alpha)

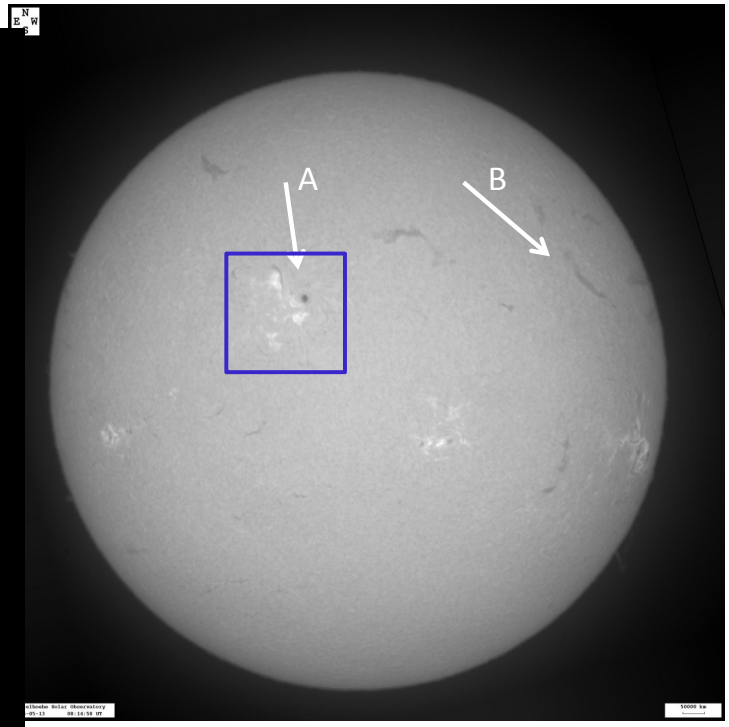

Both regions have filaments along the polarity inversion line

The Sunspot Region “A” Erupts

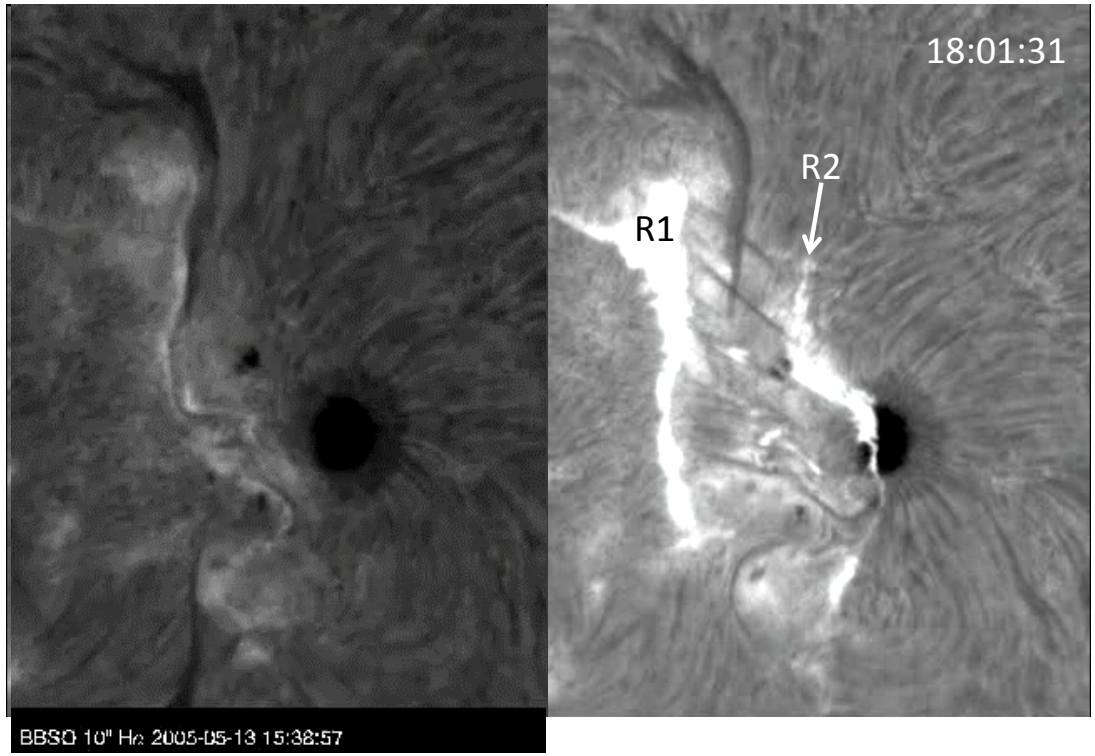

There is also wave going away from
the eruption region. Part of the filament disappears

Flare arcade

Filament eruption

Difference image (SOHO/EIT)

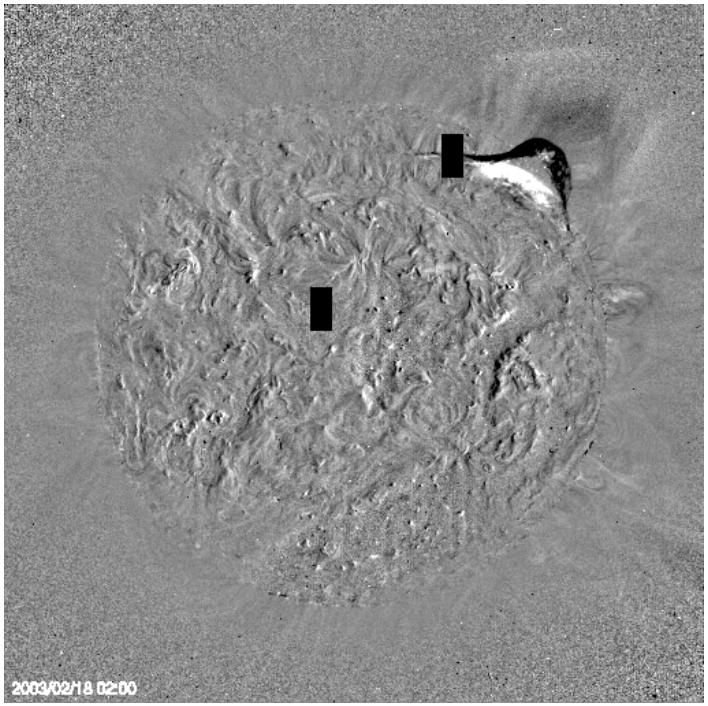

Flare from a non-sunspot region

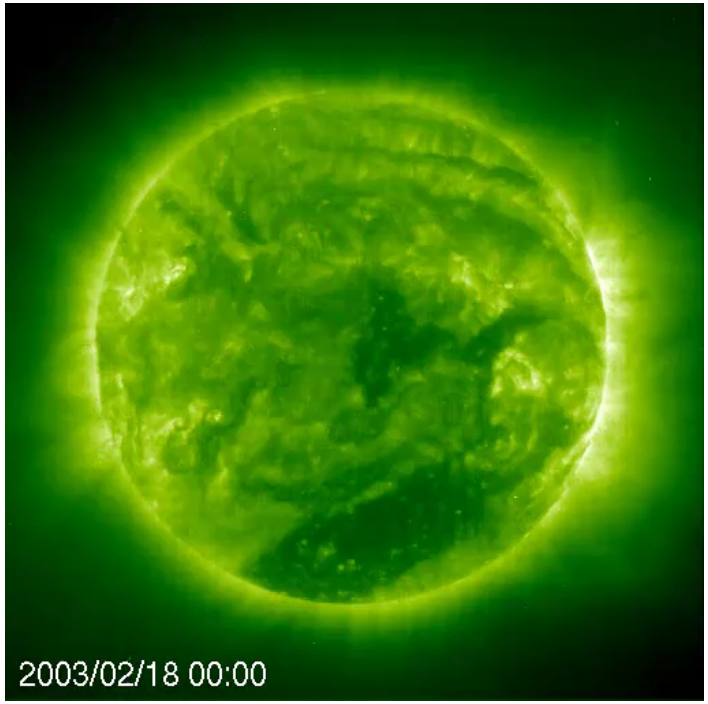

Note the CME overlying the filament in EUV

Filament Eruption in EUV

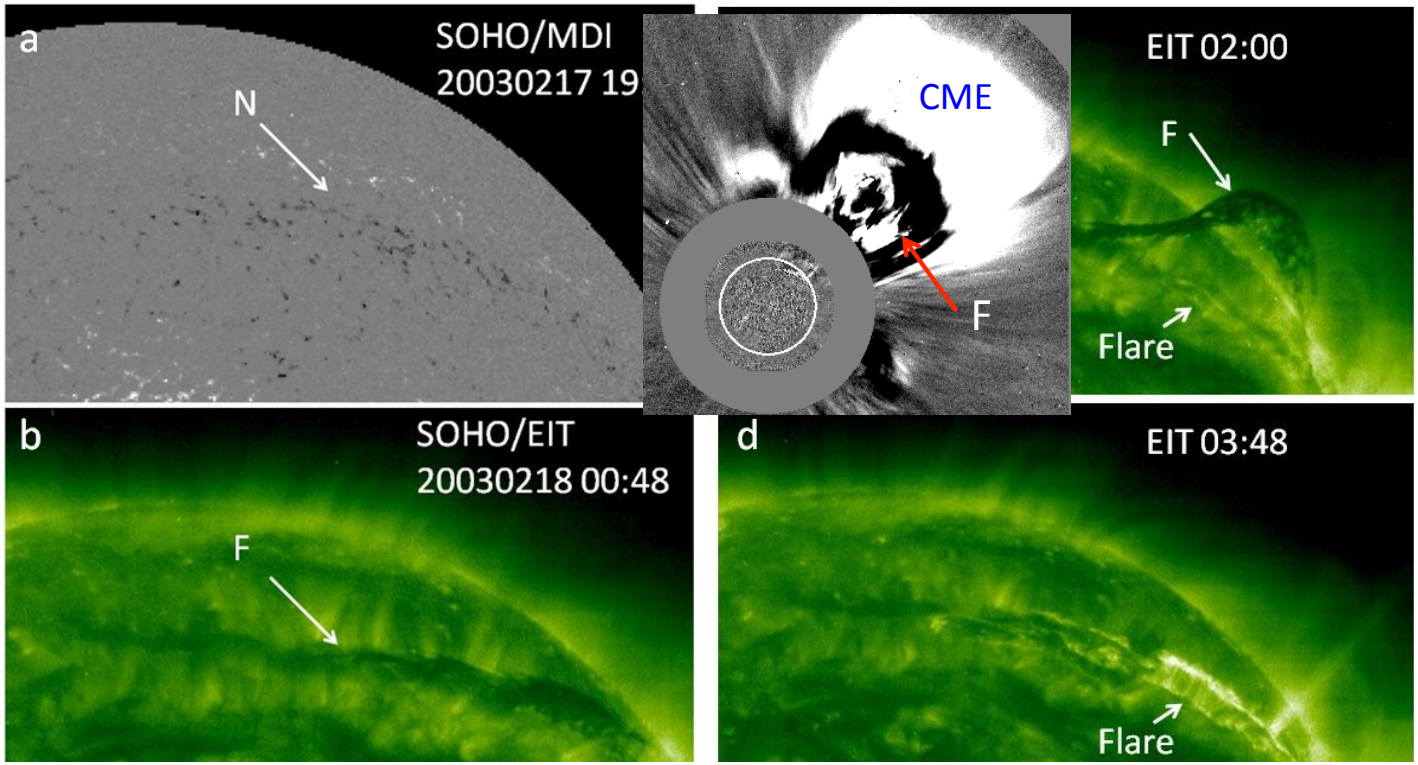

Filament (F) along neutral line (N). Flare loops under F; F becomes substructure of CMEs

Coronal Dimming and Eruption Geometry

PIL – polarity inversion line (between + and -)
D1, D2 – dimming regions in which the flux rope (FR) is rooted
PEL – post eruption loops
R1, R2 – flare ribbons with hard X-ray (HXR) and microwave (μ) source locations.

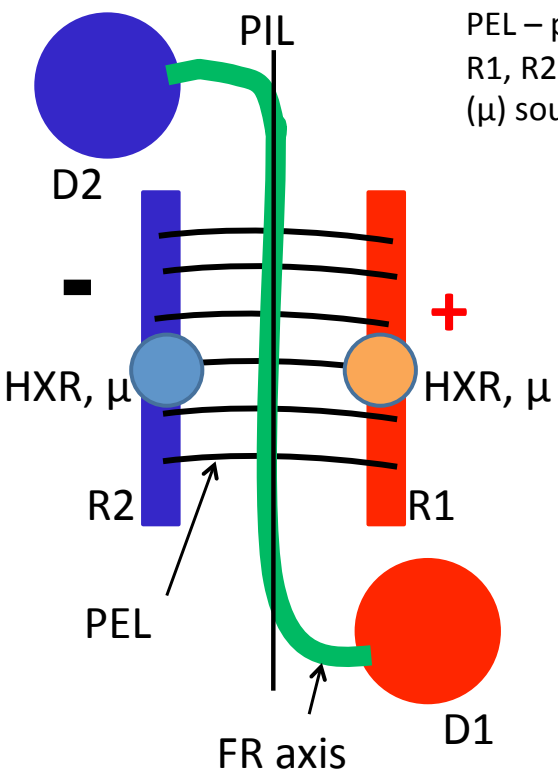

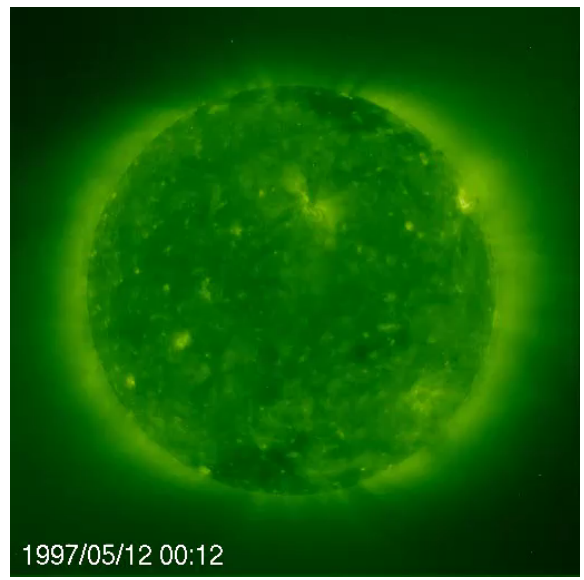

Dimming: Sites of flux rope legs?

Where does the energy come from?

Extrapolated field lines on TRACE coronal images

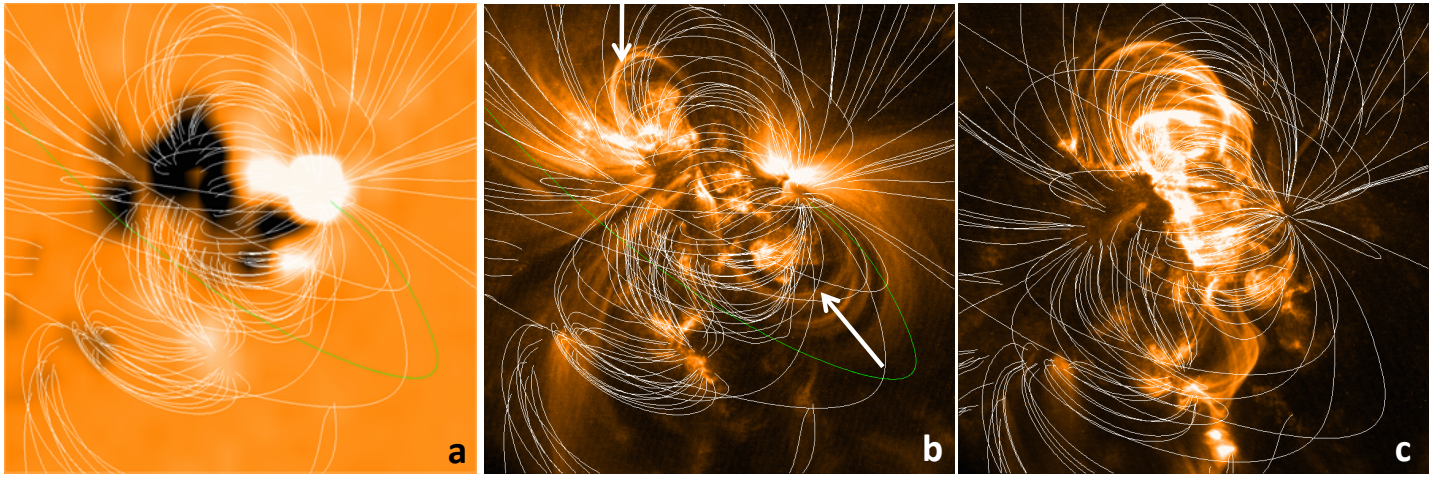

2005/05/13 14:56:00

Photospheric magnetogram with potential field extrapolation

2005/05/13 15:25:56

Actual coronal structure is "distorted" from potential field → free energy (FE)
Distortion due to current J.
Lorentz force JxB propels the CME

2005/05/13 21:26:36

Free energy went into the CME kinetic energy
Arcade is now potential (no more current J)

De Rosa & Schrijver

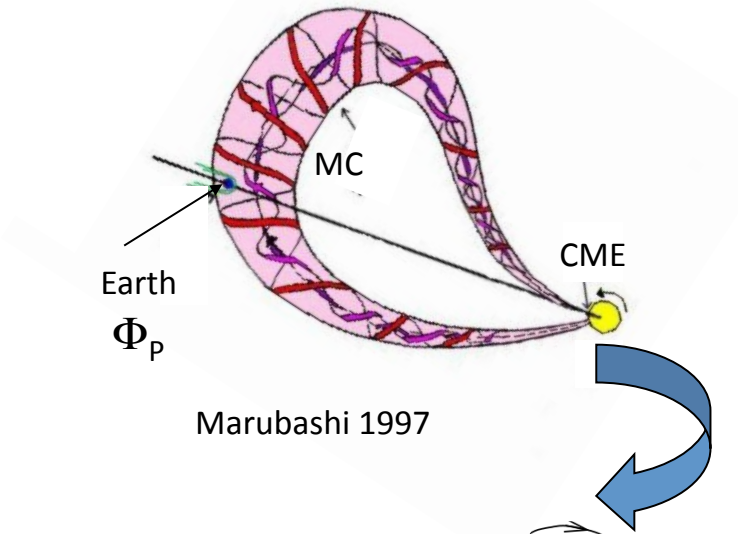

Marubashi 1997

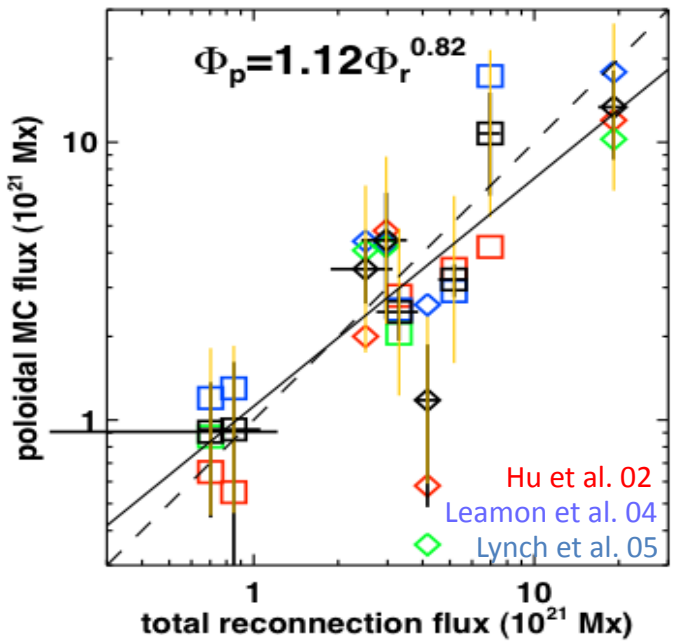

Qiu et al. 2007

Longcope & Beveridge 2007

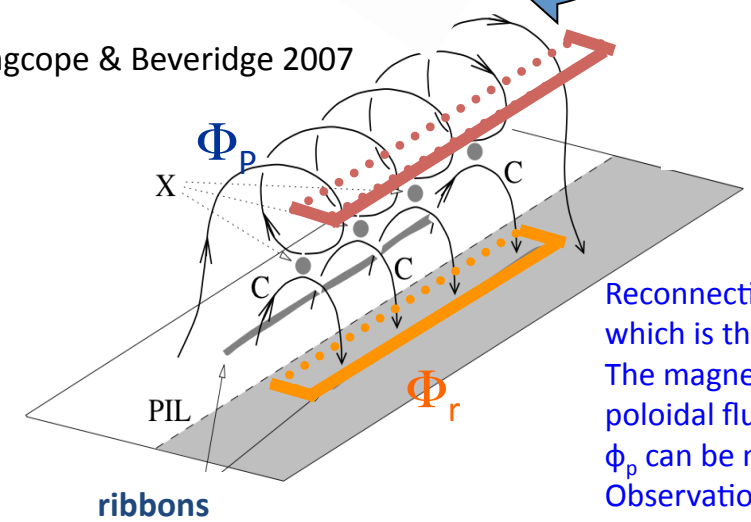

Reconnection forms the flare arcade and the flux rope, which is the fundamental magnetic structure of a CME. The magnetic flux in the flare ribbons (ϕ_r) and the poloidal flux of the flux rope (ϕ_p) must be the same. ϕ_p can be measured when the flux rope reaches earth. Observations support this flare CME connection

CMEs & Space Weather

10,000

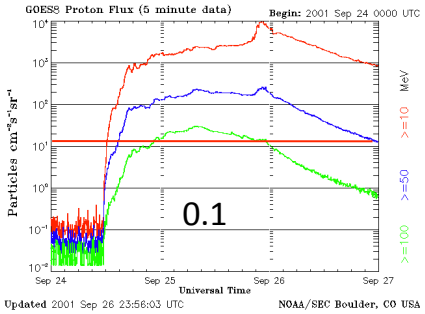

CMEs

Dst (nT)

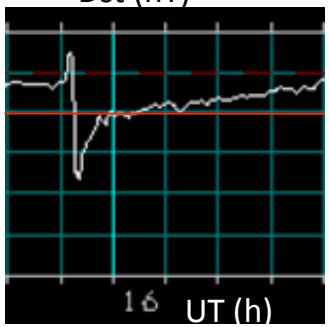

0
- 100
- 200
- 300
- 400
- 500

On the way and upon arrival

SEPs

Shock-driving Capability is Crucial

$V_{CME} - V_{SW} > V_{MS}$

Space systems
Airplanes
atmosphere

Magnetic storms

Upon arrival at Earth

Space systems
Magnetosphere
Ionosphere
Atmosphere
Ground

CME's Magnetic Structure Is Crucial (Bz <0)

The “Dark Side” of the Sun

SOHO image in white light

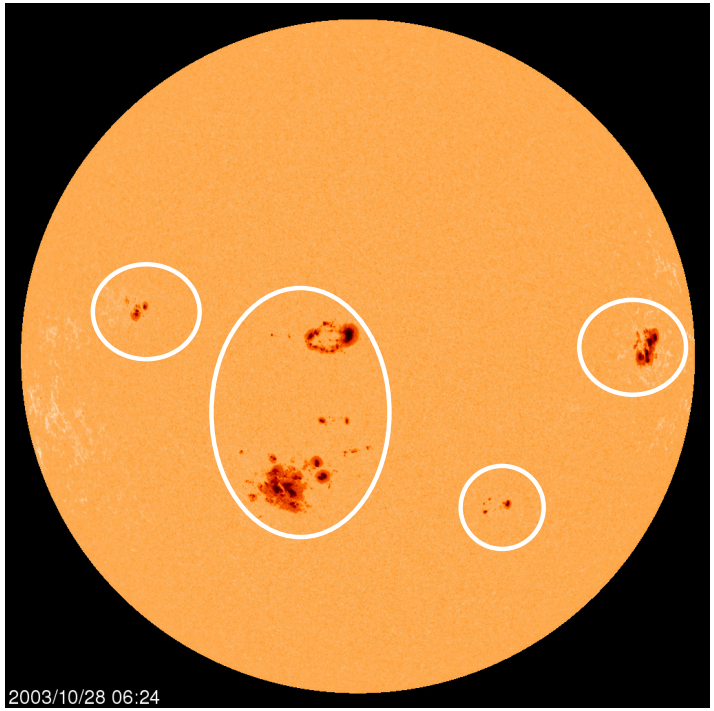

SOHO image in EUV

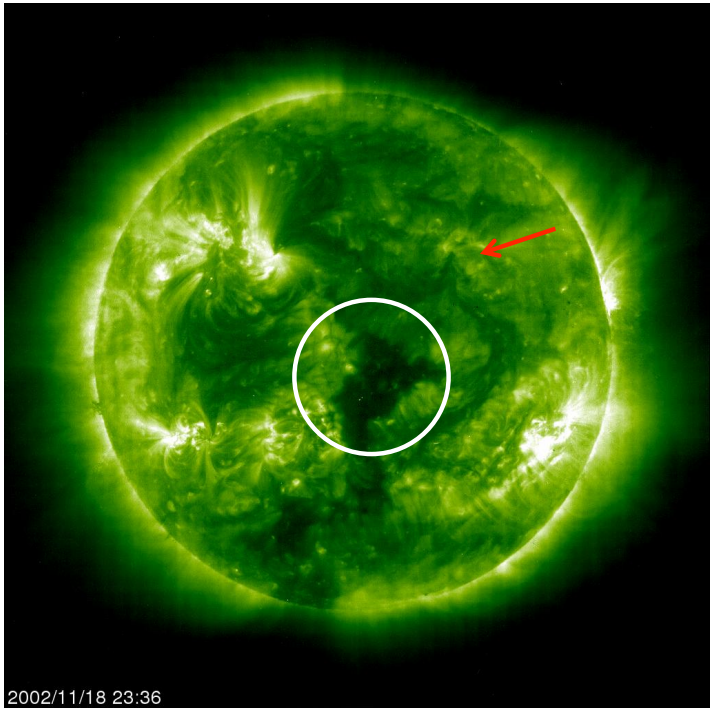

Sunspots

Coronal Hole

Filament

Two different Magnetic Topologies

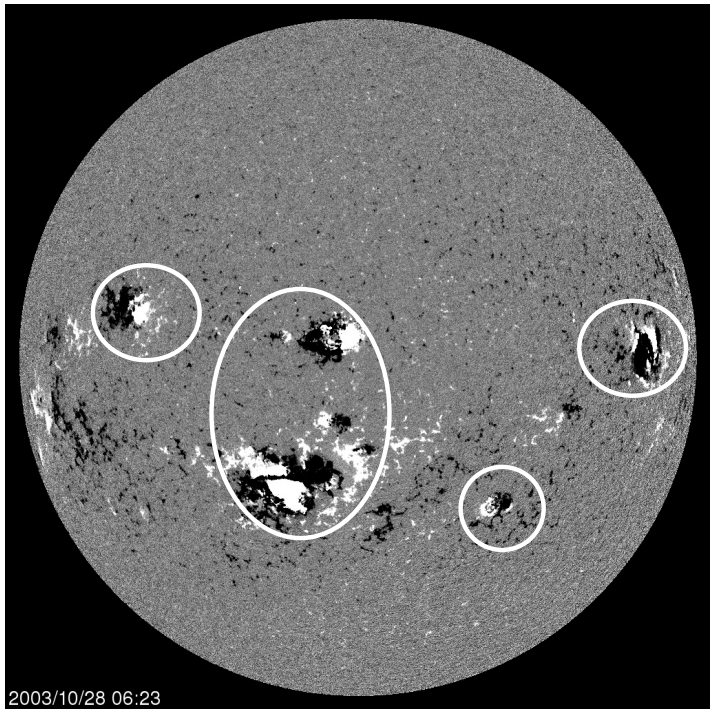

Closed and Open

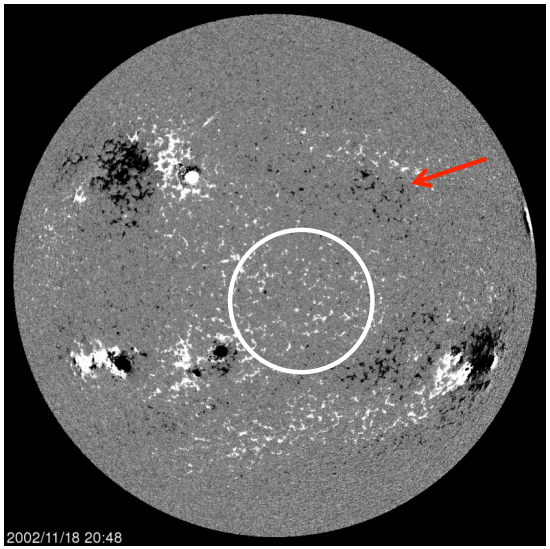

Active Region, Filament Region, and Coronal Hole

Sites of Particle Acceleration: Flare-CME Connection

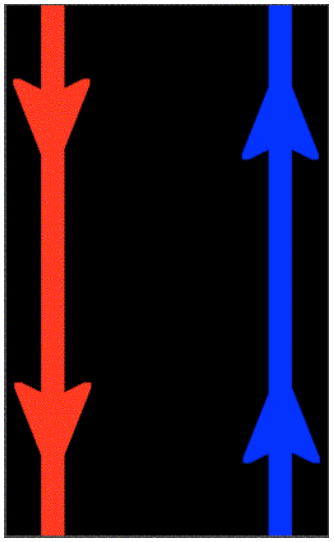

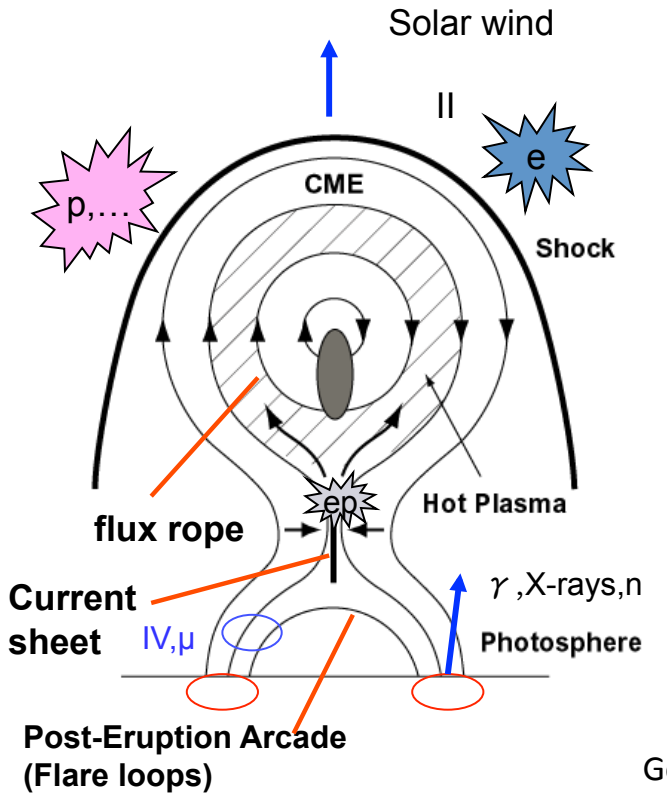

Gopalswamy 2006
adapted from Martens & Kuin 1989

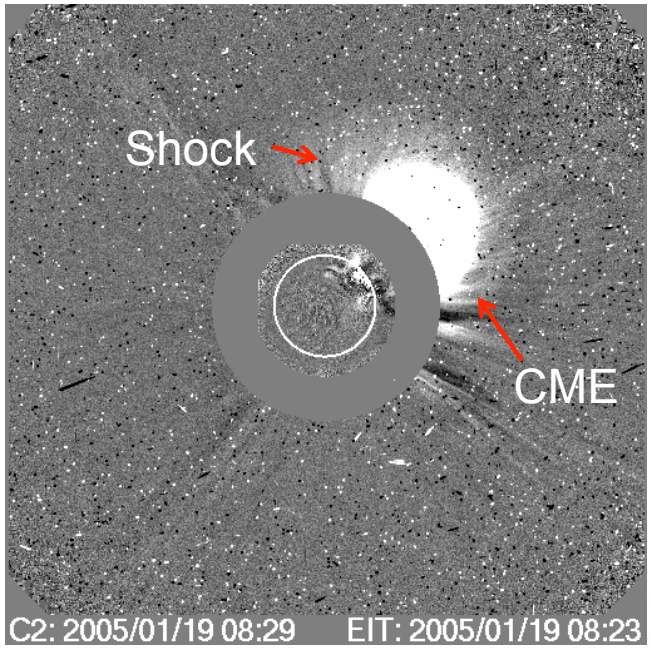

A fast CME driving a shock
(cdaw.gsfc.nasa.gov)

Solar Energetic Particles (SEPs) propagate along magnetic field lines in helical paths

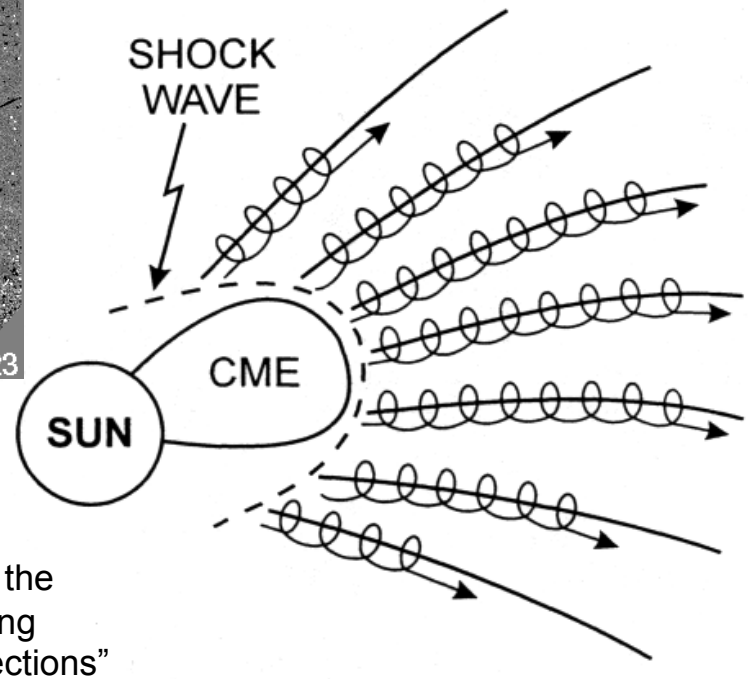

"energetic protons are accelerated in the shock front just ahead of the expanding loop structures observed as mass ejections"
Kahler, Hildner, & Van Hollebeke (1978)

CME, Flare, Shock, Type II, SEP – All Closely Related

IP shocks detected in situ by Spacecraft such as Wind, ACE and SOHO

shock at 1 AU

Shocks accelerate electrons and ions

Type III bursts are due to electrons from flares

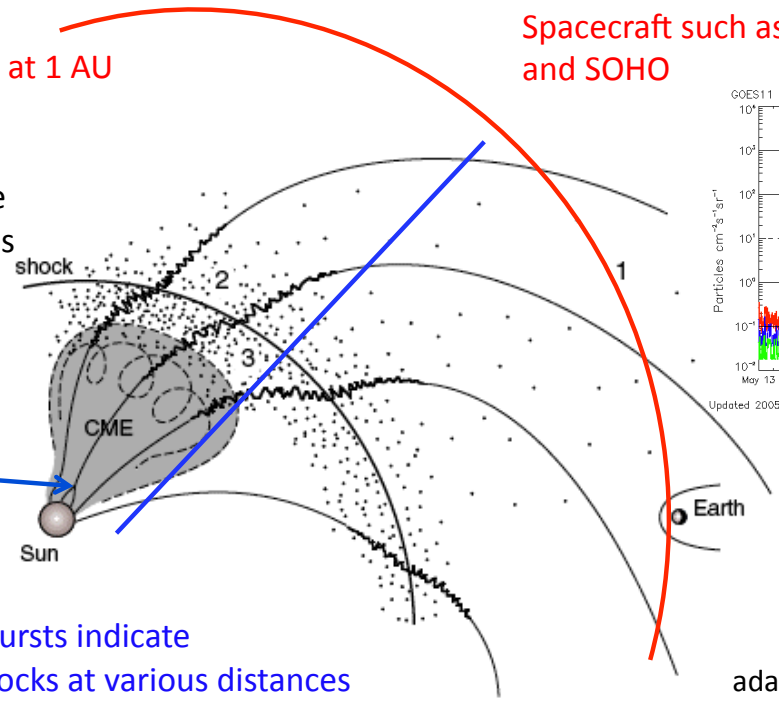

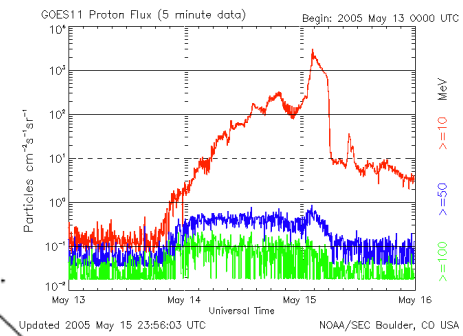

Type II Radio Bursts indicate CME-driven shocks at various distances from the Sun (emitted by accelerated electrons)

adapted from Lee 1997

Shocks studied using type II bursts, CMEs, and in-situ plasmag observations

SEP Producing CMEs

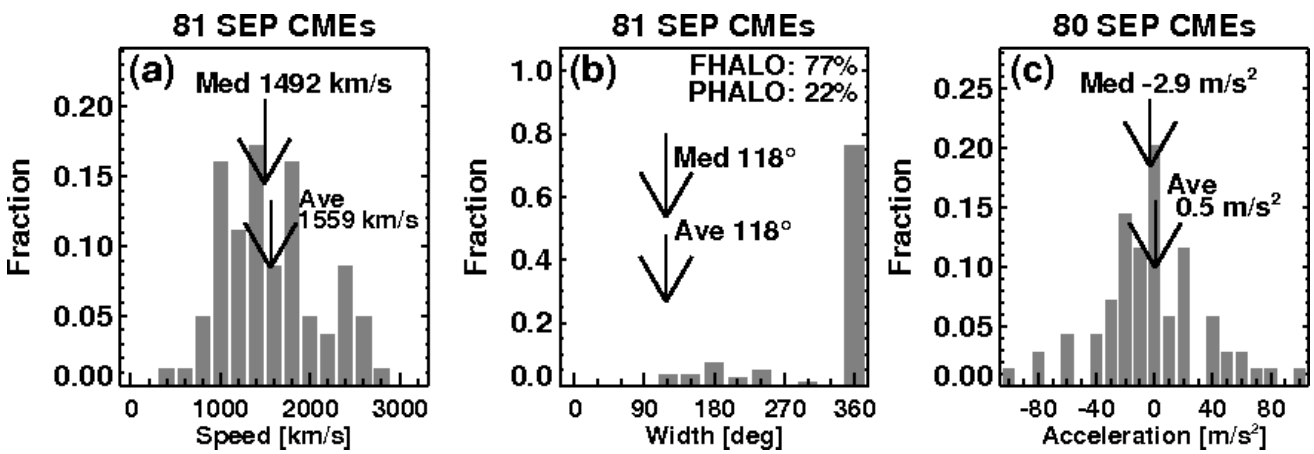

The CMEs are very fast
Almost all CMEs are halos or partial halos
Halo CMEs are generally wide

SEP-producing CME Sources

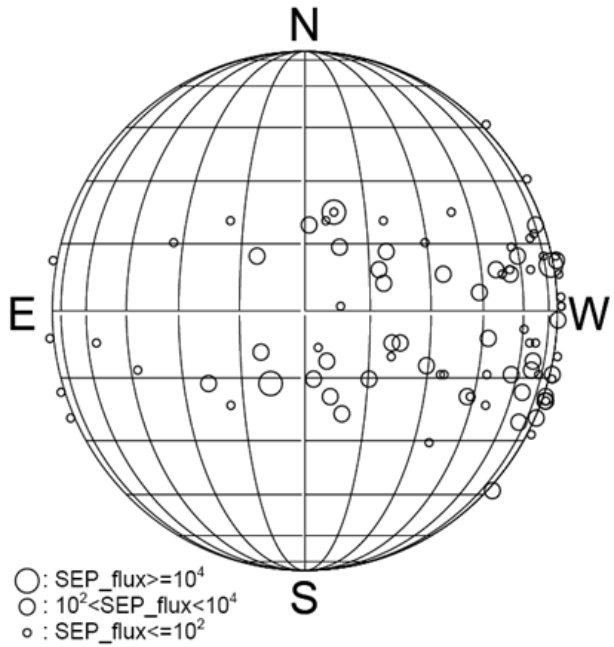

CMEs need to drive shocks
Source region needs to be magnetically connected to Earth

Galactic Cannibalism

CME Cannibalism

Gopalswamy et al. 2001

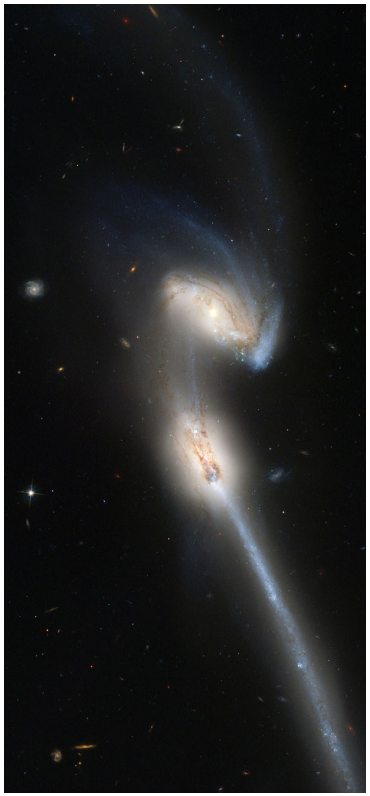

Hubble

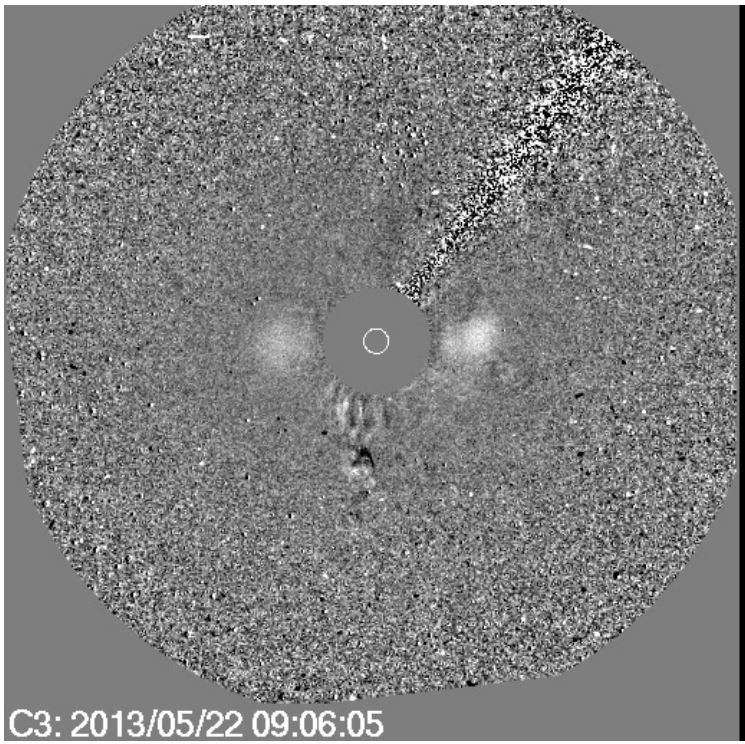

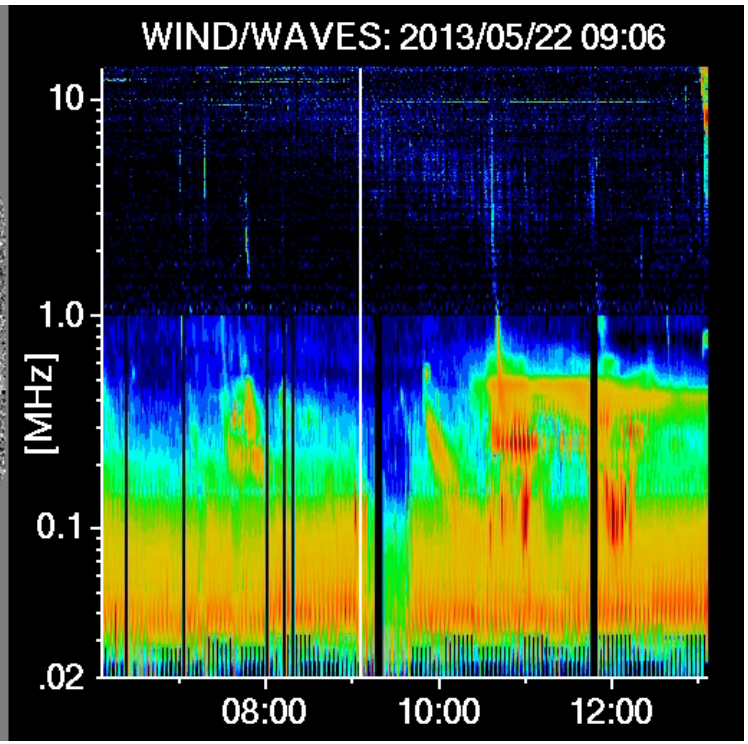

Radio direction finding points the radio source to the interaction region

SEP association higher when type II occurs at metric and longer wavelengths

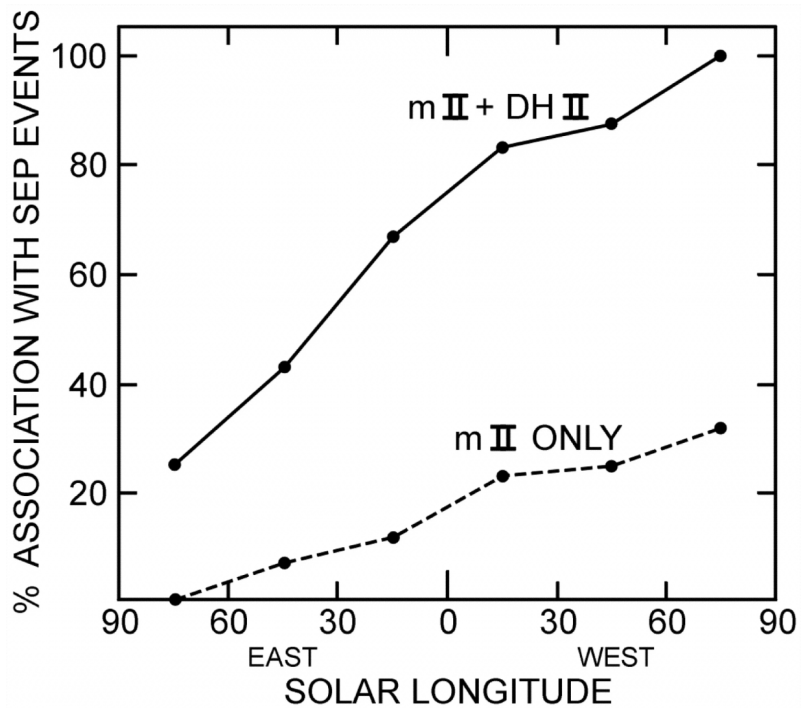

What Fraction of Radio-loud CMEs Produce SEPs?

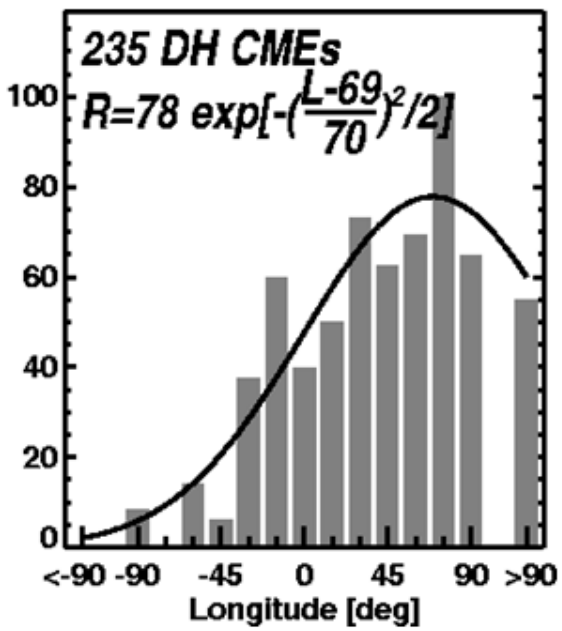

Sources of CMEs associated with DH type II bursts

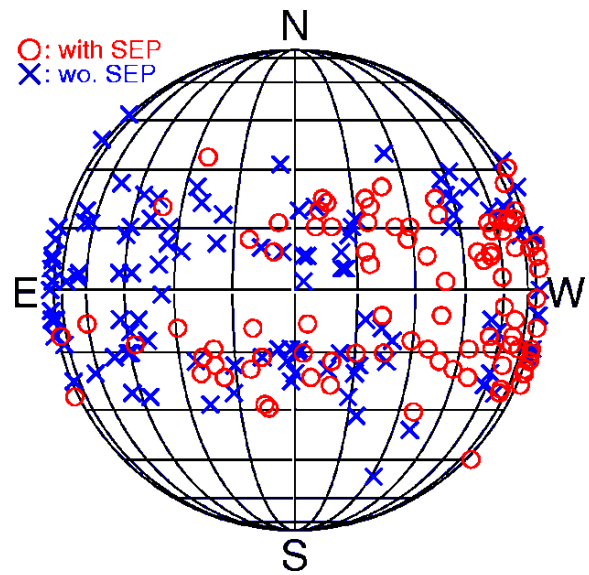

Answer: About 50% because magnetic connectivity needed for SEPs, not for EM radiation

Physical Relation Among Shock-related Phenomena

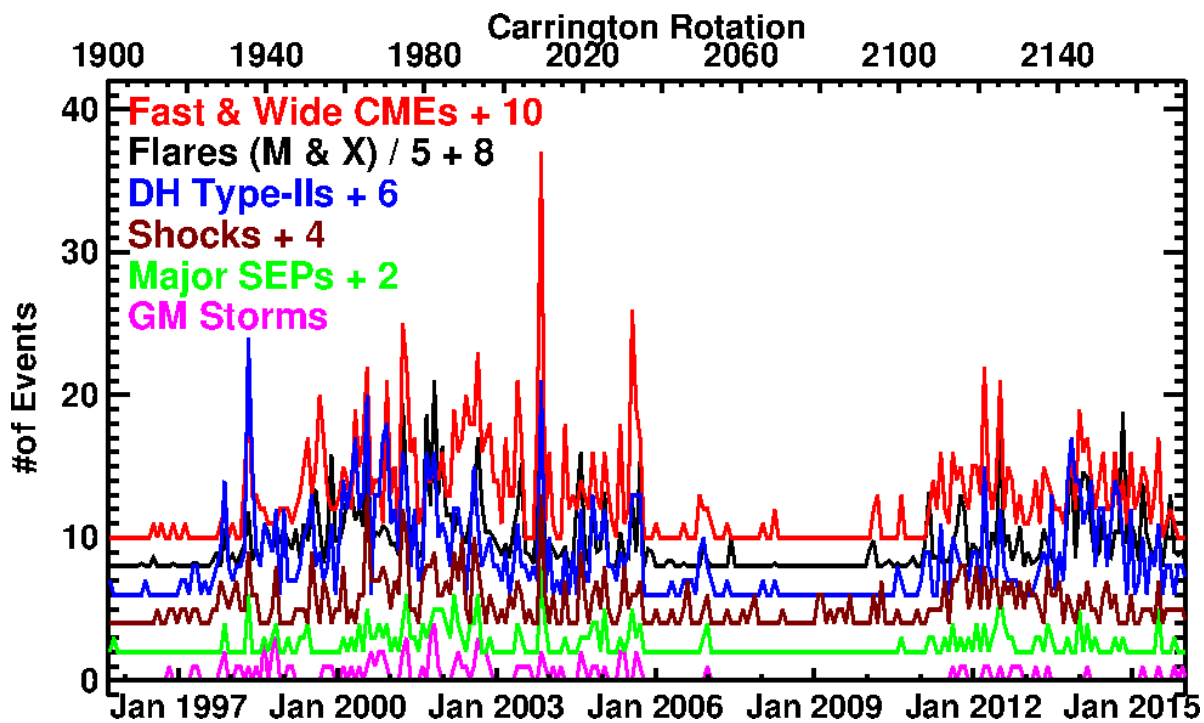

Height of Shock Formation Large for FE SEP Events

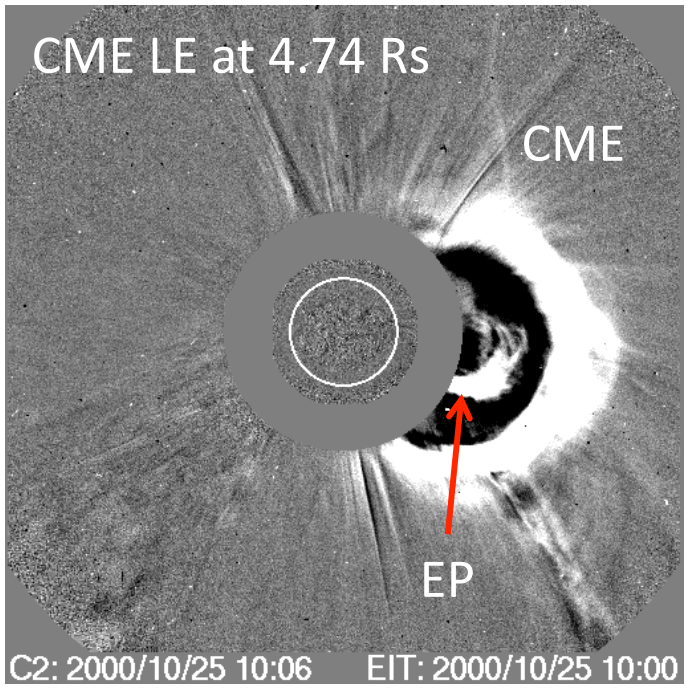

No Metric type II; IP starts at 10 MHz
at 09:26 UT CME at 3.39 Rs

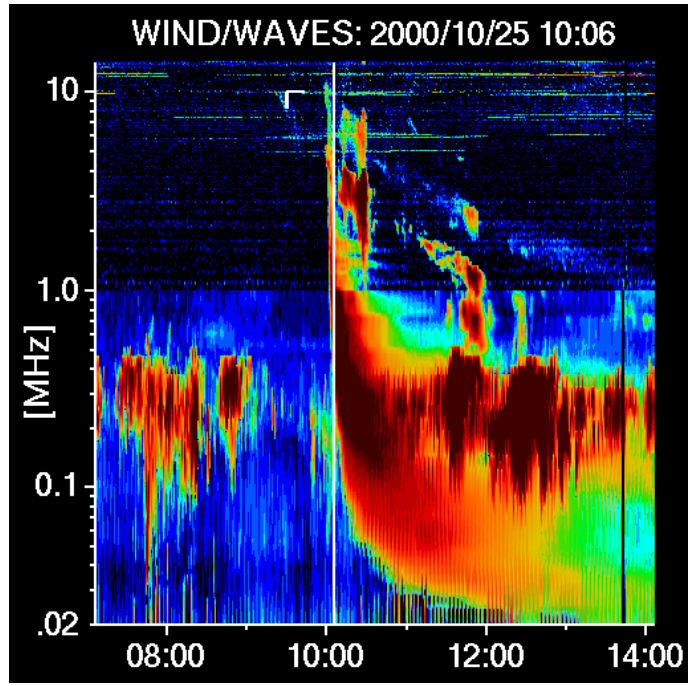

Height of Shock Formation Small for GLEs

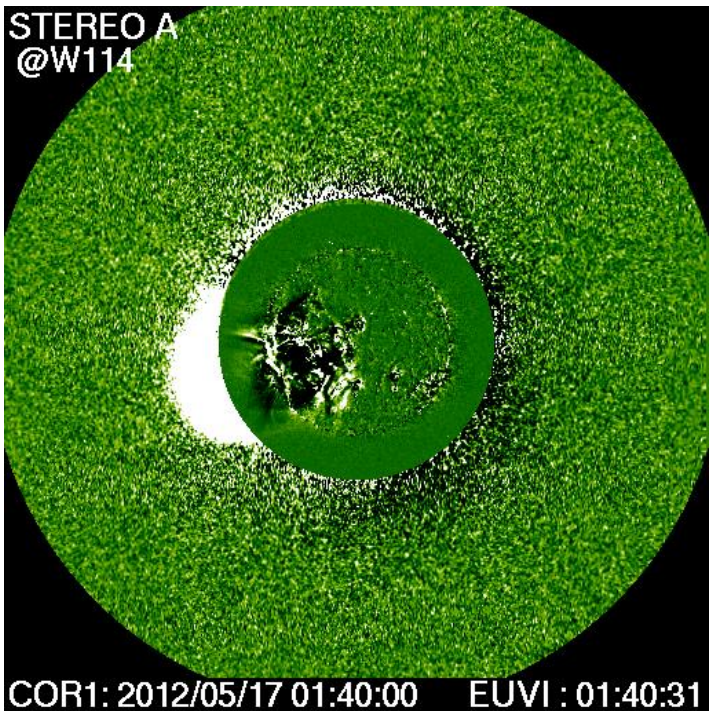

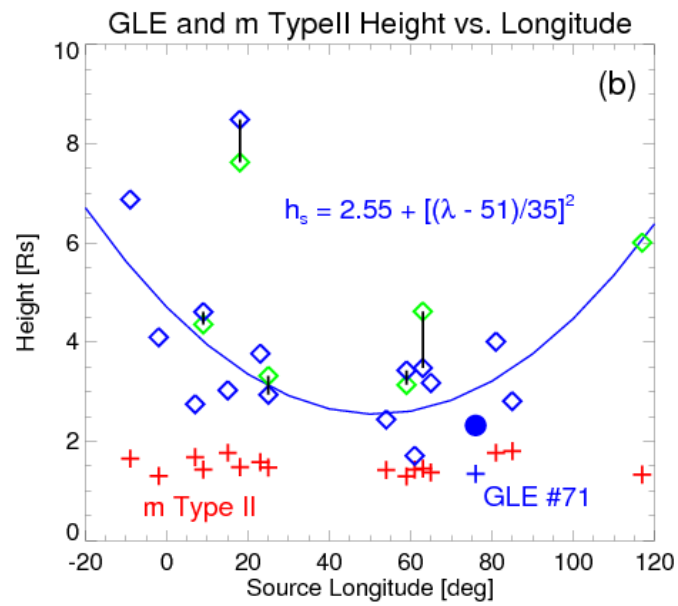

CME acceleration, shock formation height, and spectral index

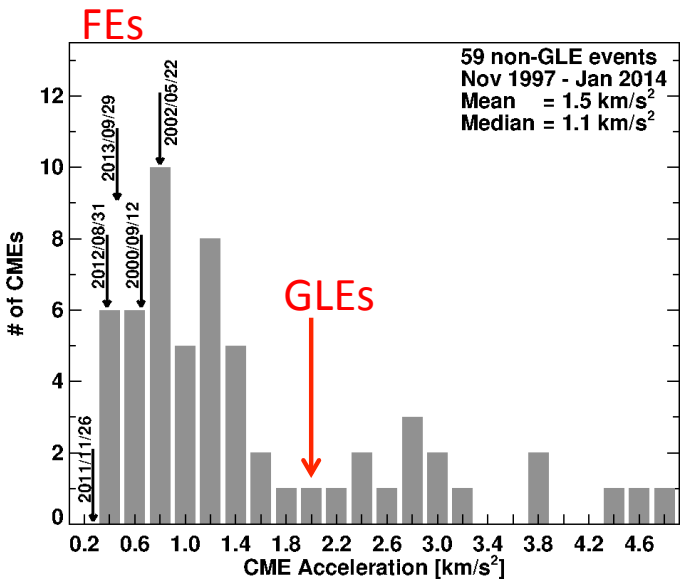

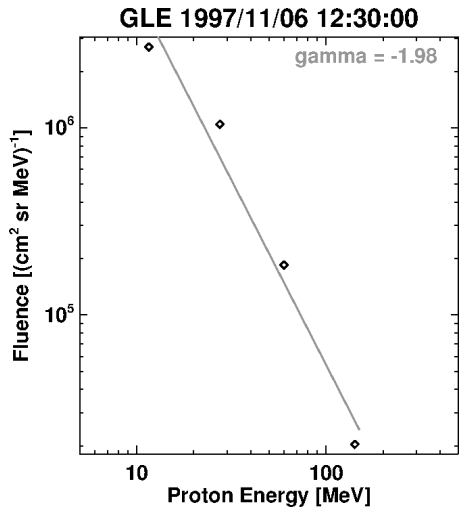

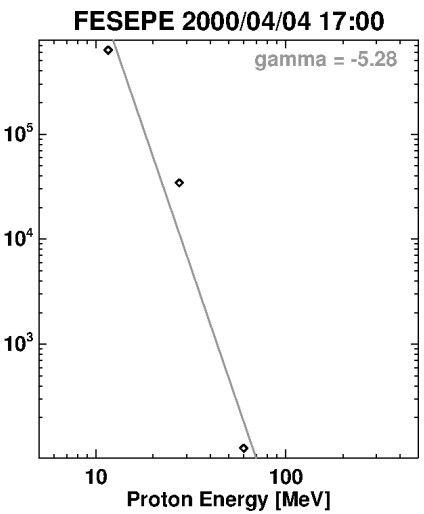

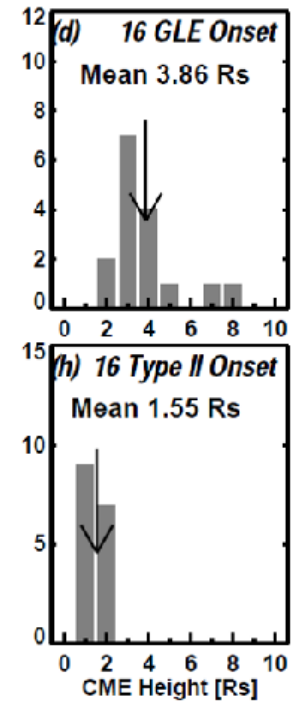

Slow CME acceleration → large shock formation heights
- GLE events: <1.5 Rs, FE SEP events: >3 Rs
- IP Type II Bursts (no metric or very low starting frequency)

Steep spectrum in FE SEP events: particles are not accelerated to very high energies because shock formation in weaker magnetic field region

Mäkelä et al. 2015; Gopalswamy et al. 2015

Energy Comparison

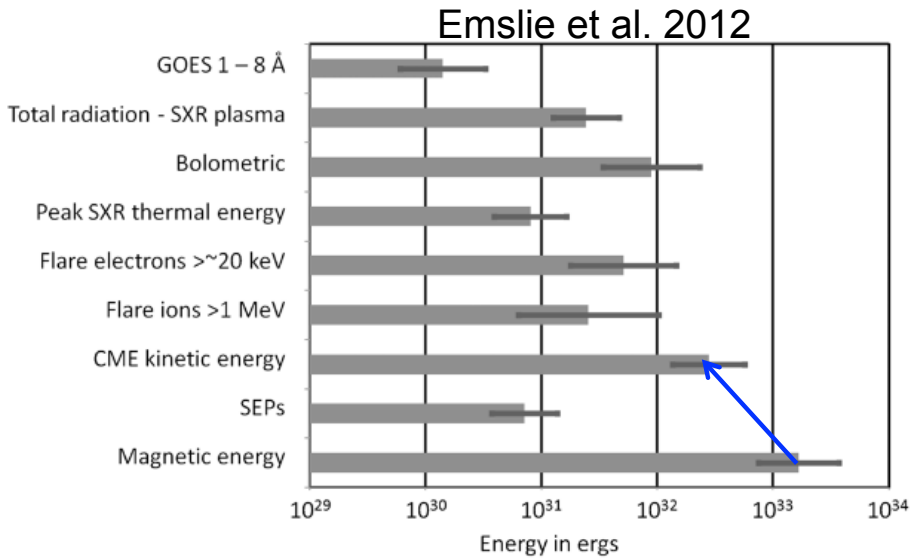

CMEs and Geomagnetic Storms

- Direct impact of CME plasma on Earth's magnetosphere
- Causes ring current enhancement
- Acceleration of electrons inside the magnetosphere
- Sudden commencement and exposure of geosynchronous satellites to the interplanetary space

Satellites Exposed to Interplanetary Space during Geomagnetic Storms

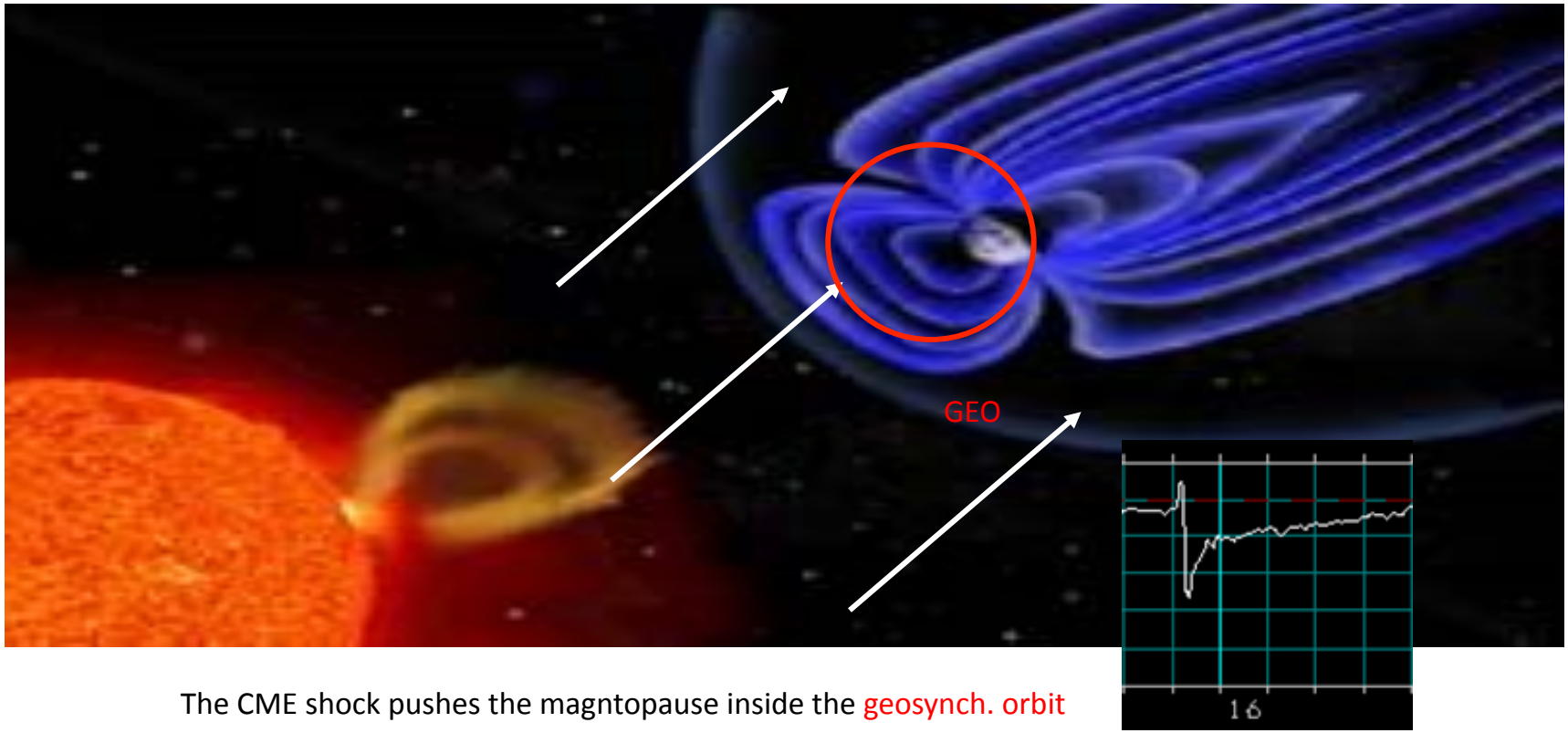

The CME shock pushes the magntopause inside the geosynch. orbit

CME Near Earth

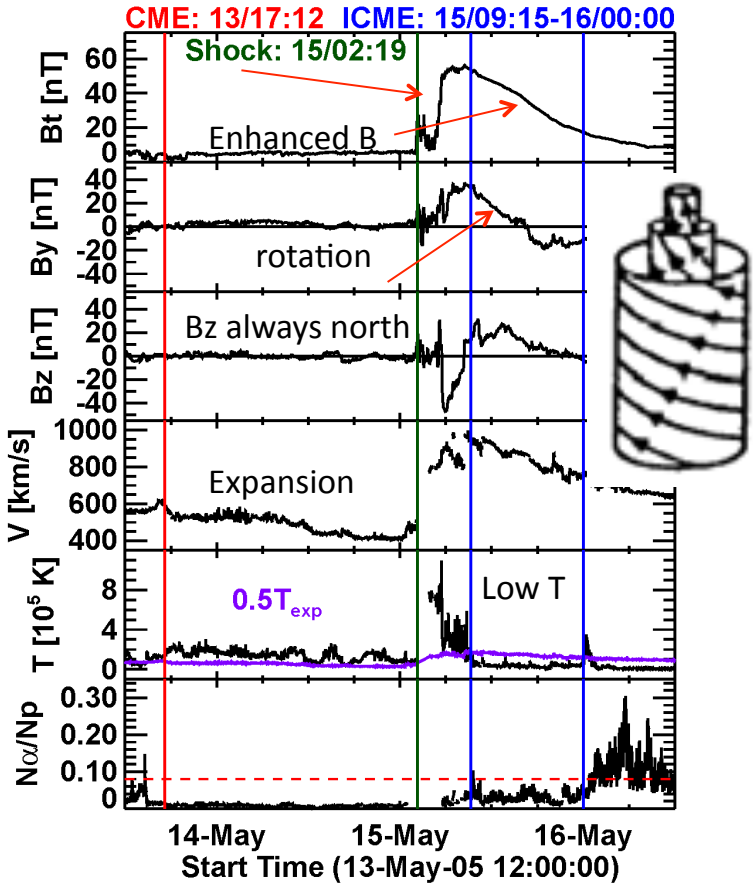

SOHO CME

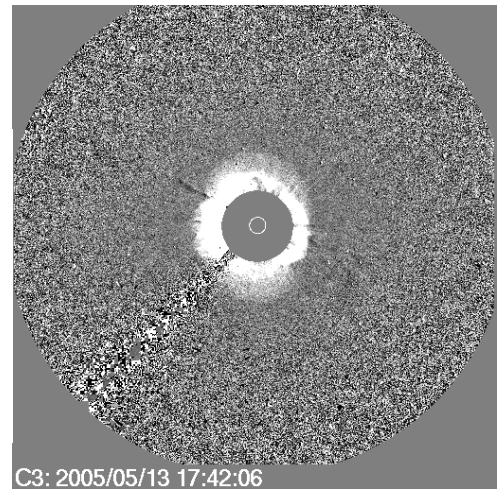

Clear magnetic field signature
Temperature signature is also clear
Alpha to proton ratio not clear
Solar wind speed clear

Shock – Sheath - Ejecta

Flux rope in white light: Chen et al. 1997

Out of the Ecliptic B from CMEs

- Normal Parker-spiral field does not have a Bz component
- CMEs with flux rope structure (magnetic clouds) naturally produce the Bz component
- Magnetic field draping in the shock sheath can also cause Bz (Gosling & McComas, 1987; Tsurutani & Gonzalez, 1988)
- Corotating interaction regions and fast wind have Alfven waves that represent Bz, but the magnitude is relatively small

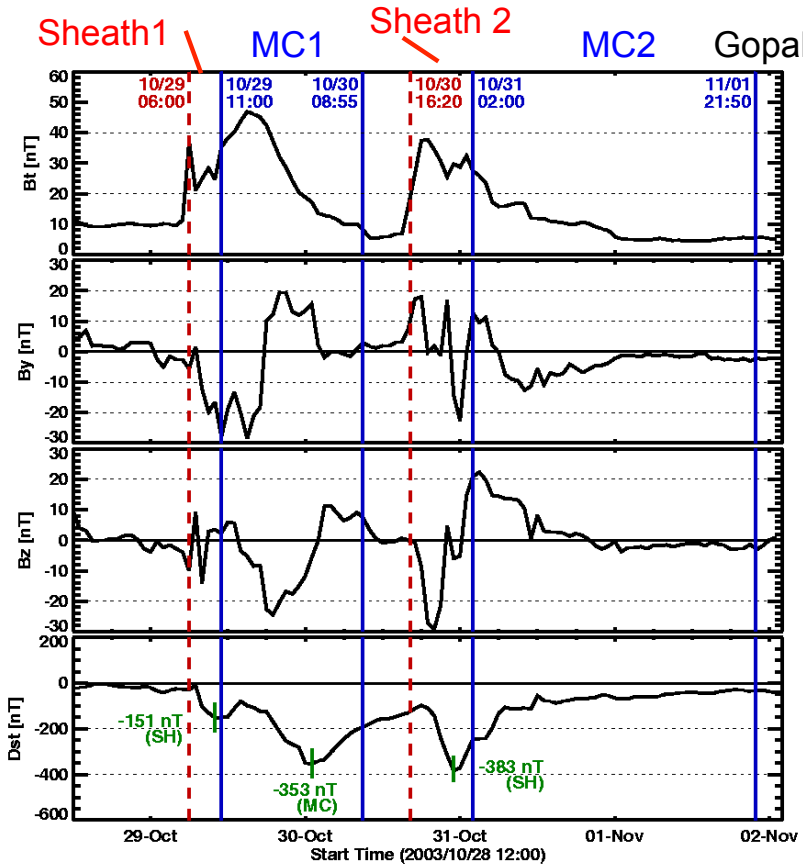

Gopalswamy et al., 2008

Sheath Superstorm

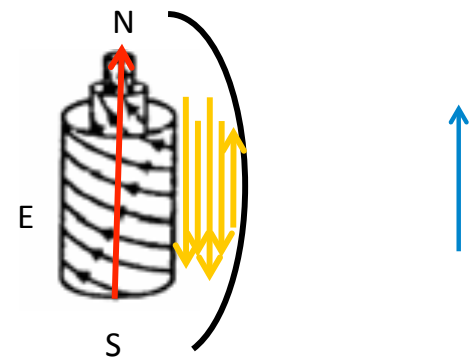

ENW (FN)

When MCs have high inclination the rotation is in the Y direction. In the Z-direction, the field will be always to the north or south. In this example, Bz is always north pointing so no storm. But there was a big storm due to the sheath consisting of intense south pointing Bz

Gosling and McComas1987; Tsurutani et al 1988

Summary of MC Structure

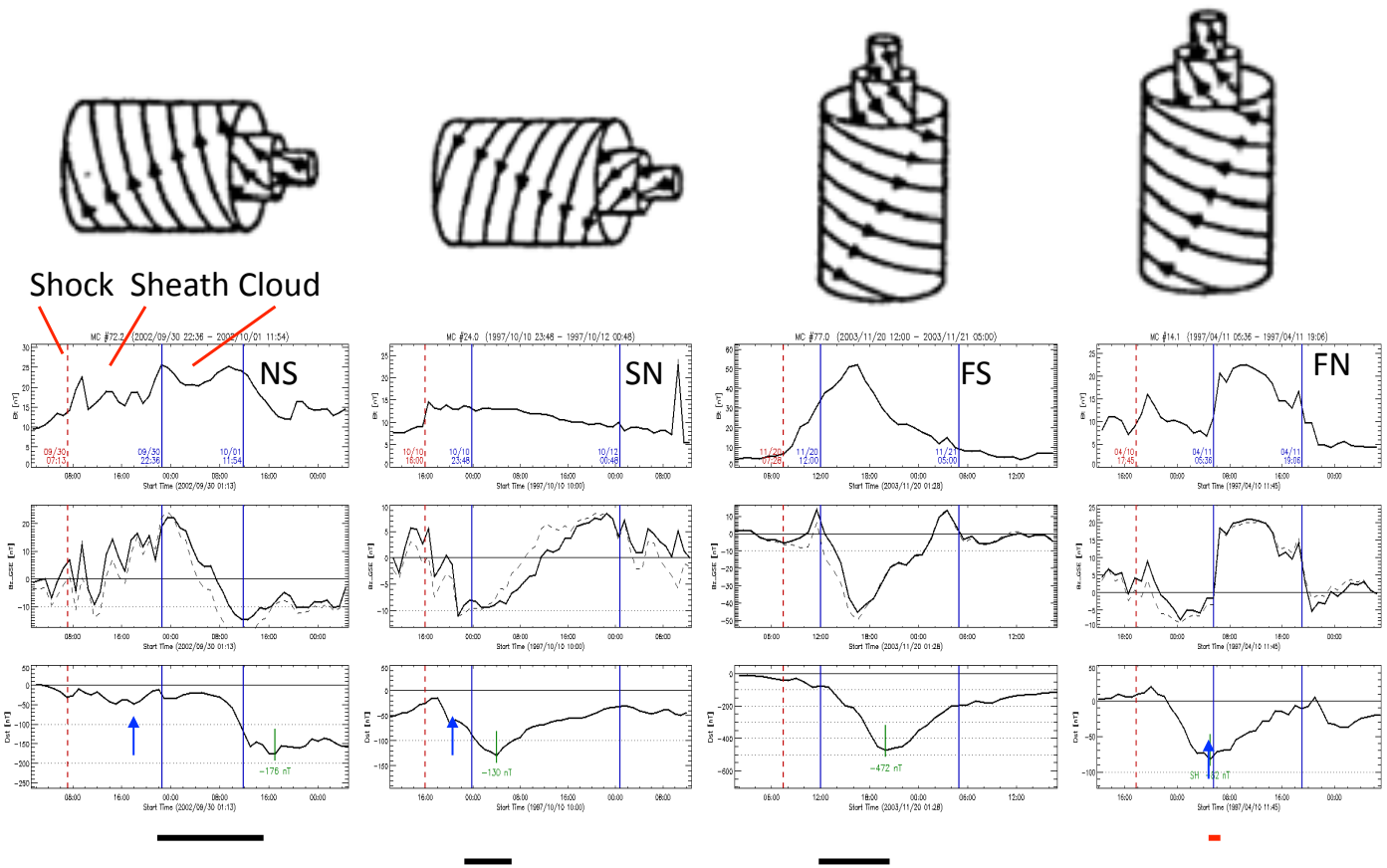

Cloud & Sheath Storms

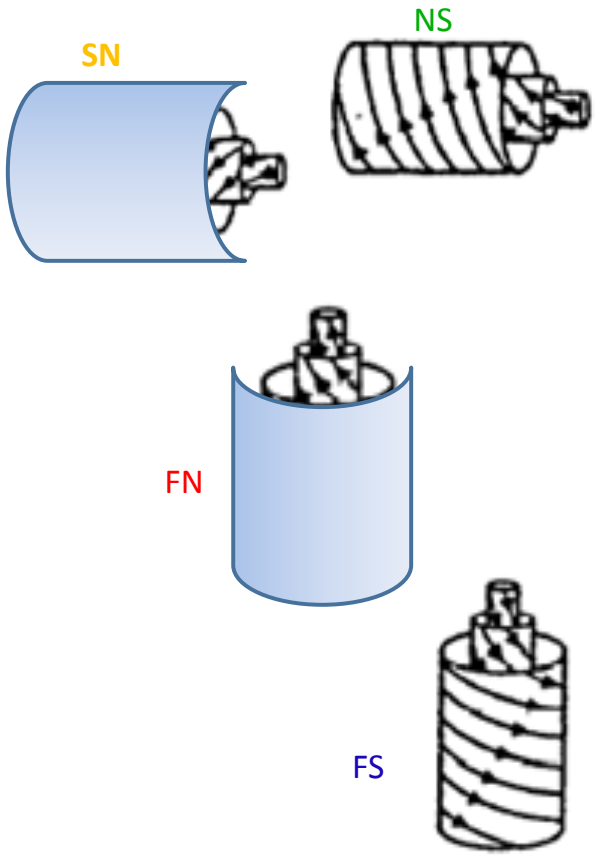

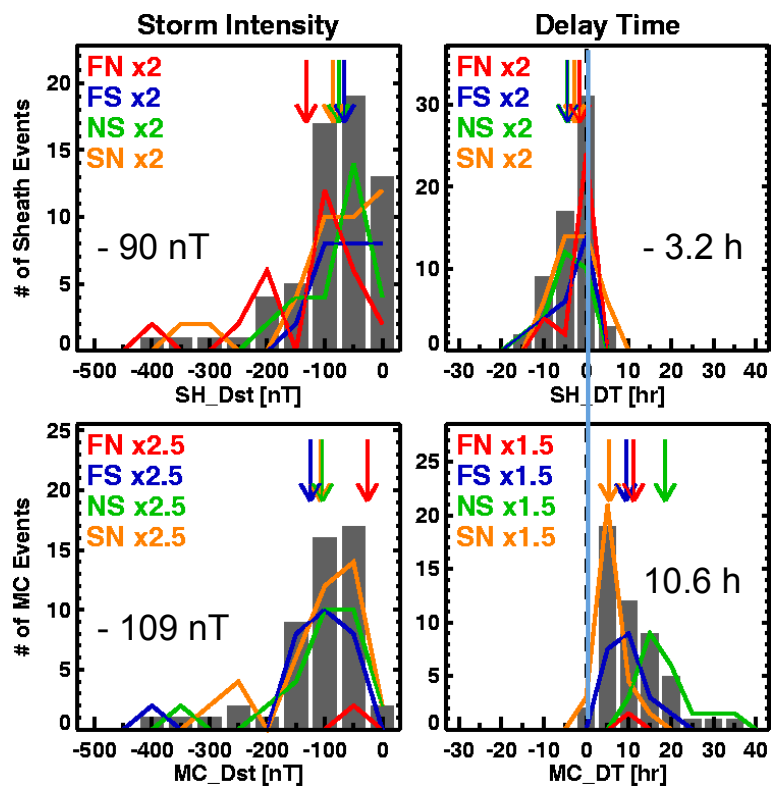

CMEs Producing Geomagnetic Storms

Large Dst (≤ -100 nT) events from cycle 23 and the associated LASCO CMEs considered

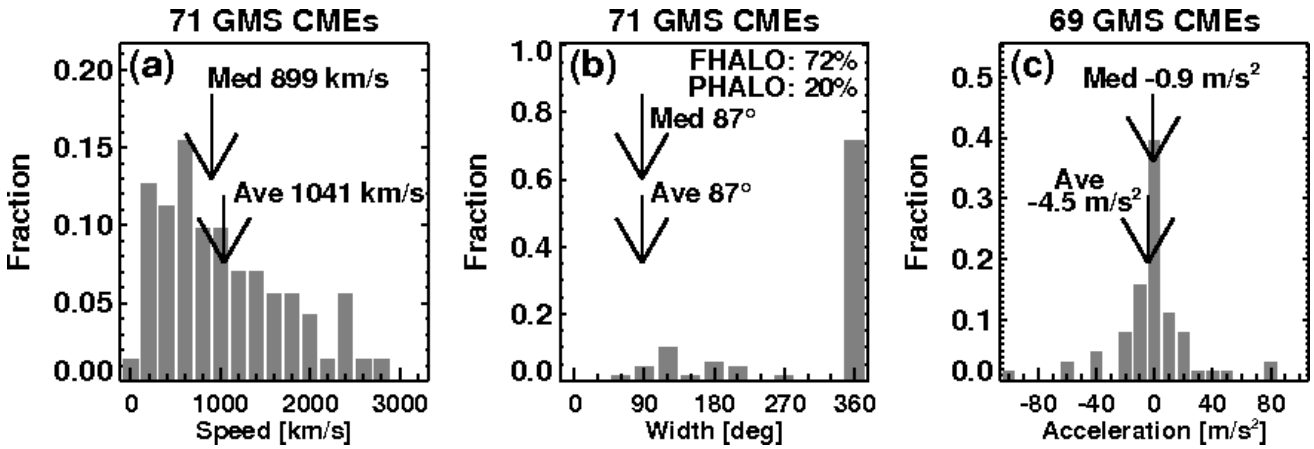

The CMEs are very fast (projected speed ~1041 km/s)
Almost all CMEs are halos or partial halos (92%)

Solar Source location important for Earth Impact

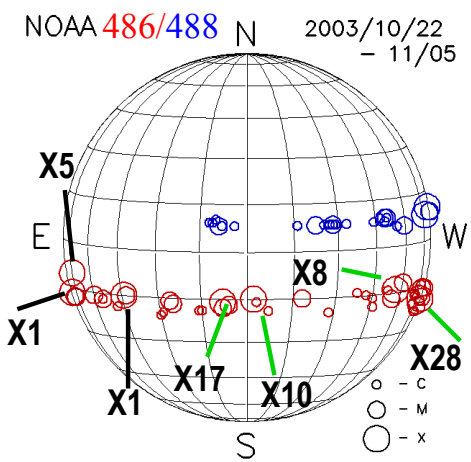

Heliographic coordinates of the CME source location. CMEs occurring near the disk center head directly toward Earth causing storms (e.g. CMEs associated with the X17 and X10 flares)

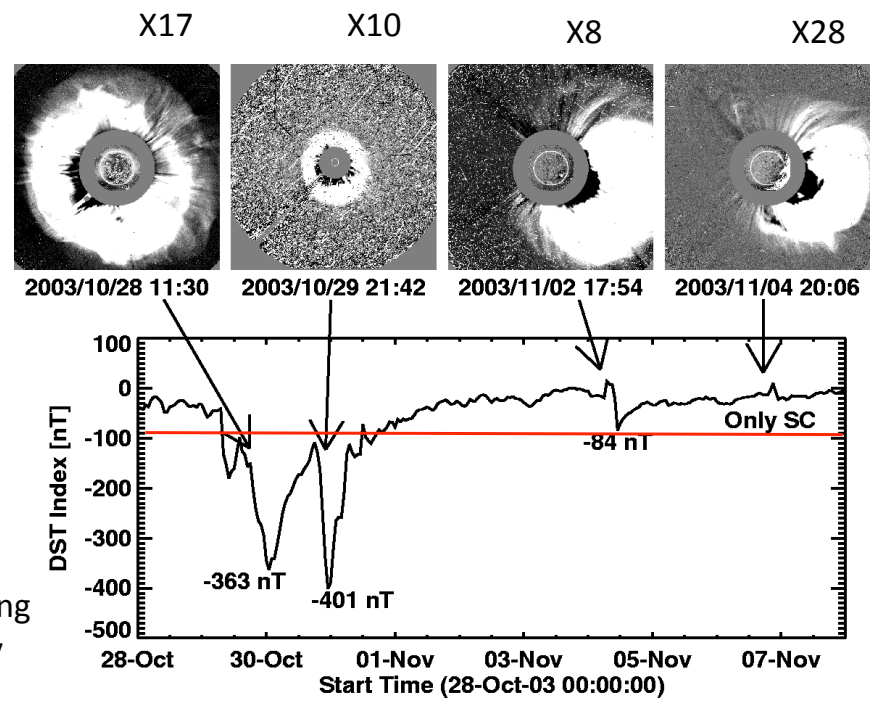

Dst index measures an average horizontal field of the Sun
Storm conditions when Dst< -30 nT
Major storms when Dst < -100 nT

Geomagnetic Storm and CME parameters

$Dst = -0.01VB_z - 32$ nT

The high correlation suggests
That V and Bz are the most
Important parameters
(- Bz is absolutely necessary)

V and Bz in the IP medium are
related to the CME speed and
magnetic content

Gopalswamy 2008

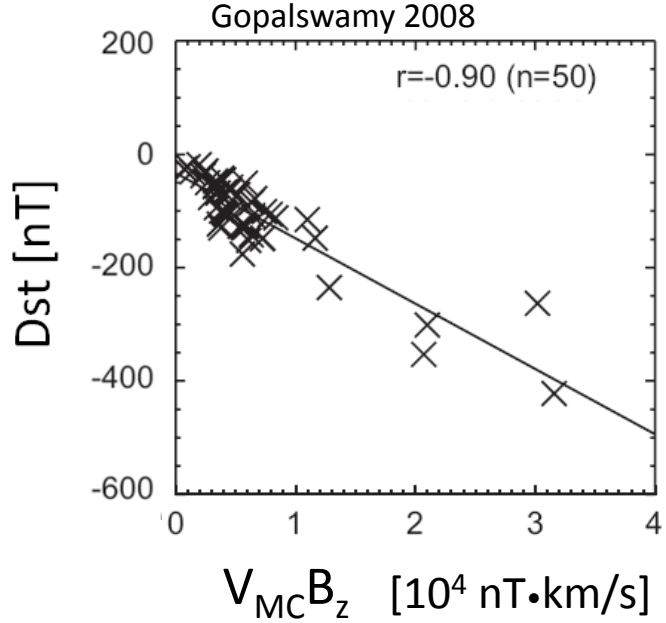

Carrington Event: VBz = 1.6 10^5 nT•km/s

V = 2000 km/s, Dst = -1650 nT → Bz = -81 nT

Origin of V and B

$$Dst = -0.01VB_z - 32 \ \ nT$$

Solar Wind speed
CIR Speed
CME speed

Active Region
Free energy

Alfven waves
CIR: Amplified Alfven waves
ICME: Sheath & Flux rope

Heliospheric
Mag Field

Active Region
Mag Field

Geoeffective & SEP-producing CME Sources

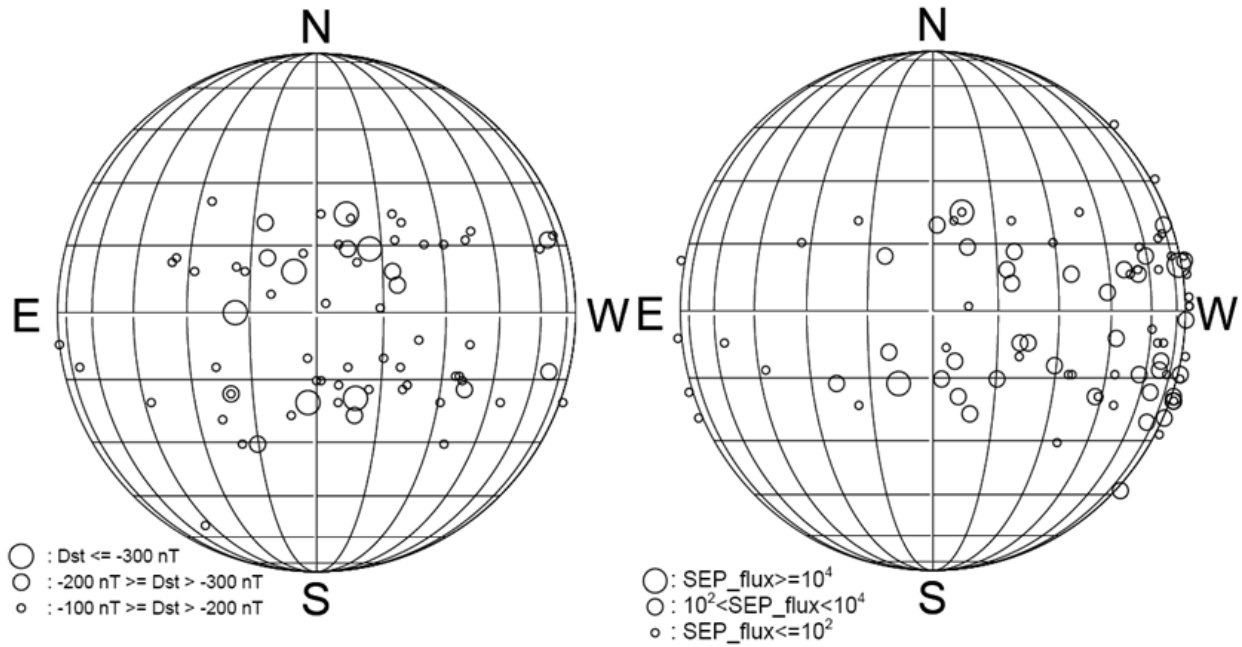

CMEs need to arrive at Earth
CMEs must contain Bz South
Similar to MC and Halo CME sources

CMEs need to drive shocks
Source region needs to be magnetically connected to Earth

Many double-whammy events

CME Speed Range & Important CMEs

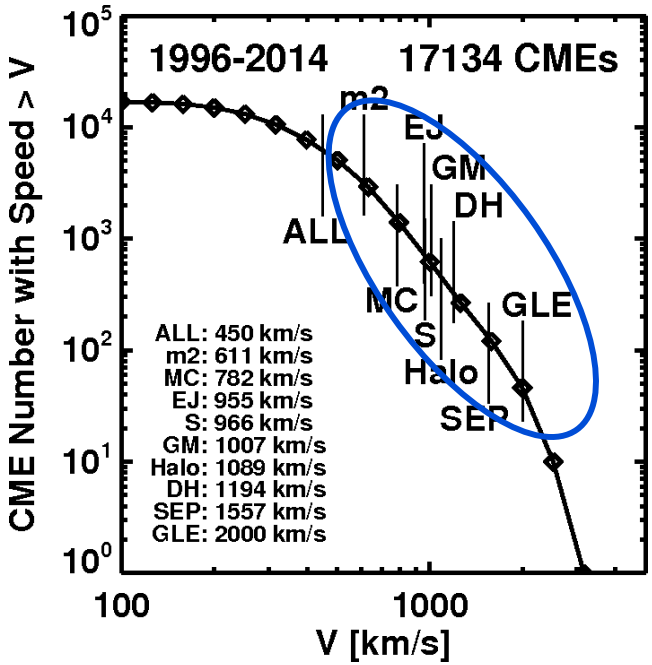

CME population	<V> km/s
All CMEs	471
metric II CMEs	610
MC CMEs	774
Geoeffective CMEs	1042
Halo CMEs	1052
mkm II CMEs	1500
SEP CMEs	1600
GLE CMEs	2000

CME speed < ~4000 km/s → Limit to the Free energy available in active regions

10% of CMEs are wide (W ≥120°) ~2100
Fast and wide CMEs ~500
Halo CMEs ~600 (some are slower than 900 km/s)
MCs ~100; intense storms ~100; SEPs ~100
GLEs : 16

Potential Field Energy ~ Free Energy

Emslie et al. 2012

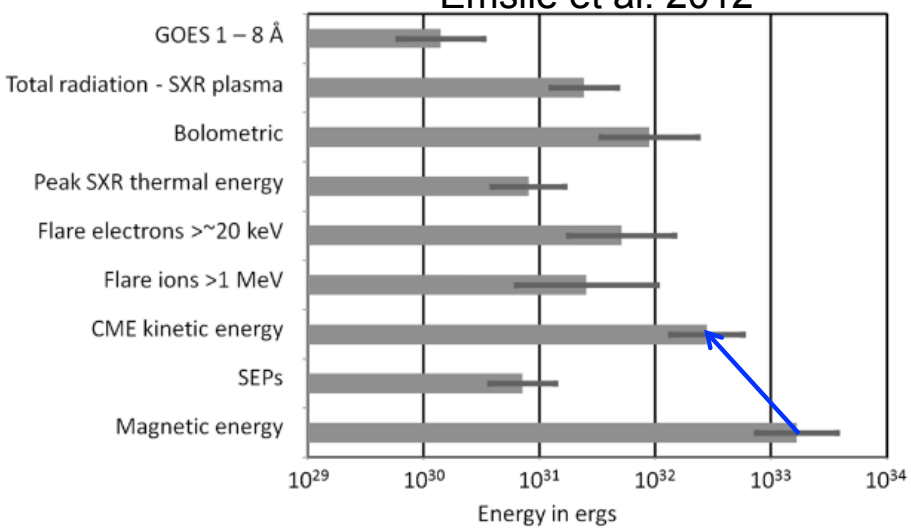

depending on Max observed A and B

B ~ 6100 G (Livingston et al. 2006)

A ~ 6132 msh (Newton 1955)

→ E ~ 3.8×10^{36} erg → Vmax ~7500 km/s

Gopalswamy et al., 2010

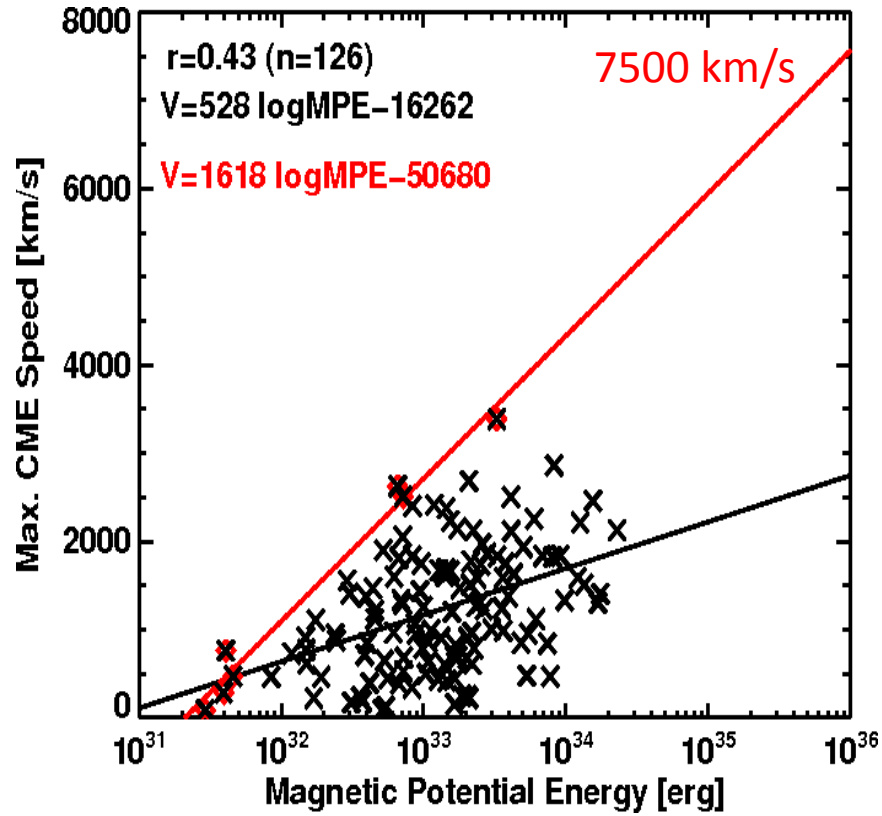

Stellar Flares

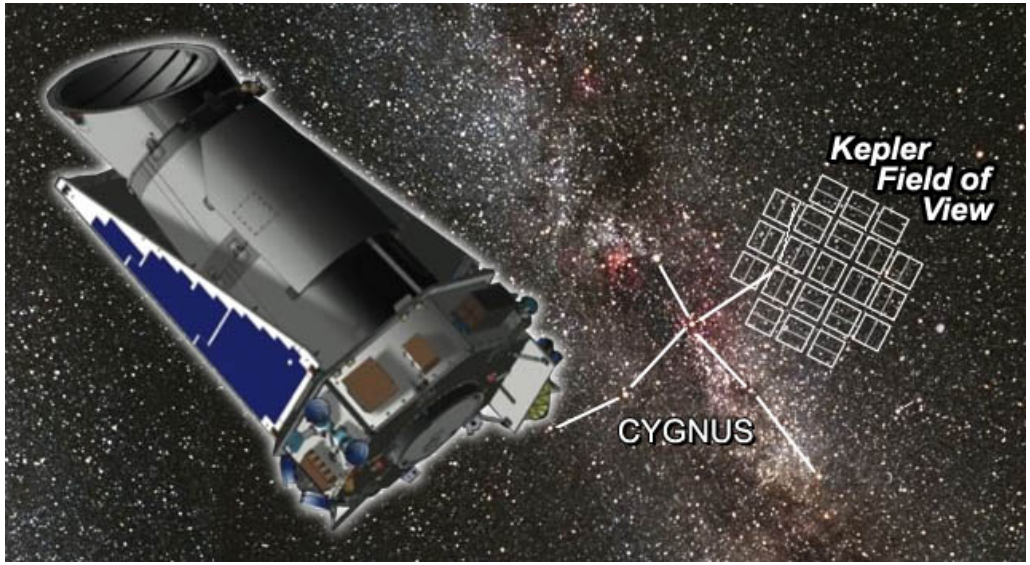

Kepler Mission, NASA

In the solar case, CMEs are ten times more energetic than the associated flares. In the stellar case?

Stellar CMEs?

Kepler has observed stellar flares that are 1000 times more powerful than solar flares.

There is a small probability that such flares can occur on the Sun

Maehara et al. (2012)

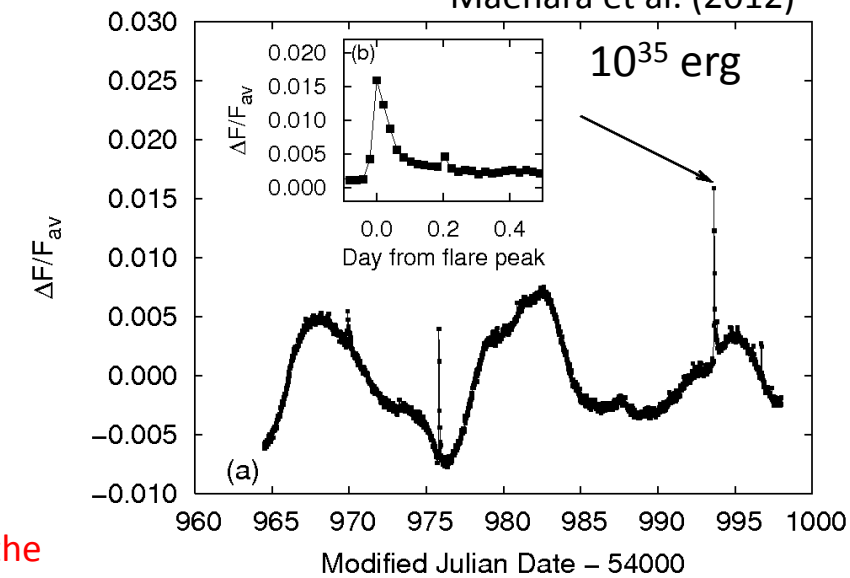

CME Interactions

- Non-radial motion of CMEs during the minimum phase
- CME – CME interactions during solar maximum
- CME – Coronal hole interaction during the declining phase
- CMEs tend to align with the heliospheric current sheet: CME rotation

Non-radial Motion: Toward Equator

NoRH PE: Gopalswamy and Thompson, 2000 JASTP

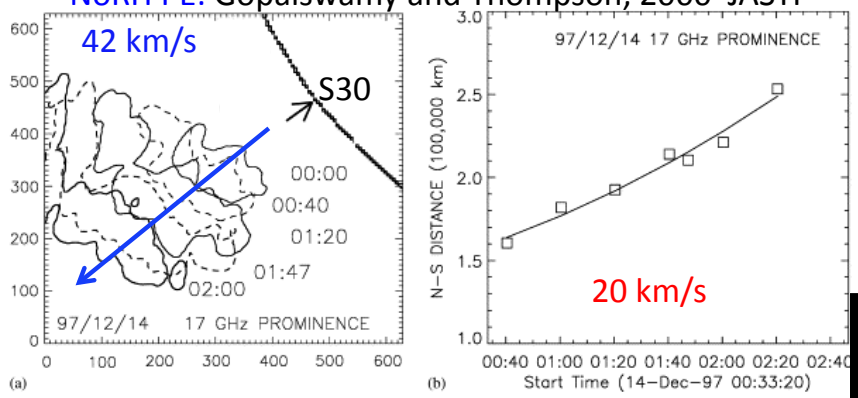

Hildner, 1977
MacQueen et al. 1986
Gopalswamy et al. 2000
Plunkett et al. 2001
Cremades et al. 2004
Gopalswamy et al. 2003,2009
Panasenco et al. 2010
Byrne et al. 2010
Lugaz et al. 2009

Deflection by 30°

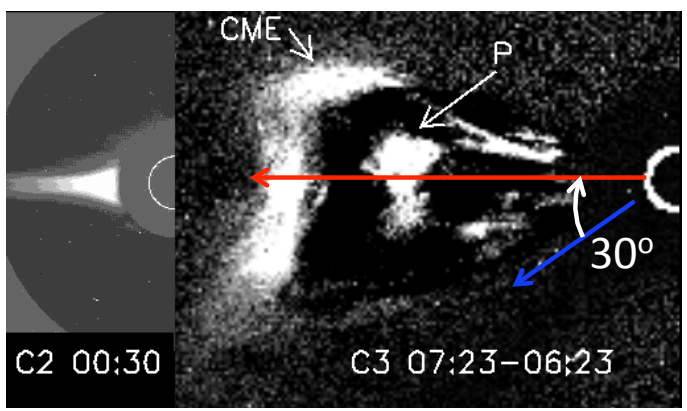

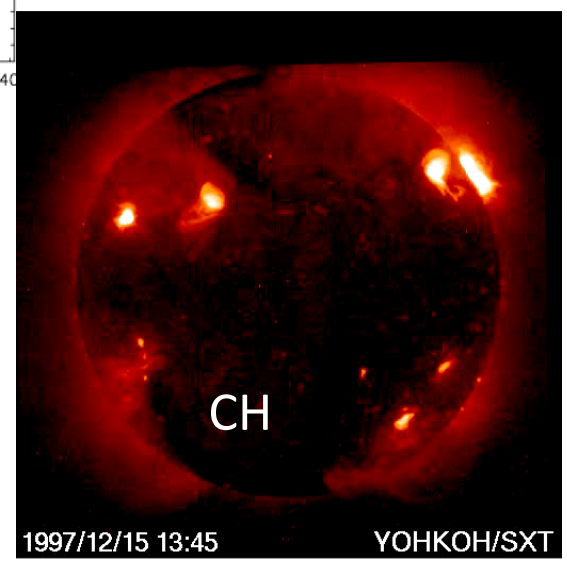

A Bad Example: 2014 January 7

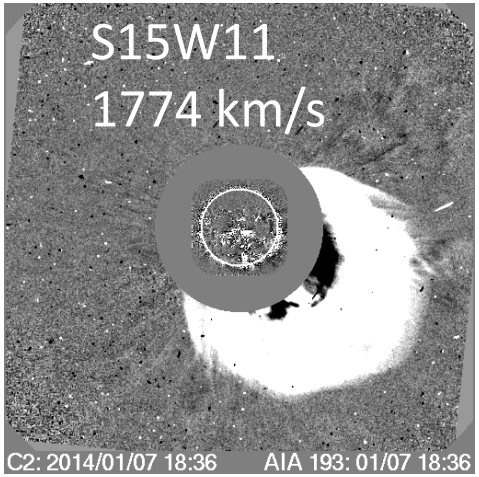

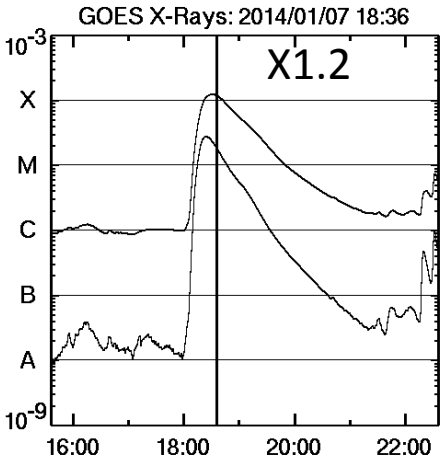

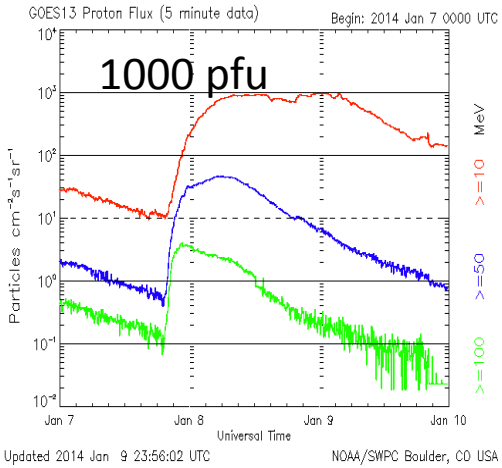

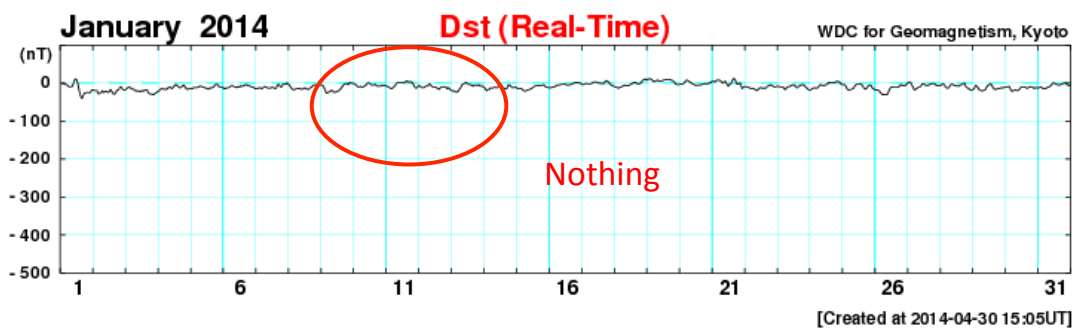

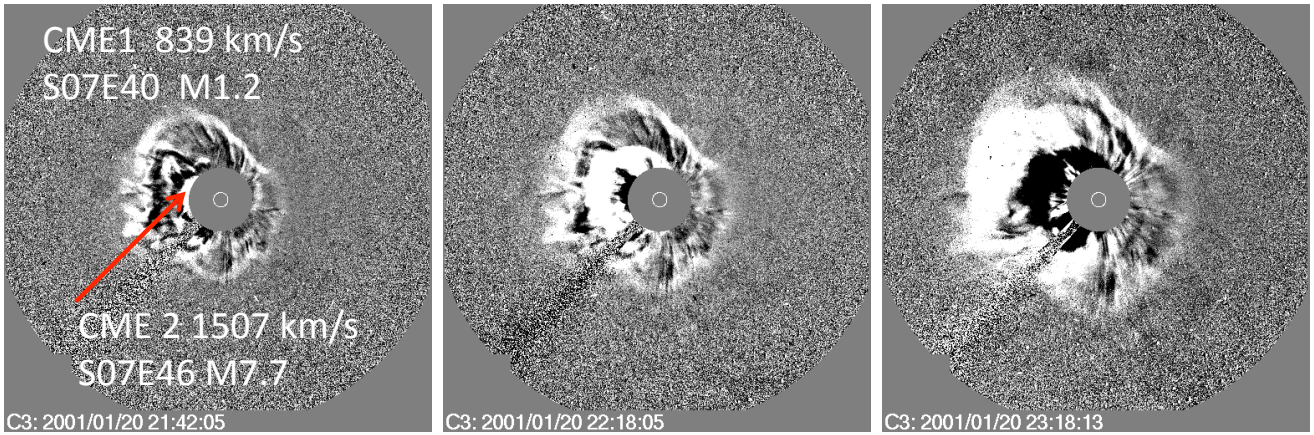

CME Cannibalism

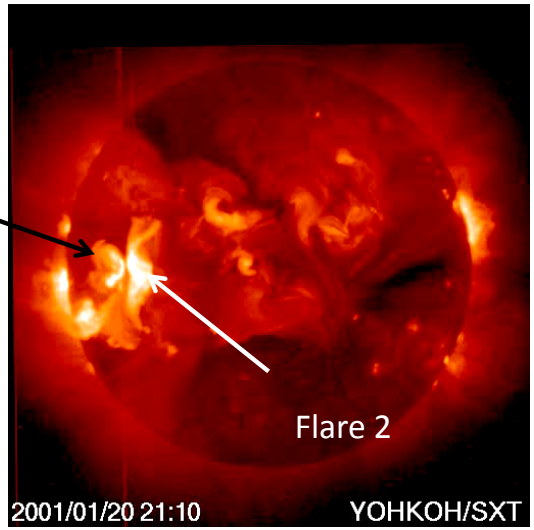

Two CMEs from the same region AR

Dst -61 nT moderate storm

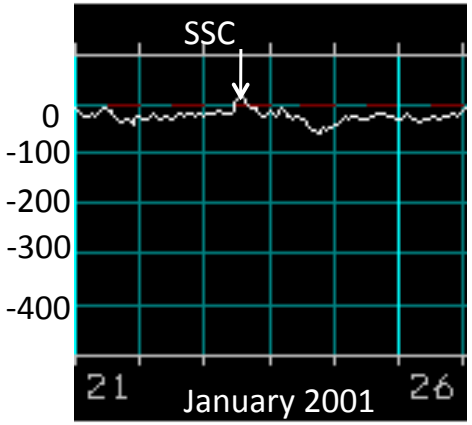

Single shock

The Sun-Earth System

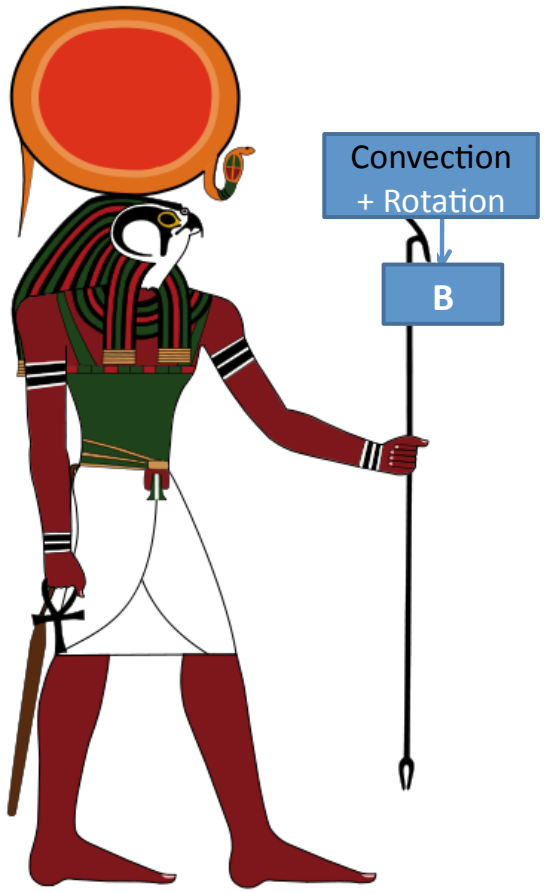

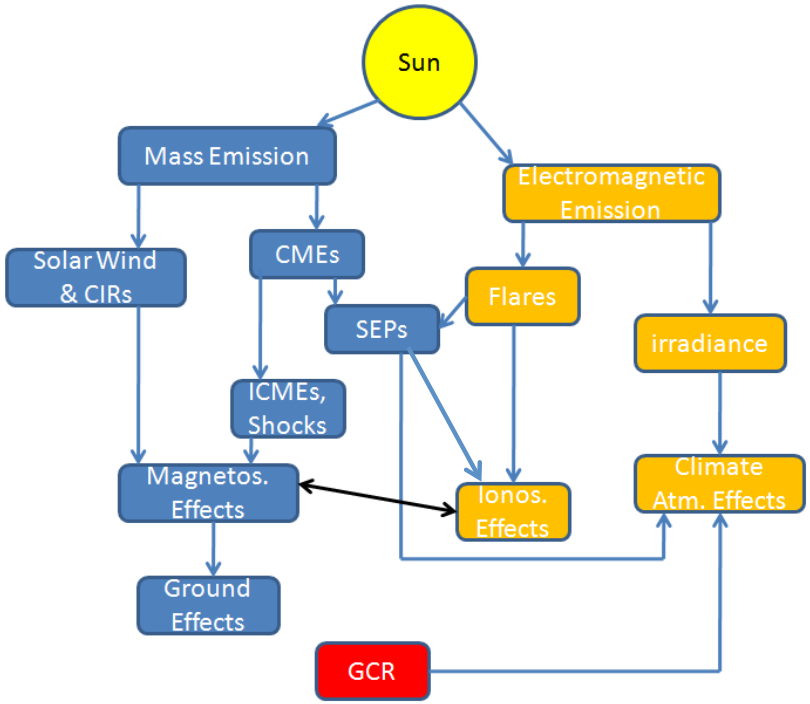

Summary

- Solar Magnetism and its variability is ultimately responsible for space weather via flares and CMEs
- CMEs cause wide-ranging space weather effects: SEPs, geomagnetic storms and the related effects
- CMEs drive shocks that accelerate SEPs
- CME magnetic structure and the sheath are responsible for large geomagnetic storms

References

- Boischot, A., 1957, Comptes Rendus Acad. Sci., Paris, 244, 1326
- Burlaga, L., Sittler, E., Mariani, F., & Schwenn, R., 1981, J. Geophys. Res., 86, 6673
- Forbes, T., 2000, J. Geophys. Res., 105, 23153
- Gold, T, 1962
- Gopalswamy, N., Lara, A., Yashiro, S., Nunes, S., & Howard, R. A., 2003, Solar variability as an input to the Earth's environment, Ed.: A. Wilson. ESA SP-535, Noordwijk: ESA Publications Division, p. 403
- Gosling, J. T., 1993, J. Geophys. Res., 98, 18937
- Sonett et al., 1964, Phys. Rev. Lett